Identification and analysis of Arabidopsis thiamine pyrophosphate transporters

Bandar Saleh Aljuaid

A thesis submitted for the degree of Doctor of Philosophy

Department of Biological Sciences

University of Essex

March 2017

Acknowledgements

I would like to express my sincere gratitude to my supervisor, Professor Christine A. Raines, for for the continuous support of my Ph.D study, for her encouragement and guidance from my project's beginning. I would also like to thank Dr Ulrike Bechtold, my PhD advisor for her constant support and her valuable feedback during supervisory meetings.

My sincere thanks also goes to Professor Donald Ort and Dr Paul F South, who provided me an opportunity and gave access the laboratory and research facilities.

Special thanks to all Christine's group members for helping and supporting throughout this project.

Last but not the least, I would like to thank my family for supporting me spiritually throughout writing this thesis and my life in general.

Abstract

Thiamine pyrophosphate (TPP) serves as a cofactor in universal metabolic pathways, including glycolysis, the pentose phosphate pathway (PPP) and the tricarboxylic acid cycle; moreover, it is essential for the proper functioning of all organisms. Recently, several steps of the plant thiamine biosynthetic pathway have been characterised, and a mechanism of feedback regulation for thiamine biosynthesis via riboswitching has been unravelled. In plants, thiamine is made in the chloroplasts and then transferred to the cytosol to generate the active form of thiamine, TPP. The mitochondria and chloroplasts must import TPP from the cytosol because both organelles contain TPP-dependent enzymes. In *Arabidopsis*, two members of the mitochondrial carrier family (MCF), AtTpc1 and AtTpc2, export TPP to the mitochondria, but the chloroplast TPP carrier is still unknown. This project aims to identify thiamine chloroplast transporter(s) and investigate mitochondrial thiamine transporters in *Arabidopsis*. The approaches used to achieve the aims of this project include phylogenetic analysis, mutant analysis, polymerase chain reaction techniques and gene construct techniques. AtTpc1 and AtTpc2 have a limited effect on plant growth under normal conditions, at least in terms of stem length and secondary stem length. Moreover, phylogenetic analysis showed that AtFolt1 (Arabidopsis folate transporter) and CTT (AT3G51870) are putative chloroplast TPP transporters. The inhibition of AtFolt1 by about 50% and CTT by about 80% was associated with reduced TPP levels in leaves. Thus, AtFolt1 and CTT may be chloroplast TPP transporters.

Table of Contents

Table of figures

Abbreviations

acetyl CoA	acetyl coenzyme A
AIR	5-aminoimidazole ribonucleotide
Amp	ampicillin
AtFolt1	*Arabidopsis* folate transporter 1 (At5g66380)
AtFolt1i	AtFolt1 transgenic plant using RNAi
ATP	adenosine triphosphate
AtTPC1	mitochondrial TPP transporter (At3g21390)
AtTPC2	mitochondrial TPP transporter (At5g48970)
bp	base pair
cDNA	complementary DNA
CO_2	carbon dioxide
C-terminal	carboxy terminal
cTP	chloroplast transit peptide
CTT	putative chloroplast transporter (AT3g51870)
CTTi	CTT transgenic plant using RNAi
DmTpc1p	*Drosophila* TPP transporter
DNA	deoxyribonucleic acid
dNTP	deoxyribonucleotide triphosphate
DPX	1-deoxy-D-xylulose-5-phosphate
dsH_2O	double-sterilised water
DTT	dithiothreitol
DW	dry weight
DXS	1-deoxy-D-xylulose 5-phosphatesynthase
E. coli	*Escherichia coli*
EDTA	ethylenediaminetetraacetic acid
ER	endoplasmic reticulum
g	gram
YFP	The yellow fluorescent protein
HET-P	4-methyl-5-b-hydroxyethylthiazole phosphate
HMP-P	hydroxymethyl pyrimidine phosphate
HMP-PP	hydroxymethyl pyrimidine diphosphate

HMT-PP	pyrimidine
HPLC	high-performance liquid chromatography
h	hour
Hyg	hygromycin
IPP	
IPTG	isopropyl β-D-1-thiogalactoside
Kan	kanamycin
Kb	kilobase
KDa	kilodalton
LB	Luria–Bertani broth medium
LB agar	Luria–Bertani agar/broth
M	DNA marker
MCF	mitochondrial carrier family
MDB	membrane desalting buffer
MEP	non-mevalonate pathway
mg	milligram
min	minute
ml	millilitre
mM	millimolar
mRNA	messenger RNA
MS	Murashige and Skoog
MTT	mitochondrial thiamine transporters
MW	molecular weight
NaCl	sodium chloride
NAD	nicotinamide adenine dinucleotide
NADPH	nicotinamide adenine dinucleotide phosphate
NASC	National Arabidopsis Source Centre
N-terminal	amino terminal
PCR	polymerase chain reaction
PDB	The protein data bank
pH	measure of acidity or alkalinity
pmole	picomole

PPP	pentose phosphate pathway
PRPP	5-phosphoribosyl 1-pyrophosphate
R-5-P	ribulose-5-phosphate
rpm	revolutions per minute
RMSD	The root mean square deviation
RNA	ribonucleic acid
RNAi	RNA interference
RT-PCR	reverse transcription PCR
Rubisco	ribulose-1,5-bisphosphate carboxylase/oxygenase
s	second
SAR	systemic acquired resistance
SDS	sodium dodecyl sulphate
SE	standard error
TAIR	The Arabidopsis Information Resource
TBE	tris-orthoboric acid EDTA
TCA	citric acid
Th1	HET-P synthase
TK	transketolase
Tm	melting temperature
TMP	thiamine monophosphate
Tpc	human TPP carrier
Tpc1p	yeast TPP carrier
TPK	thiamine diphosphokinase
TPP	thiamine pyrophosphate
Tris	Tris(hydroxymethyl)aminomethane
Tris-HCl	Tris-hydrochloric acid
TTP	thiamine triphosphate
Tween 20	polyoxyethylene sorbitan monolaurate
UTR	untranslated region
v	volt
WT	wild type
X-gal	5-bromo-4-chloro-3-indolyl-β-D-galactopyranoside
3'UTR	3' untranslated region
µg	microgram

µl	microlitre
°C	degrees Celsius
%	percentage

Chapter 1: Introduction

1.1. Introduction

Thiamine, commonly called vitamin B1, is an essential substance for all living organisms. Thiamine pyrophosphate (TPP; also called thiamine diphosphate, ThDP) is considered to be the metabolically active form of thiamine. TPP functions as a cofactor and is involved in regulating enzymes in a number of metabolic pathways, such as glycolysis, reductive carbohydrate metabolism, oxidative decarboxylation and transketolase (TK) reactions (Frank et al., 2007). Recent research has also reported its function in the tolerance of DNA damage and in activating genes in plants for disease resistance (Ahn et al., 2007).

Through a complex pathway, TPP is biosynthesised in microorganisms (prokaryotes and fungi) and plants, but not in humans or animals (Jenkins et al., 2007). Thus, humans and animals must obtain this nutrient from dietary sources. Moreover, it has a high turnover rate and the body is incapable of storing it; hence, a continuous supply of this vitamin is needed.

The importance of thiamine is well known, and low thiamine intake is a public health concern, particularly in nations where polished rice is the main part of the diet, such as in Asian countries. The rice-polishing process removes thiamine from the bran, and those who eat such rice as a staple tend to become thiamine deficient. Thiamine deficiency is also associated with beriberi, cardiac problems, peripheral neuropathy, alcoholic brain disease and other neurological disorders (Martin et al., 2003). It is therefore of great clinical importance to augment our knowledge concerning the pathways of its biosynthesis in plants to aid us in the production of thiamine for our own benefit. This review aims to gather evidence from the literature on thiamine biosynthesis and its transport in plants.

1.2. Thiamine pyrophosphate

Thiamine pyrophosphate, or thiamine diphosphate, is a cofactor for several enzymatic reactions, including glycolysis, the tricarboxylic acid cycle and the pentose phosphate pathway (Krampitz, 1969). TPP also influences ThiC gene expression by binding to the riboswitch that is involved in the pyrimidine biosynthesis pathway (Miranda-Rios, 2007).

1.2.1. The importance of thiamine pyrophosphate

1.2.1.1. Functions of thiamine pyrophosphate as a cofactor

As mentioned above, TPP is the active form of thiamine and works as a cofactor in important metabolic pathways, such as glycolysis, the pentose phosphate pathway (PPP) and the citric acid (TCA) or Krebs cycle to synthesise energy (Pohl et al., 2004). for example, with TK, pyruvate dehydrogenase and alpha-ketoglutarate (Fattal-Valevski, 2011). In conjunction with TPP, these three enzymes are essential for producing energy in cells after breaking down carbohydrates. Consequently, a decrease in TPP will cause a decrease in the activity of these reactions.

Glycolysis takes place in the cytosol, producing pyruvate, which is then transported to the mitochondrial matrix where it is further metabolised (LeClere et al., 2004). The TPP pyruvate dehydrogenase complex (PDC) in this pathway catalyses the reaction which produce pyruvate, then, the enzyme pyruvate dehydrogenase (PDH) converts the pyruvate to acetyl coenzyme A (acetyl CoA), a reaction in which TPP serves as a cofactor also. The acetyl CoA is used in the citric acid cycle and links glycolysis to the citric acid cycle (LeClere et al., 2004). At this

point, when acetyl CoA is produced, the TCA cycle can begin. The TCA cycle involves a series of enzyme-catalysed chemical reactions that occur in the mitochondrial matrix to generate an energy source. In this cycle, TPP combines with α-ketoglutarate dehydrogenase to produce succinyl-CoA through the oxidative decarboxylation of α -ketoglutarate (Fattal-Valevski, 2011). There are also two TPP enzymes which participate in branched amino acids pathway, the TPP dependent enzyme acetolactate synthase (ALS) and branched chain ketoacid dehydrogenase (BCKDH) in Arabidopsis. The first enzyme (ALS) catalyses a reaction which produce 2-acetolactate from pyruvate (Binder, 2010). The second enzyme participates I the breakdown the branched amino acids and produce branched chain acyl-CoA which is converted later to acetyl-CoA (Peng et al., 2015) (Figure 1.1).

TPP also serves as a cofactor for the pyruvate decarboxylase reaction, which converts pyruvate into acetaldehyde and carbon dioxide (CO_2) during ethanolic fermentation in yeast (Rivoal et al., 1990, Lee and Langston-Unkefer, 1985).

There is an alternative pathway for glucose oxidation called the pentose phosphate pathway (PPP); this pathway represents a process wherein nicotinamide adenine dinucleotide phosphate (NADPH) is generated by oxidising glucose to ribose-5-phosphate (R-5-P). A key enzyme in this pathway is TK, which also participates in the Calvin cycle. TK catalyses two reactions in the PPP and the Calvin cycle. In the first reaction, TK catalyses the transfer of a two-carbon glycolaldehyde from a keto-sugar to an aldose-sugar to form sedoheptulose 7-phosphate and glyceraldehyde 3-phosphate using TPP (Schenk et al., 1998). In the second reaction, TK also uses TPP as a cofactor to transfer a two-carbon fragment from D-xylulose-5-P to aldose erythrose-4-phosphate, giving fructose 6-phosphate

and glyceraldehyde-3-P (Kruger and von Schaewen, 2003). In the Calvin cycle, TK catalyses the same two reactions, but in the opposite direction (Teige et al., 1998, Lindqvist et al., 1992) (Figure 1.1).

TPP is also required in the non-mevalonate pathway (MEP) to synthesise IPP and DMAPP (Rohmer, 1999). The 1-deoxy-D-xylulose-5-phosphate (DXP) synthase enzyme catalyses the first reaction in the MEP using TPP as a cofactor. In this reaction, DXP synthase catalyses the condensation of pyruvate and glyceraldehyde 3-phosphate to produce DXP (Lange et al., 1998, Lois et al., 1998, Sprenger et al., 1997).

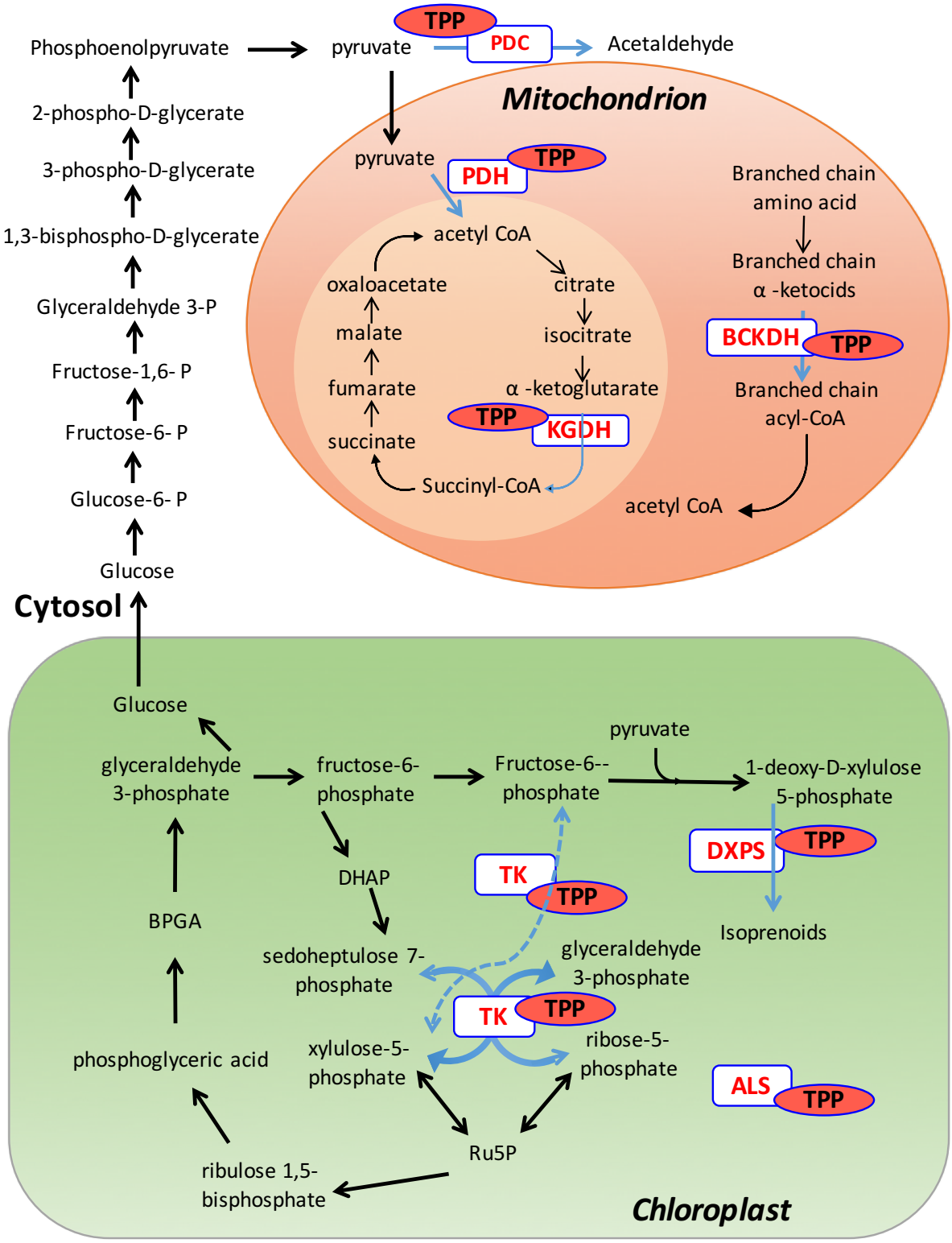

Figure 1.1: TPP-dependent enzymes and their cellular location. thiamine pyrophosphate (TPP); pyruvate decarboxylase (PDC); pyruvate dehydrogenase (PDH); a-ketoglutarate dehydrogenase (KGDH); (BCKDH) branched-chain a-ketoacid dehydrogenase (KGDH); transketolase (TK); 1-deoxy-D-xylulose-5-phosphate synthase (DXS); acetohydroxyacid synthase (ALS).

Insufficient amounts of thiamine result in a reduction in the activity of these important enzymes. This decrease in activity is different for each enzyme, and it is strongly dependent on the type of cell (Butterworth et al., 1993). Studies have demonstrated this reduction in activity in autopsied human tissues and in thiamine-deficient experimental rat models (Bubber et al., 2004, Butterworth et al., 1993, Blass and Gibson, 1977). A stoppage in the production of adenosine triphosphate (ATP) and a subsequent decrease in ATP levels may result from the diminished activity of pyruvate dehydrogenase and alpha-ketoglutarate following a deficiency in thiamine. This reduction in ATP levels causes an energy deficiency in the cells and ultimately cell death (Aikawa et al., 1984). In addition, decreased pyruvate dehydrogenase activity results in decreased pyruvic acid entry into the Krebs cycle. This causes an accumulation of lactic acid in the cells, which also results in cell death (Fattal-Valevski, 2011). A deficiency in thiamine gives rise to the failure of acetyl CoA production, thereby decreasing the production of acetylcholine, which is an important neurotransmitter in the nervous system (Heinrich et al., 1973).

TK plays a part in the oxidative PPP, as mentioned above. This pathway produces a reducing compound, NADPH, which is utilised for different synthetic reactions in cells. One example of this is that TK is significant in maintaining the redox state in cells (Fattal-Velevski, 2011). This pathway also produces riboses, which are used in making nucleic acids and nucleotides. Therefore, a deficiency in thiamine results in a flawed ribonucleic acid (RNA) synthesis of ribose. In summary, the end result of a thiamine deficiency with TK includes a reduction in the production of myelin sheaths in nerves, reduced synthesis of fats and sugars and decreased synthesis of branched amino acids.

1.2.1.2. *Thiamine and its phosphate esters function as non-cofactors*

Thiamine function is important in cells; it not only serves as a coenzyme in cell metabolism but also has a structural role. Thiamine plays a role in membrane function and structure, including in mitochondrial and axoplasmic membranes. It counteracts the cytotoxicity induced by various agents. Thiamine also has an important role in axonal growth, myelinogenesis, the formation of synapses and cell differentiation (Goldberg et al., 2004).

Numerous studies have also demonstrated the importance of thiamine function in cells, particularly in the tissues of the nervous system. These studies claim that in rat models, thiamine deficiency can definitely result in spinal cord deficits, insufficiencies in brain enzymes and decreased lipogenesis and myelinogenesis (Fournier and Butterworth, 1990, TROSTLER and SKLAN, 1978).

Thiamine may also provide a substitute approach for the management of plant diseases. A study conducted by Ahn et al. (2005) demonstrated that thiamine encourages systemic acquired resistance (SAR) among plants. Their results showed that rice plants (and other crop plants) given thiamine demonstrated resistance against bacterial, viral and fungal infections. In addition, they determined that thiamine treatment promotes stronger and faster production of pathogenesis-related genes and an increase in the activity of protein kinase C. This disease-resistant property of thiamine and the production of the gene was organised systematically throughout the plant and lasted more than 15 days after treatment. These results show that thiamine promotes SAR in plants via the salicylic acid and calcium-related signalling pathways (Ahn et al., 2005).

1.2.2. Structure of thiamine pyrophosphate (TPP)

Thiamine consists of two moieties, namely 4-methyl-5-β-hydroxyethyl thiazolium (thiazole ring) and 4-amino-2-methyl-5-pyrimidyl (pyrimidine ring). These are linked together by a methylene bridge (Figure 1.2; (Jurgenson et al., 2009).

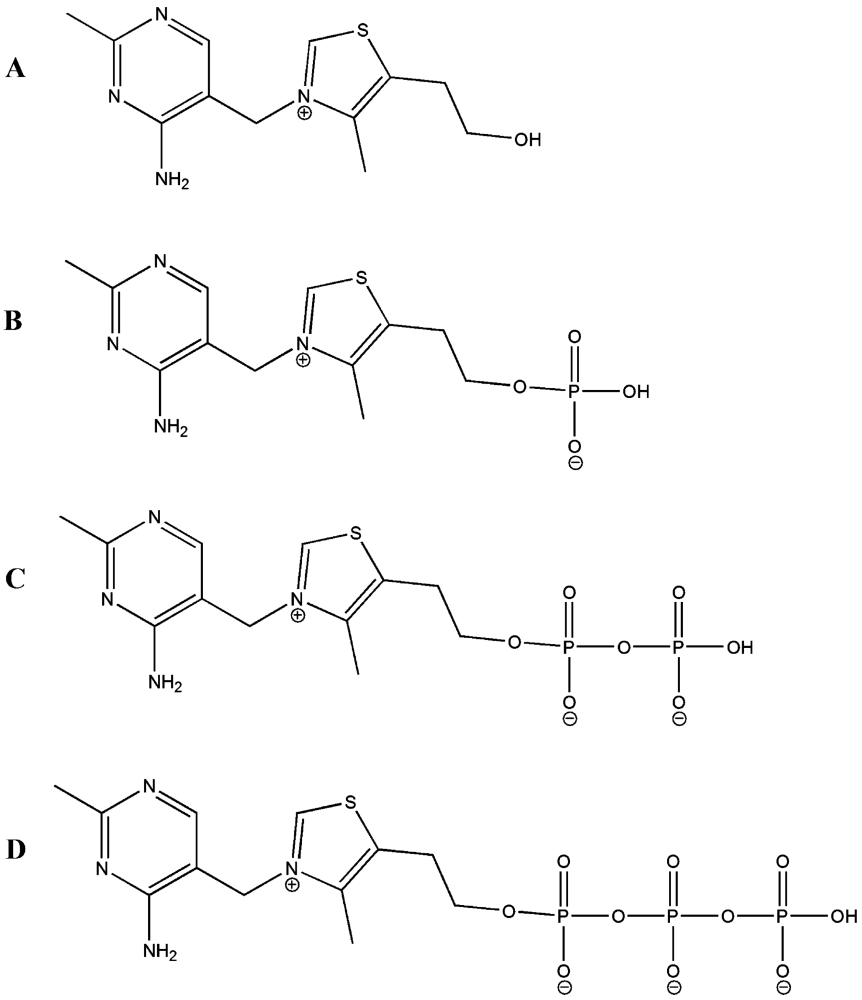

Figure 1.2: Structures of thiamine forms: (A) thiamine ion, (B) thiamine monophosphate (TMP), (C) thiamine pyrophosphate (TPP), (D) thiamine triphosphate (TTP; Alvarado et al., 2016).

1.3. Thiamine pyrophosphate in plants

1.3.1. Thiamine pyrophosphate biosynthesis in plants

Thiamine biosynthesis in plants is similar to the biosynthesis of thiamine in yeast and bacteria. Whereas the thiazole biosynthetic pathway in plants resembles that of yeast, the plant pyrimidine ring is synthesised in a similar fashion to that of bacteria (Rapala-Kozik et al., 2007). Thiazole and pyrimidine are generated in separate pathways, and subsequently, generate thiamine by coupling the two moieties (Jurgenson et al., 2009); this process occurs in several stages (Figure 1.3). The pyrimidine moiety is synthesised from the 5-aminoimidazole ribonucleotide (AIR), which is derived from 5-phosphoribosyl 1-pyrophosphate (PRPP); this is synthesised from R-5-P, which is produced from one of the Calvin cycle reactions (Senecoff and Meagher, 1993). AIR is converted into hydroxymethyl pyrimidine phosphate (HMP-P). The bacterial enzyme ThiC catalyses this reaction, and homologues of TjiC have recently been identified in tomatoes, as well as in *Arabidopsis thaliana* (Kong et al., 2008, Raschke et al., 2007). HMP-P is phosphorylated to hydroxymethyl pyrimidine diphosphate (HMP-PP), and the enzyme of this reaction is Th1; in contrast, in bacteria, it is catalysed by ThiDase (Figure 1.3) (Rapala-Kozik et al., 2007). The thiazole moiety is derived from DXP, which is synthesised from the condensation of pyruvate and glyceraldehyde 3-phosphate. The enzyme that catalyses this reaction is 1-deoxy-D-xylulose 5-phosphatesynthase (DXS) (Julliard and Douce, 1991). Further studies on bacteria by Julliard and Douce (1991) have shown that thiazole can be synthesised from glycine, cysteine and tyrosine, which are all involved in the shikimic acid pathway production.

4-Methyl-5-b-hydroxyethylthiazole phosphate (HET-P) is synthesised from nicotinamide adenine dinucleotide (NAD), glycine and a sulphur donor (L-cysteine; (Chatterjee et al., 2008, Chatterjee et al., 2007). This reaction is catalysed by HET-P synthase (Th1), which is the only enzyme involved in thiazole biosynthesis. This lends support to the claim that the thiazole biosynthetic pathway resembles that of yeast, as the homologues of yeast HET-P synthase have been identified in several plant species, namely *Zea mays* (Belanger et al., 1995), *Alnus glutinosa* (Ribeiro et al., 1996), *Arabidopsis thaliana* (Machado et al., 1996) and *Oryza sativa* (Wang et al., 2006). As Thi4 was the first thiamine biosynthetic enzyme to be found in plants, it was named Thi1 (Goyer, 2010).

Next, the pyrimidine and thiazole precursors (HMT-PP and HET-P, respectively) are condensed, producing thiamine monophosphate (TMP). The condensation reaction is catalysed by TH1, which is also responsible for the phosphorylation of HMP-P to HMP-PP (Rapala-Kozik et al., 2007). The final step in this process is the dephosphorylation of TMP to thiamine, which has recently been shown to be carried out by the enzyme TMP phosphatase encoded by TH2 (At5g32470) (Mimura et al., 2016). The location of this hydrolysis step in the cell has not been unequivocally shown; however, there is no data to support a chloroplast location, and while a dual-targeting leader sequence was identified, which suggests that both a cytosolic and mitochondrial location are possible, the evidence in planta favours a cytosolic location (Mimura et al., 2016). The free thiamine in the cytosol is then converted to TPP catalysed by thiamine pyrophosphokinase, which is known to have a cytosolic location (TPK; Figure 1.3; Ajjawi et al., 2007b) (Figure 1.3). The implication of this finding is that it is TMP, rather than thiamine, that is transported from the chloroplast to the cytosol; in addition, TPP then has to be transported to a

number of locations in the cell, including the nucleus, mitochondria and chloroplast. At this point, the only known transporters are those that facilitate the entry of TPP to the mitochondria, as no specific transporters for TMP transport from the chloroplast or TPP transport to the chloroplast have been identified. The mitochondrial TPP transporters identified to date belong to the MCF, and it is likely that the chloroplastic TMP or TPP carriers are also members of this family. It is likely that MCF proteins function as antiporters in order to link the mitochondrial matrix and cytosolic pathways (i.e. the ADP/ATP and dicarboxylate-tricarboxylate carriers). The transportation activity differs depending on the proton-motive force, whether it is electroneutral or electrophoretic and whether the ΔpH pathways are dependent or independent (Monné and Palmieri, 2014). Therefore, it is probable that TMP and TPP utilise antiporters to move the TMP from the chloroplast to the cytosol and to transport the TPP from the cytosol to the chloroplast.

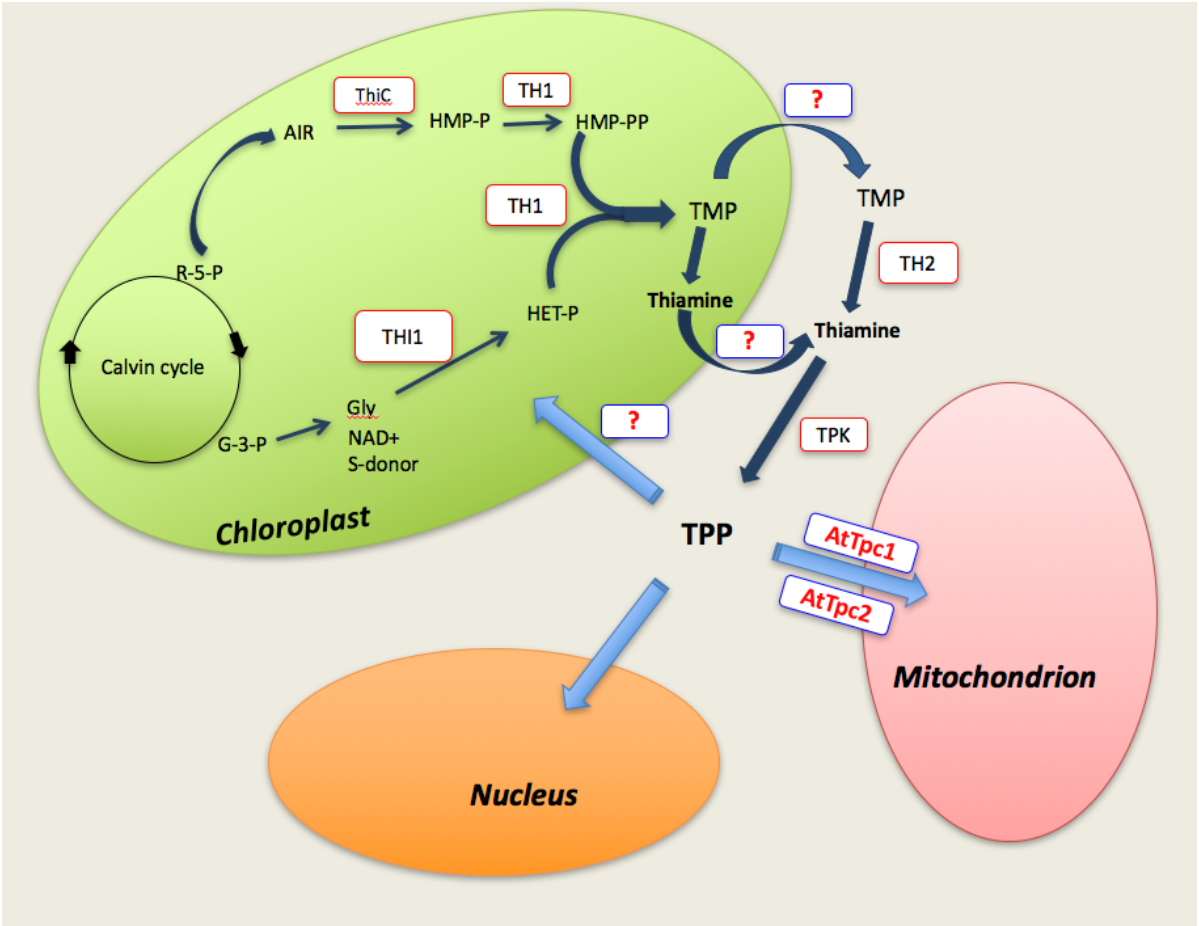

Figure 1.3: Thiamine biosynthetic pathway in plants. The scheme shows the thiamine pyrophosphate (TPP) pathway in plants. The pyrimidine moiety is synthesised from ribose-5-phosphate **(R-5-P)**, which is produced from the Calvin cycle to generate 5-aminoimidazole ribonucleotide (**AIR).** AIR is converted into hydroxymethyl pyrimidine phosphate **(HMP-P)** by the ThiC enzyme **(ThiC).** The hydroxymethyl pyrimidine phosphate is phosphorylated to hydroxymethyl pyrimidine diphosphate **(HMP-PP)** by the TH1 enzyme **(TH1).** The thiazole moiety is synthesised on a separate pathway from one of the Calvin cycle products, glyceraldehyde 3-phosphate **(G-3-P)**, which produces 4-methyl-5-b-hydroxyethylthiazole phosphate **(HET-P)** from glycine **(Gly),** nicotinamide adenine dinucleotide **(NAD^+)** and a sulphur donor **(S-donor)** via HET-P synthase **(THI1).** Thiazole and pyrimidine are combined to generate thiamine monophosphate **(TMP)** which hydrolyse in chloroplast or cytosol to form thiamine by TMPase. Finally, thiamine is converted to thiamine pyrophosphate **(TPP)** by thiamine pyrophosphokinase **(TPK)**. The responsible enzymes are shown in red (adapted from Rapala-Kozik et al., 2012).

1.3.2. Regulation of thiamine biosynthesis in plants

There is tight regulation of thiamine biosynthesis in plants, which implies that it is important to control the flow of metabolic intermediates to this pathway. There are several recognised mechanisms for the regulation of thiamine biosynthetic proteins, including gene regulation (the riboswitch mechanism) and post-translational regulation.

1.3.2.1. The Thi-box riboswitch

The Thi-box riboswitch is a widely recognised process of conformational changes within the bacterial messenger RNA (mRNA) molecules that affect the expression of gene-encoding proteins involved in the biosynthesis of the respective riboswitch substrate metabolites. For example, a riboswitch has been recognised as a regulatory mechanism in the expression of biosynthetic genes for amino acids, nucleotides and vitamins. This riboswitch has mostly been studied in bacteria, and interestingly, the TPP-sensing riboswitch is the only riboswitch found in eukaryotes (Wachter et al., 2007, Croft et al., 2007, Bocobza et al., 2007).

A TPP-sensing riboswitch has been detected in the 3' untranslated region (3'UTR) of the pyrimidine biosynthetic gene, ThiC, in many plant species (Bocobza et al., 2007). The ThiC precursor transcript can be processed into two alternative variants – an intron-retaining form and one in which the intron has been spliced out – depending on whether the second intron of the 3'UTR is retained (Goyer, 2010). These different forms of the ThiC transcript respond to changes in thiamine levels in different ways, with unchanged expression of the precursor transcript, decreased expression of the transcript in which the intron has been retained and increased expression of the intron-spliced variant (Goyer, 2010).

It has been suggested that TPP regulates the processing of the 3'UTR of the ThiC precursor transcript. More importantly, it has been found the total number of ThiC transcripts decreases in the presence of thiamine, and experiments using transgenic *A. thaliana* plants and protoplasts have revealed that TPP binding to a riboswitch is necessary for this feedback control of ThiC expression (Bocobza et al., 2007; Wachter et al., 2007). The binding of TPP to riboswitches requires the presence of Mg^{2+} ions, and it is characterised by a relatively high affinity, suggesting a precise recognition of the pyrimidine ring, as well as the diphosphate group of TPP.

Wachter et al. (2007) proposed a unified mechanism for the TPP-sensing riboswitch. They suggested that when the levels of TPP are low, the riboswitch interacts with a 5' splice site within the 3'UTR, a process that ultimately inhibits splicing. The retained intron allows specific processing of the precursor transcript, including transcript cleavage and polyadenylation, generating the intron-retaining version of the ThiC transcript; this leads to clear expression of the ThiC gene. At high levels of TPP, its extremely specific binding to the riboswitch element exposes the 5' splice site, leading to the generation of the intron-spliced version of the ThiC transcript, and this is characterised by a much higher decay rate (Wachter et al., 2007). Thus, the specific and high-affinity binding of TPP to the riboswitch within the 3'UTR of the ThiC gene triggers allosteric rearrangement within the mRNA structure, leading to a modification in gene expression and translation.

1.3.2.2. Post-translational regulation of thiamine biosynthetic proteins

Several plant thiamine biosynthetic proteins are regulated at the post-translational level. ThiC and Thi1 contain nine and three conserved cysteines,

respectively, which serve as potential targets for chloroplastic thioredoxins. It has been postulated that thioredoxins could influence the activity of these thiamine biosynthesis enzymes, possibly affecting their oxidative regulation, assembly and folding. Moreover, the ThiC enzyme contains an iron-sulphur cluster that has been suggested to facilitate the stability of the protein; its reduction could activate the enzyme (Raschke et al., 2007). Finally, recombinant HMP-kinase/TMP-synthase from *Zea mays* (Thi3) is uncompetitively inhibited by the presence of excess levels of either HMP-PP or ATP substrate (Rapala-Kozik et al., 2007).

1.4. Transporters in plants

It is known that cells have complex metabolic networks and contain several compartments, including the vacuole, peroxisomes, Golgi, endoplasmic reticulum (ER) and plastids, as well as mitochondrial organelles. All of these compartments are embedded in the cytosol and are surrounded by at least one membrane to prevent the uncontrolled exchange of intermediates. Many enzymatic reactions occur in these compartments, so each subcellular space requires specific substrates and enzymes that are obtained from the metabolic network. The transport of substrates from one part of a cell to another depends on providing various subcellular pH environments to allow for the counter-exchange operation of pathways to compete for the same substrates (Linka and Weber, 2010).

Frequently, metabolic pathways rely on the supplements of metabolic precursors and transfer them through several compartmental boundaries. This means that specific transporters are required to control and regulate the export and import of metabolites across organelle membranes. As a result, the metabolic transport of proteins is an important and essential component for connecting the cellular metabolic pathways of the cellular compartments and organelles (Lunn, 2007, Schwacke et al., 2004).

In the model plant species, *Arabidopsis thaliana,* it is estimated that there are 2705 proteins and that these transporter proteins comprise 10% of all *Arabidopsis thaliana* proteins (Linka and Weber, 2010). A complement of yeast mutations was successfully used to identify many of the plant transport proteins by various deficient transporters or metabolic functions (Frommer and Ninnemann, 1995). In recent years, good progress has been made on transporters, with a model structure of

membrane proteins consisting of hydrophobic domains and hydrophobic loops or termini. These hydrophobic domains include amphipathic α-helices or β-barrels that pass across or dip into the hydrophobic membrane lipid bilayer (Linka and Weber, 2010).

It is known that in plants, most proteins are encoded by genes located in the nucleus; the mRNA is transported to the cytosol where it is translated and expressed in the cytosol as precursor proteins. Precursor proteins carry the N-terminal targeting signal, which functions as a ticket to facilitate proteins reaching their final destination. There are different N-terminal targeting signal sequences in different organelles, and these signal sequences are called 'transit peptides' for plastids, 'presequences' for mitochondria and 'signal peptides' for the ER (Li and Chiu, 2010).

1.4.1. Thiamine transporters in plants

The thiamine biosynthetic journey starts in the chloroplast and moves to the cytosol. Then, an active form of thiamine (TPP) is moved back to the chloroplast and imported into the mitochondria to work as a cofactor in enzymatic reactions (Figure 1.3).

As mentioned above, TMP is generated in the chloroplast, and the dephosphorylation of TMP to thiamine is catalysed by a newly identified TMP phosphatase enzyme (Mimura et al., 2016; Ajjawi et al., 2007; Raschke et al., 2007; Belanger et al., 1995).

TPK, the enzyme responsible for converting thiamine to TPP, appears solely in the cytosol (Ajjawi et al., 2007a). Thus, TPP has to be imported to the

chloroplasts and mitochondria, because both of them contain TPP-dependent enzymes (Ajjawi et al., 2007a; Rapala-Kozik et al., 2008; Goyer, 2010). This also occurs in mammals and yeast, where mitochondria must import TPP from the cytosol because TPK is cytosolic (Marobbio et al., 2002, Barile et al., 1990). TPP mitochondrial transporters have been identified in humans, *Drosophila* and yeast (Tpc, DmTpc1p and Tpc1p, respectively) These transporters refer to the mitochondrial carrier family (MCF) (Marobbio et al., 2002; Lindhurst et al., 2006; Iacopetta et al., 2010). The mitochondrial carrier family (MCF)

The MCF is a group of eukaryotic proteins located in the mitochondrial membrane, peroxisome and the chloroplast membrane (Millar and Heazlewood, 2003). MCF proteins have been shown to exist in animals, yeast and plants (Palmieri, 2004, Picault et al., 2004, Kaplan, 2001, Palmieri et al., 2000, Belenkiy et al., 2000, Palmieri, 1994). Early studies on non-plant mitochondrial carriers showed that each protein had a tripartite structure that contained three domains and consisted of 100 amino acids. Each domain consists of two transmembrane α-helices (Palmieri, 1994; Belenkiy et al., 2000). Recently, with the advantage of more developed techniques, progress has been made in identifying many proteins with the characteristic features of mitochondrial carriers in various organisms. Thirty-five MCF proteins have been identified in *Saccharomyces cerevisiae*, and about 50 MCF carriers have been found in humans (Palmieri et al., 2000; Palmieri, 2004). In plants, screening the *Arabidopsis* genome sequence resulted in the identification of many MCF members. In the past decade, 58 putative mitochondrial carriers have been reported for *Arabidopsis* (Picault et al., 2004).

Based on a phylogenetic analysis, four candidate plant TPP transporters that show homology to known TPP transporters in various species have been identified (Frelin et al., 2012). Furthermore, these four plant proteins—two in Arabidopsis (AtTpc1 and AtTpc2) and two in maize (GRMZM2G118515 and GRMZM2G124911)—are related to the TPP MCF carriers in animals and S. cerevisiae. A functional complementation assay was conducted to investigate TPP transport activity in a yeast tpc1Δ mutant. Each of these four transporters (AtTpc1, AtTpc2, GRMZM2G118515 and GRMZM2G124911) were cloned into yeast expression vector Pyes2/CT and then transformed into a yeast tpc1Δ strain. The results showed that the four candidate plant TPP carriers were able to restore thiamine on an SM medium with galactose in the absence of Tpc1 (the yeast TPP transporter). These findings suggested the possibility that one of these proteins carried TPP into the mitochondria, while another transported it into the chloroplast. However, a study of the subcellular localisation of all four proteins (AtTpc1, AtTpc2, GRMZM2G118515 and GRMZM2G124911) showed that they are all localised in the mitochondria, which means that the chloroplast transporter is still unknown (Frelin et al., 2012). Although Frelin et al. (2012) investigated the transport activity of AtTpc1 and AtTpc2 in reconstituted liposomes, no data has yet been presented to clearly demonstrate that these putative transporters are capable of transporting TPP. The authors suggest that this is due to improper renaturation of these proteins in the liposomes. Therefore, further in vivo studies are required in order to unequivocally demonstrate the transport function of the AtTpc1 and AtTpc2 proteins.

One member of the MCF is a folate transporter in plants (AtFolt1). This is a 34-kDa protein, and it was identified in the MCF because of its structure (Palmieri, 2004). AtFolt1 is homologous to the mitochondrial folate transporters in mammalian

cells (Bedhomme et al., 2005), and it functions as a folate transporter in the Chinese hamster; in addition, it is able to take up exogenous folic acid when it is expressed in Escherichia coli. However, in plants, a localisation study using transient expression analysis of the full-length AtFolt1 protein tagged with the green fluorescent protein (YFP) and western blot analysis showed that this protein is located in the chloroplast envelope (Bedhomme et al., 2005). In addition, the disruption of Arabidopsis AtFolt1 did not affect the folate level in the chloroplast and exhibited the wild-type (WT) level (Bedhomme et al., 2005).

1.5. Location of thiamine biosynthesis and thiamine transport in plants

In *Arabidopsis* and *Zea mays*, HET-P synthase has been detected in the chloroplast (Chabregas et al., 2003, Chabregas et al., 2001, Belanger et al., 1995). With regard to pyrimidine biosynthesis, HMP-P synthase was located in the stroma (Raschke et al., 2007; Kong et al., 2008). In silico investigation has suggested that the phosphorylation of HMP-P synthase and the condensation of HMP-PP synthase and HET-P are catalysed by bifunctional enzymes in *Brassica napus* that appear in the chloroplast. Overall, HET-P, HMP-P synthase, HMP-PP synthase and bifunctional HMP-kinase are expressed in leaves, lower roots and stems (Goyer, 2010).

Subsequently, all intermediates in the thiamine biosynthetic pathway are generated inside chloroplasts, with the exception of TPP, which is made in the cytosol. This means that TMP or thiamine must be delivered from the chloroplasts to the cytosol. The transport of thiamine appears to occur not only at the subcellular level, but also between the cells and tissues of the plant, as plant roots cannot synthesise thiamine in quantities adequate for normal growth based on the thiamine delivered from the leaves. In addition, roots are capable of taking up thiamine from the medium, and exogenous free thiamine can be transported throughout plant tissues (Goyer et al., 2010).

1.6. Objectives of this study

As previously discussed, chloroplasts and mitochondria contain TPP-dependent enzymes, and TPK – which catalyses the conversion of free thiamine to TPP – is cytosolic, meaning that TPP is made in the cytosol. Chloroplasts, such as mitochondria, must import TPP. The main aims of this project are to study and determine the chloroplastic thiamine transporter(s) using plant mitochondrial transporter sequences and to determine the relative importance of the different transporters for plant growth. A further aim is to study the expression of the transporters in vivo.

The following approaches are taken to answer these aims: Phylogenetic analyses are conducted to determine the sequence homologues of mitochondrial thiamine transporters (MTT) that contain an N-terminal chloroplast transit peptide (cTP). Mutant analysis and RNAi constructs are used to study the importance of these transporters for plant growth. Furthermore, high-performance liquid chromatography (HPLC) is employed to determine the TPP content.

Chapter 2:

Materials and methods

2.1. Materials

2.1.1. Bacterial strains

One Shot® TOP10 chemically competent *E. coli* cells were purchased from the Invitrogen™ supplier (https://www.lifetechnologies.com) and used throughout the project. Regarding plant transformation, *Agrobacterium tumefaciens* strain GV 3101 was used.

2.1.2. Plasmid and expression vectors

- **pENTR/D-TOPO vector**

The pENTR/D-TOPO vector was purchased from Invitrogen™ and used to transfer a blunt end of the PCR product into the expression vector. It contains attL1 and attL2 sites to combine the entry clone with a destination vector. It contains the T7 gene as a translational enhancer and the rrnB sequence as a terminator. The origin of replication is pUC.

- **pGWB41**

The pGWB41 is one of the pGWB series used as binary vectors and obtained from Nakagawa Lab. This vector contains the 35S promoter, is tagged by the YFP gene in C–terminal and has resistance to kanamycin and hygromycin.

Table 2.1: Plasmids and bacterial strains were used in this staduies.

A. Plasmids:

Plasmid name	Cassette description
pENRE/D-TOPO	**attL1-pUC ori-Kanamycin-attL2**
pGWB41	**P35S-attR1-Cmr-ccdB-attR2-EYFP-TNOS**
AtTpc1::RNAi	**Hyg-P_{35S} – AtTpc1-intron-A. AtTpc1-T_{NOS}**
AtTpc2::RNAi	**Hyg-P_{35S} - AtTpc2-intron-A. AtTpc2-T_{NOS}**
CTT::RNAi	**Hyg-P_{35S} -CTT-intron-A. CTT -T_{NOS}**
AtFOLT1::RNAi	**Hyg-P_{35S} – AtFolt1-intron-A. AtFolt1-T_{NOS}**

B. Bacterial strains:

Bacterial type	Bacterial strain
E coli.	TOP10
Agrobacterium tumefaciens	GV 3101

2.1.3. Enzymes and antibiotics

The restriction enzymes and antibiotics used were provided in our laboratory and purchased from Invitrogen™. The digestion procedure was conducted as described by the manufacturer, using the appropriate buffer. DreamTaq, which was used for PCR analysis, was purchased from Thermo Scientific. SuperScript II RT was purchased from Invitrogen™ to generate the cDNA that was used as a template for semi-quantitative and quantitative PCR analysis. Phusion Hot start II DNA polymerase was purchased from Life Technology and used to produce a blunt-end product. The antibiotics used during this study are listed in Table 1.

Table 2.2. Antibiotics list:

Antibiotic	Stock concentration	Storage
Hygromycin	100 mg mL^{-1} in H_2O	-20 °C
Gentamycin	50 mg mL^{-1} in H_2O	-20 °C
Kanamycin	100 mg mL^{-1} in H_2O	-20 °C
Rifampicin	50 mg mL^{-1} in H_2O	-20 °C
Ampicillin	50 mg mL^{-1} in H_2O	-20 °C
Spectinomycin	100 mg mL-¹ in H²O	-20 °C

2.1.4. Primers

All primers used in this research were designed by using the Pimer3Plus server (Untergasser et al., 2007) and obtained from Sigma. The primer stock solution was 100 pmole μl^{-1} and diluted 1:10 to make the working primer solution 10 pmole μl^{-1} . The primers were stored at -20°C.

2.1.5. Plant materials

The wild-type *Arabidopsis thaliana* Col. 0 was used throughout this study, and all T-DNA mutants were obtained from the National Arabidopsis Source Centre (NASC). *Nicotiana benthamiana* were used in the transit assay. Fisons Levington F2+S soil was used for plant growth during the study.

2.2. Methods

2.2.1. Bacterial propagation

E. coli cells were allowed to grow at 37 °C overnight after appropriate antibiotics were added to either the Luria agar medium or the liquid Luria broth (LB) medium. *Agrobacterium* cells were grown at 28 °C after suitable markers were added.

2.2.2. Preparation of *Agrobacterium* competent cells

A colony of *Agrobacterium* strain GV 3101 was incubated in 10 ml of the LB medium and incubated in a shaker at 28 °C for two days. The cells were chilled on ice and centrifuged at 3,000 x g at 4 °C for 15 min. The supernatant was removed and the pellet was washed with 10 ml of ice-cold, double-sterilised water (dsH_2O), which was repeated 4 times. The pellet was resuspended in 200 µl of 10% glycerol. The 40 µl of cells were divided into 1.5-ml microcentrifuge tubes and stored at -80 °C.

2.2.3. Transformation of *E. coli* competent cells using heat shock

A total of 2–5 µl of plasmid was incubated in 50 µl of *E. coli* cells and placed on ice for 30 min. The cells were then heat shocked in a water bath at 42 °C for 30 s, and then the samples were chilled on ice for 2 min. The cells were shaken at 37 °C in a shaker for 1 hr after 200 µl of LB media were added. The samples were centrifuged in a bench-top centrifuge for 5 min at 5,000 rpm. The pellet was suspended in 150 µl of LB media. A total of 150 µl of the sample was spread on LB agar plates containing the appropriate antibiotics, and then the plates were incubated overnight at 37 °C.

2.2.4. Transformation of *Agrobacterium* competent cells using electroporation

On ice, 2–5 µl of plasmid was incubated in 50 µl of *Agrobacterium* competent cells for 20 min. The *Agrobacterium* competent cells with the expression vector containing a target were transferred into electroporation cuvettes that were pre-chilled on ice. The electroporation system (Easy ject prima EQUIBIO Limited, UK) was set up at 2,500 volts, and then the mixture was electroporated twice. Next, the cells were placed immediately on ice, after adding 200 µl of cold LB medium to resuspend the cells inside the cuvettes. The samples were incubated in a 28 °C shaker for 1.5 h, so they would grow. Next, the samples were centrifuged in a bench-top centrifuge for 5 min at 5,000 rpm. Finally, the pellet was resuspended in 150 µl of LB media. A total of 150 µl of the sample was spread on LB agar plates containing the appropriate antibiotics, and then the plates were incubated at 28 °C for two days and screened by PCR.

2.2.5. Isolation and purification of plasmid DNA

2.2.5.1. DNA purification

It is important to remove any primer dimers that could exist in a PCR product and to improve the DNA purification before sequencing or cloning. Consequently, the NucleoSpin® PCR Clean-up Column kit was used to clean up the PCR product, and it was purchased from MACHEREY-NAGEL (MN) Company. The protocol was operated as described in the manufacturer's user manual. A total of 100 µl of NT1 buffer was added to 50 µl of the PCR product and mixed well. After transferring the sample into a NucleoSpin® PCR Clean-up Column, the sample was centrifuged at

11,000 x g for 1 min to bind the DNA to the silica membrane. The flow-through was discarded, and the column was placed back into the collection tube. A total of 400 µl of NT3 buffer was loaded into the column and centrifuged again at 11,000 x g for 1 min to wash the silica membrane. The flow-through was discarded, and the centrifugation was repeated to remove the NT3 buffer completely. Finally, the column was placed into a new 1.5-ml microcentrifuge tube, and 50 µl of sterilised water was loaded directly on a silica membrane inside the column. After the incubation at room temperature for 2 min, the sample was centrifuged at 11,000 x g for 2 min to elute the DNA and stored at -20 °C.

2.2.5.2. Plasmid DNA isolation using Miniprep kit

The Thermo Scientific GeneJET Plasmid Miniprep kit was used to obtain a high-purity, quality plasmid DNA in order to be suitable for sequencing and restriction digestion. This kit was purchased from Thermo Scientific, and the procedure was conducted throughout as described in the company's protocol. A positive colony was cultured in LB media after appropriate antibiotics were added to allow bacterial growth overnight. The cells were centrifuged at 3,000 g at 25 °C for 30 min. All supernatant was removed, and the pellet was redissolved in 250 µl of resuspension solution and mixed well. The sample was transferred into a new 1.5-ml microcentrifuge tube, 250 µl of lysis solution was added, and the tube was inverted 4 to 6 times. A total of 350 µl of neutralisation solution was added, and the tube was inverted again 4 to 6 times. Next, the tube was centrifuged at 12,000 rpm in a bench-top microcentrifuge for 5 min to pellet cell debris. The supernatant was transferred to the Thermo Scientific GeneJET Spin Column and centrifuged at 12,000 rpm in a bench-top microcentrifuge for 1 min. The sample was washed by

adding 500 µl of wash solution and centrifuged at 12,000 rpm in a bench-top microcentrifuge for 1 min, and then the sample was washed again and centrifuged for 1 min. The flow-through was discarded, and the empty column was centrifuged for 1 min to remove any wash solution remaining in the column. Finally, the column was transferred into a new 1.5-ml microcentrifuge tube, 50 µl of elution buffer was added and incubated for 2 min at room temperature, and then the sample was centrifuged at 12,000 rpm for 2 min and stored at -20 °C for further use.

2.2.5.3. Restriction enzyme digestion of DNA

The DNA digestion was performed throughout by using a suitable enzyme with the recommended buffer, according to the manufacturer's instructions. The digestion reaction consisted of 1 µg of plasmid DNA, 2–5 µl of buffer and 1 µl of enzyme, and the total volume of the reaction was increased to 20 µl with pure sterile water. Then the reaction was incubated at 37 °C for 1–16 hr, depending on the enzyme activity period, as described in the manufacturer's protocol.

2.2.6. Plant genomic DNA extraction

The DNA extraction procedure was carried out as described in (Edwards et al., 1991) with some modifications. A small amount of tissue (about 10 mg) was collected from the plant, and then this tissue was ground by adding 200 µl of DNA extraction buffer (200 mM Tris-HCL pH 7.5, 250 mM EDTA, as well as 0.5% SDS). The samples were centrifuged at 13,400 rpm in a bench-top microcentrifuge for 5 min. The supernatant was transferred to a new 1.5-ml microcentrifuge and mixed 4 times with 500 µl of isopropanol. Afterwards, the DNA was precipitated by centrifugation at 13,400 rpm in a bench-top microcentrifuge for 10 min. The

supernatant was removed, and the samples were centrifuged for 10 min, as described above. The samples were air-dried at room temperature for 20 min. Finally, the pellet was suspended in 50 µl of TE buffer (Tris 10 mM, EDTA 1mM in a total volume of 100 ml). The DNA was stored at 4 °C.

2.2.7. Plant RNA extraction from seeds

Dry and imbibed seeds were ground in liquid nitrogen, and then the XT buffer (sodium borate decahydrate, 0.2 M; EGTA, 30 mM; SDS, 1%; sodium deoxycholate 1%; pH 9) and proteinase K were added to each tube, 1 ml and 44 µl, respectively. Next, all tubes were vortexed and incubated in a water bath at 42 °C for 30 min. Then each sample was divided into two tubes, and 56 µl of 2 M KCl were added; all tubes were incubated on ice for 60 min to remove debris. The supernatant was transferred to new microcentrifuge tubes and mixed with 252 µl of 8 M LiCl. The samples were incubated at -20 °C for 2 hr to precipitate the RNA and then centrifuged at 13,000 rpm at 4 °C for 20 min. Afterwards, both pellets were redissolved in 100 µl of dsH_2O. A total of 100 µl of phenol: chloroform: isomylalcoho (25:24:1) solution was added, and the sample was centrifuged at 7,550 g in a bench-top centrifuge for 10 min. The top phase was transferred into a new 1.5-ml microcentrifuge tube. To remove traces of phenol from the sample, 25:1 chloroform: isoamyl-alcohol was added and centrifuged at 7,550 g for 10 min. Then the top phase was transferred carefully into a new 1.5-ml microcentrifuge tube, and the sample was precipitated by placing it on ice for 30 min after 2.5 volume of absolute ethanol and 20 µl of 3 M sodium acetate pH 7.0 were added. Finally, the pellet was air-dried, resuspended in 30 µl of double-sterilised water and stored at -80 °C (modified from Sambrook et al., 1989).

2.2.8. Plant RNA extraction from seeds using a rapid, TRIzol®-based two-step method

The RNA extraction from seeds is quite challenging, and the advantage of the rapid, TRIzol®-based two-step method resulted in obtaining a high-quality RNA without DNase I treatment. The procedure was operated as described by (Meng and Feldman, 2010). The seeds were ground in liquid nitrogen until fine powder was produced, then 1.2 ml of EB was added immediately and mixed well by inverting. The mixture was transferred into a new 2-ml Eppendorf tube, vortexed for 5 min and then centrifuged at 11,000 g for 10 min, using a bench-top centrifuge. The supernatant was transferred into a new 2-ml Eppendorf tube, and 500 µl of chloroform was added and then vortexed for 2 min. After vortexing the sample, 0.5 volume of acid phenol was added and vortexed again for 2 min, and then the sample was centrifuged for 15 min at 11,000 g. The top phase was transferred carefully into a new 1.5-ml microcentrifuge tube, and then 90 µl of sodium acetate (pH 5.2) and 600 µl of isopropanol were added and mixed well by inverting before incubation for 10 min. After the sample was spun for 10 min at 11,000 g, the upper phase was discarded, and the pellet was washed by adding 1 ml of 75% ethanol. The sample was centrifuged for 10 min at 11,000 g, and the supernatant was discarded. The pellet was air-dried for 5 min at room temperature and resuspended in 1 ml of TRIzol® reagent. Next, the sample was vortexed immediately until the pellet was dissolved. A total of 200 µl of chloroform was added and mixed by inverting 5–10 times and then incubated for 3 min before the sample was centrifuged at 11,000 g for 15 min at 4 °C. Then the top phase was transferred into a new 1.5-ml microcentrifuge tube, and 500 µl of isopropanol was added and mixed before the sample was incubated for 10 min. When the incubation was completed,

the sample was centrifuged at 11,000 g at 4 °C for 15 min. Next, the pellet was washed by adding 1.2 ml of 75% ethanol and centrifuged at 11,000 g at 4 °C for 10 min. The supernatant was removed, and the pellet was air-dried for 10 min before it was dissolved in 100 µl of double-sterilised water. Then 10 µl of 3M sodium acetate (pH 5.2) and 200 µl of absolute ethanol were added and mixed well. After incubation for 20 min, the sample was centrifuged at 11,000 g at 4 °C for 15 min. The RNA pellet was washed with 1.2 ml of 75% ethanol and centrifuged at 11,000 g at 4 °C for 10 min. Finally, the supernatant was removed, and the pellet was air-dried for 10 min before it was dissolved in 50 µl of double-sterilised water and stored at -80 °C.

2.2.9. Plant RNA isolation using NucleoSpin® RNA kit

NucleoSpin® RNA kit was purchased from MACHEREY-NAGEL (MN) Company. The protocol was operated as described in the manufacturer's user manual The procedure was carried out with the following steps. In the presence of liquid nitrogen, 100 mg of plant leaves were ground to fine powder. Then the ground tissue was transferred into a 1.5-ml microcentrifuge tube and kept on dry ice. A total of 350 µl of buffer RP1 containing 1% ß-mercaptoethanol was added to the frozen sample and mixed well immediately. The mixture was processed through the NucleoSpin® Filter and centrifuged for 1 min at 11,000 g. Next, the NucleoSpin® Filter was discarded, and the homogenised lysate was collected in a collection tube. The sample was washed by adding 350 µL of 70% ethanol and mixed 5 times by pipetting it up and down. Then the sample was applied into a column and centrifuged for 30 s at 11,000 g to allow the RNA to bind to the column membrane. The column was placed into a new collection tube, and 350 µL of membrane desalting buffer (MDB) was added into the column and centrifuged for 1 min at

11,000 g to dry the membrane. Then the rDNase was treated by adding 95 µL of rDNase reaction mixture (90% rDNase reaction buffer, 10% rDNase) into the column and incubating it for 15 min at room temperature. After the rDNase treatment was completed, the rDNase was inactivated by adding 200 µL of RA2 buffer to the column and centrifuging it at 11,000 g for 45 s. Then the column was placed into a new collection tube, 600 µL of RA3 buffer was added, and it was centrifuged again at 11,000 g for 45 s. The column was placed into a new collection tube, washed again by adding 250 µL of RA3 buffer and centrifuged at 11,000 g for 2 min. Finally, the column was placed into a new 1.5-ml microcentrifuge tube, 50 µL of sterilised water was added, and it was centrifuged at 11,000 g for 1 min to elute the RNA. The RNA was stored at -80 °C.

2.2.10. Plant RNA extraction from leaves

The RNA producer was extracted as described by (Hilario and Mackay., 2007), with some additional steps. A total of 100 mg of tissue was ground with liquid nitrogen, collected in a 1.5-ml microcentrifuge tube and then placed on dry ice immediately. Tri reagent (1 ml) was added to isolate the RNA from the plant sample mixture, then vortexed immediately for 1 min and incubated at room temperature for 5 min. The sample was centrifuged at 12,000 g at 4 °C for 10 min to precipitate insoluble materials. The supernatant was transferred into a new 1.5-ml microcentrifuge tube, and 200 µl of chloroform was added and inverted about 20 times before incubating it at room temperature for 5 min, and then the sample was centrifuged at 12,000 g at 4 °C for 15 min to separate the phases. Next, the aqueous phase was removed carefully and transferred to a new 1.5-ml Eppendorf tube. A total of 500 µl of absolute isopropanol was added, mixed well and then incubated at room

temperature for 5 min. Then the sample was centrifuged at 12,000 g at 4 °C for 15 min to precipitate the RNA. The supernatant was poured off, and the pellet was washed with 75% ethanol and centrifuged at 12,000 g at 4 °C for 5 min. Then the supernatant was removed, and the pellet was dried by kept in air dry for 10 min. Afterwards, the pellet was redissolved in 400 µl of dsH_2O, then 400 µl of chloroform was added, and the sample was centrifuged again at 12,000 g at 4 °C for 5 min. Next, the upper phase was removed carefully and transferred to a new 1.5-ml microcentrifuge tube. The next step was the RNA precipitation, which included the addition of 30 µl of 3 M sodium acetate and 750 µl of ice-cold ethanol, and the samples were then centrifuged at 12,000 g at 4 °C for 15 min. After this, the sample was left on dry ice for 20 min. Next, the pellet was washed with 75% ethanol and centrifuged again for 5 min. Finally, the supernatant was discarded, and the pellet was redissolved in 40 µl of dsH_2O and then stored at -80 °C for further studies.

2.2.11. Agarose gel electrophoresis of nucleic acids

Agarose gel electrophoresis is a technique used to separate nucleic acid in a matrix of agarose. The Tris-Acetate-EDTA (TAE) buffer was used for the gel preparation and as the running buffer in the gel tanks. The stock concentration of TAE was 50X and diluted to a working concentration of 1X. Three gel sizes were used during this study, as follows: large (150 ml of 1% agarose), medium (100 ml of 1% agarose) and small (50 ml of 1% agarose). The gel was run at 100 volts for 40 min in the TAE buffer. For the DNA markers throughout the study, GeneRular 1kb DNA Ladder plus (purchased from Fermentas) and GeneRular Low Range DNA Ladder were used for the high and low ranges, respectively. A loading sample was between 5 µl and 20

µl, with 1 µl of loading buffer added for each 5 µl of DNA. The gel was screened by using the InGenius3 Gel Documentation system.

2.2.12. PCR reactions

2.2.12.1. Reaction mix

The PCR reaction used in normal PCR and RT-PCR analysis was as follows: the PCR totalled 20 µl, including 2 µl of DreamTaq Buffer, 2 µl of primers, 0.3 µl of dNTPs, 0.3 µl of DreamTaq, 14.4 µl of water, as well as 1 µl of DNA. The PCR reaction was run by using 2720 Thermal Cycler and Veriti 96-Well Thermal Cycler, both from Applied Biosystems Company. The reaction mix used in qPCR analysis totalled 15 µl, including 6 µl of diluted cDNA and 9 µl of SYBR® Green master mix, purchased from Life Technology Company. The qPCR reaction was run by using the CFX Connect Real-Time PCR Detection System from Bio-Rad Company.

2.2.12.2. First-strand cDNA synthesis using superscript II RT

The cDNA was generated from 1 µg of total RNA by using Invitrogen™'s SuperScript II Reverse Transcriptase kit. The experimental procedure was performed as described in the manufacturer's instructions. The cDNA was utilised as a template in qRT-PCR, with the use of suitable primers.

2.2.12.3. Amplification programmes

In all studies, the PCR cycling conditions were 95 °C for 5 min [94 °C for 5 s, 45–60 °C for 30 s, 72 °C for 1–2 min] (25–35 cycles) and 72 °C for 7 min. On the other hand, the qPCR cycling conditions were 95 °C for 2 min [95 °C for 5 s, 60 °C for 10 s, 72 °C for 5 s] (45 cycles), 65 °C for 5 s, followed by 90 °C for 5 s.

2.2.12.4. Bacterial PCR colony screening

Screening colonies by using PCR is a fast and easy approach for selecting a positive colony that contains a target of interest. A single colony was taken from a plate and dissolved in 20 µl of water; 1 µl was used as a template, and 19 µl of master mix (2 µl of DreamTaq Buffer, 2 µl of primers, 0.3 µl of dNTPs, 0.3 µl of DreamTaq, as well as 14.4 µl of water) was added, containing appropriate primers.

2.2.13. Gateway® technology

The Gateway® technology is a rapid and efficient technique to provide a way to transfer a DNA fragment into multiple-expression vectors, depending on a proprietary set of recombination of bacteriophage lambda (Landy, 1989). To use the Gateway® system, the entry clone was generated by the TOPO clone DNA fragment of interest into the pENTR/D-TOPO vector. In the TOPO cloning reaction, the PCR product was cloned by adding 4 bases (CACC) into the forward primer; these bases were linked with the overhang in the pENTR/D-TOPO vector (GTGG), and as a result, the target sequence was inserted in the correct orientation. Then the entry clone was transferred into competent *E. coli*, One Shot® TOP10. Next, the LR reaction was performed by using the Gateway® LR Clonase® II enzyme mix to recombine the entry clone into the appropriate destination vector and to generate the expression clone, which was then transferred into Arabidopsis. This method was carried out as described in Invitrogen™'s user guide for pENTR™ Directional TOPO® Cloning kits (2012).

2.2.14. Golden gate technology

The RNA-interface RNAi technique was used to inhibit a gene expression of interest. The target reign was selected from cDNAs, so a construct was designed with an antisense and sense orientation linked by an Actin intron that consisted of 515 bp, as described by (Hirai and Kodama, 2008). The designed construct was sent to Invitrogen™ for synthesis. Once the synthesis construct arrived in level-0 module, a level-1 acceptor was created by using type IIS restriction enzyme *BsaI* and NEB T4 ligase to assemble the p35S promoter, target sequence and NOS terminator in the level-1 acceptor. Then these fragments were assembled with a selection marker in the level-2 acceptor, using *BpiI* and NEB T4 ligase. Finally, the level-2 plasmid was transferred into *Agrobacterium tumefaciens* (Engler et al., 2008).

2.2.15. Plant tissue culture

All *Arabidopsis thaliana* mutant and wild-type seeds were sterilised and stored in a refrigerator at 4 °C for 2 days. Next, the plants were grown on MS media (Murashige and Skoog, Sigma) under controlled conditions at 22 °C, with 16-hr light and 8-hr dark periods. After 3 weeks, all plants were moved to the soil and used for further studies. Other plants were grown under different concentrations of TPP to study gene expression in response to TPP.

2.2.15.1. Seed sterilisation

Seeds were immersed in 75% ethanol for 2 min, using a 1.5-ml microcentrifuge tube. The ethanol was removed, and 30% bleach solution (sodium hypochlorite with one drop of Tween) was added to the seeds and incubated for 15 min. Next, the

bleach solution was removed, and the seeds were washed 4 times by double-distilled water to remove the bleach. The seeds were stored in a refrigerator at 4°C for two days for stratification to encourage uniform germination of the seeds on the media and then germinated on MS media.

2.2.15.2. Plants grown in soil

The plants transferred from the media were grown in small pots containing soil (Fison Levington F2+S compost). Then they were moved to grow under a controlled environment, with 16 h in the light period and 8 h in the dark period at 22 °C. Some plants were grown directly in the soil and incubated at 4°C for two days before being placed in a cabinet under the controlled environment described above. The plants were watered 3 times weekly with tap water.

2.2.15.3. Arabidopsis plant transformation using infiltration method

Healthy *Arabidopsis* plants were grown in the soil for long days until they flowered, and the first bolts were clipped to encourage the proliferation of many secondary bolts. After 6 days, *Agrobacterium tumefaciens* strain GV 3101 that carried a gene of interest on a destination vector was prepared by allowing it to grow in 10 ml of liquid LB culture and incubating it overnight at 28 °C. The *Agrobacterium* cells were spun at 3,000 x g at 28 °C for 25 min and were then resuspended in 5% sucrose to obtain OD = 0.5 to 0.8. After 0.02% of Silwet L-77 was added and mixed well, the plants were infiltrated by dropping 1–2 µl of *Agrobacterium* solution on the top of the flowers. The plants were covered and placed in a dark room overnight and then placed back in the growth room under the controlled condition of long days. The

plants were watered normally until the seeds matured, and then stopped. Dry seeds were harvested and collected in bags to be screened (Clough and Bent, 1997).

2.2.15.4. Transient expression assay by agroinfiltration

Transient expression assay is an alternative method of stable transformation to enable a fast analysis of gene expression. The procedure was performed as follows. One day before a binary vector was transferred into the plant leaves, 10 ml of LB culture with the Agrobacterium that had been transferred with the binary vector was incubated overnight at 28 °C and 180 rpm after the appropriate selection of antibiotics was added. The next day, the cells were pelleted by centrifuging them at room temperature at 3,000 g for 30 min. The supernatant was removed, and the pellet was resuspended in 3–10 ml of infiltration media (10 mM MES pH = 5.5, 10 mM MgCl2 and 150 µg/ml Acetosyringone). Then the absorbance was measured at 600 nm of 1 ml of cells, and the OD of the culture was calculated by multiplying the OD value by 10; the final OD600 was about 0.5 to 0.6. The cells were left for 3 hr at room temperature, and the plant was placed in a laboratory room under a white fluorescent lamp for 1 hr before infiltration to open the stomata fully. A healthy plant with large leaves was selected to obtain a high rate of transformation, as the transformation rate would depend on the viability of the plant and the Agrobacterium. The selected leaves were labelled clearly with a marker pen. Once everything was ready, 1 ml of the resuspended Agrobacterium sample was infiltrated, using a syringe without a needle. Finally, the plant was placed back in the growth room cabinet under normal conditions. After 4 days, the infiltrated zone of the leaf tissue was excised, placed on a glass microscope slide and screened (Sparkes et al., 2006).

Gene name	RNAi lines	type	The name of line
AtTpc1	5	RNAi construct	AtTpc::RNAi
AtTpc2	6	RNAi construct	AtTpc2::RNAi
CTT	3	RNAi construct	CTT::RNAi
AtFolt1	4	RNAi construct	AtFolt1::RNAi

Table 2.3a: Transporter mutants identified

Gene name	Collection insertion lines	Insertion mutant lines	identified name
AtTpc2	sail	1	AtTpc2_127
AtTpc2	GK	3	AtTpc2_GK

Table 2.3b: Insertion mutant identified.

2.2.15.5. Plant tissue storage

All plant materials used in RT-PCR and qRT-PCR were collected and placed immediately in liquid nitrogen. These materials were then stored at -80 °C. The plant materials that were used to extract genome DNA were collected, and the DNA was immediately isolated and then stored at -20 °C. Regarding the seeds, the plants were harvested, and the seeds were collected in seed bags and then stored in boxes.

2.2.16. Microscopic analysis

The sample was imaged with the use of a confocal microscope with a 63X oil-immersion objective, as described by (Wei and Wang, 2008) . The YFP was excited at 488 nm to 514 nm.

2.2.17. Bioinformatics tools

The DNA and protein sequences were obtained from The Arabidopsis Information Resource (TAIR) (https://www.arabidopsis.org/) and the Universal Protein Resource (UniProt) (http://www.uniprot.org/). ClustalW was used for sequence alignment (Larkin et al., 2007), and the TM-align server (Zhang and Skolnick, 2005) and the PyMOL Molecular Graphics System (Version 1.7.4) were used for structural. A phylogenetic tree was built by using MEGA5 (Tamura et al., 2011). Regarding the 3D structure, more than one software was used to obtain more reliable results, including the Phyre2 server (Kelley and Sternberg, 2009) and The PyMOL Molecular Graphics System (Schrödinger, 2015).

2.2.18 Thiamine extraction and measurement analysis

Thiamine was extracted,as described in (Lu and Frank, 2008) with some modifications. Leaf tissue (100 mg) was frozen in the liquid nitrogen, then crushed and homogenised in 1 ml of 0.01 M hydrochloric acid (HCl). The sample was transferred to a 1.5 ml Eppendorf™ tube and centrifuged for 15 minutes at 4 °C at 14 000 rpm. The supernatant was carefully removed and placed in a new 1.5 ml Eppendorf™ tube and stored at – 20 °C. Before measuring the TPP, the thiamine was derivatised by adding 50 µl of a freshly prepared mix of 1% potassium ferricyanide and 15% NaOH. The measurement was carried out by HPLC.

Chapter 3:

The importance of mitochondrial TPP transporters for growth in *Arabidopsis*

3.1. Introduction

TPP serves as a cofactor in universal metabolic pathways (Frank et al. (2007). In plants, thiamine is made in the chloroplasts and then transferred to the cytosol to create the active form of thiamine, which is TPP, via TPK, which appears to be exclusively cytosolic (Ajjawi et al. (2007). The mitochondria and chloroplasts must import TPP from the cytosol because both chloroplasts and mitochondria contain TPP-dependent enzymes.

The AtTpc1 and AtTpc2 proteins are members of the MCF. This is a large group of proteins located in the inner mitochondrial membrane, the chloroplast or the peroxisomes in the eukaryote (Palmieri et al., 2001; Bedhomme et al., 2005; Haferkamp, 2007; Gennaro et al., 2011; Bernhardt et al., 2012). These genes are homogenous to known mitochondrial TPP transporters in three species, namely yeast, humans and *Drosophila* (Marobbio et al., 2002; Lindhurst et al., 2006; Iacopetta et al., 2010; Frelin et al., 2012). This leads to the hypothesis that AtTpc1 and AtTpc2 may encode TPP transporter proteins. A functional complementation assay was performed on the yeast Tpc1 mutant, with the results showing that AtTpc1 and AtTpc2 restored its mitochondrial TPP level (Frelin et al., 2012). In addition, the localisation of AtTpc1 and AtTpc2 was studied, and the results showed that both targeted the mitochondria, as described by Frelin et al., (2012). However, the importance of AtTpc1 and AtTpc2 *Arabidopsis* genes in plant growth and development is as yet unknown; they may have other functions aside from encoding mitochondrial TPP carriers.

This chapter considers how both AtTpc1 and AtTpc2 were knocked out using either the T-DNA insertion or RNA interface techniques. Following this, a growth analysis experiment was performed to determine the importance of these genes for plant growth.

3.2. Results

3.2.1. Identification and characterisation of *Arabidopsis* MTT insertion lines

3.2.1.1. Identification of homozygous mutant lines of AtTpc1

To identify the mutant insertion in AtTpc1, two criteria were considered. The first was the type of insertion, which was T-DNA. The second condition was the location of the insertion, which was to be in the exon or very close to the exon. These criteria were used to choose the mutants for all genes investigated in this study.

After searching the *Arabidopsis* gene-mapping tool, the T-DNA express database (http://signal.salk.edu), identified one T-DNA mutant that met the selection standards previously explained, namely SALK_007543.49.60.x. The T-DNA SALK database reported that this mutant was located in the exon (Figure 3.1A). Plants were screened by PCR using the specific primers in a gene-specific reaction and a combination of insert-specific primers (right border) and SALK primers (left border) to identify the presence of T-DNA insertion. The PCR analysis results showed that the PCR screening failed to identify homozygous lines for T-DNA SALK_007543.49.60.x, and all screened lines appeared to be the WT (Figure 3.1).

(A)

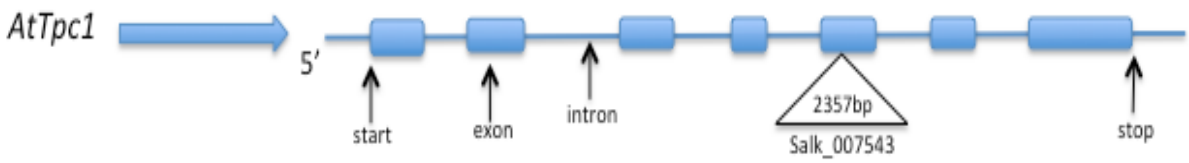

(B)

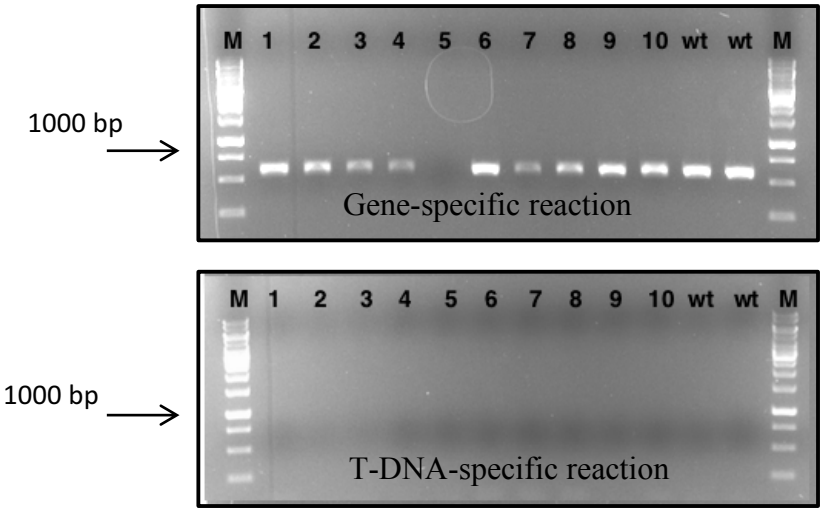

Figure 3.1: Analysis of SALK_007543 mutant in Arabidopsis AtTpc1. (A) Exon–intron structure of AtTpc1 indicating the location of SALK_007543. (B) *Arabidopsis* AtTpc1 characteristics. PCR analysis indicated plant genotypes employing primer pairs specific to the T-DNA SALK_007543 insertions in AtTPC1. The product size of SALK_007543 was 520 bp. Molecular marker (M), wild type (wt), numbers indicate the mutant lines.

3.2.1.2. Determining the homozygous mutants of AtTpc2

The SALK T-DNA and TAIR databases were searched, and two suitable AtTpc2 insertion mutants were identified according to the aforementioned criteria for the selection of T-DNA mutants. These mutants were SAIL_127_G03 and GK-870B10-026116. Homozygous plants for SAIL_127_G03 were identified by PCR using specific gene and insertion primers (see Table 3.1 for the primers used and Figure 3.2a for PCR analysis). The amplification fragment of the insertion-specific PCR reaction was sequenced to determine the specific site of the insertion. This result confirmed that the insertion was located at the fourth exon. The transcript expression level of this line was screened to determine the impact of insertion on transcript AtTpc2 expression using semi-quantitative RT-PCR analysis. The primers used in this study are shown in appendix 1. β-Actin was used as a reference for cDNA amplification. The actin primers were the forward primer, CGT CTT CCC CTC CAT CG, and the reverse primer, CTC GTT AAT GTC ACG CAC. Different cycles of amplification were used. A signal appeared in the WT samples at 25 cycles, and in contrast, a very weak signal was obtained at 35 cycles in the homozygous line (Figure 3.2c). This result was confirmed by quantitative RT-PCR analysis, by which it was seen that the transcript expression was reduced more than four times compared to the WT. Considering this result, the expression of AtTpc2 in this line appeared to be knocked out (Figure 3.2).

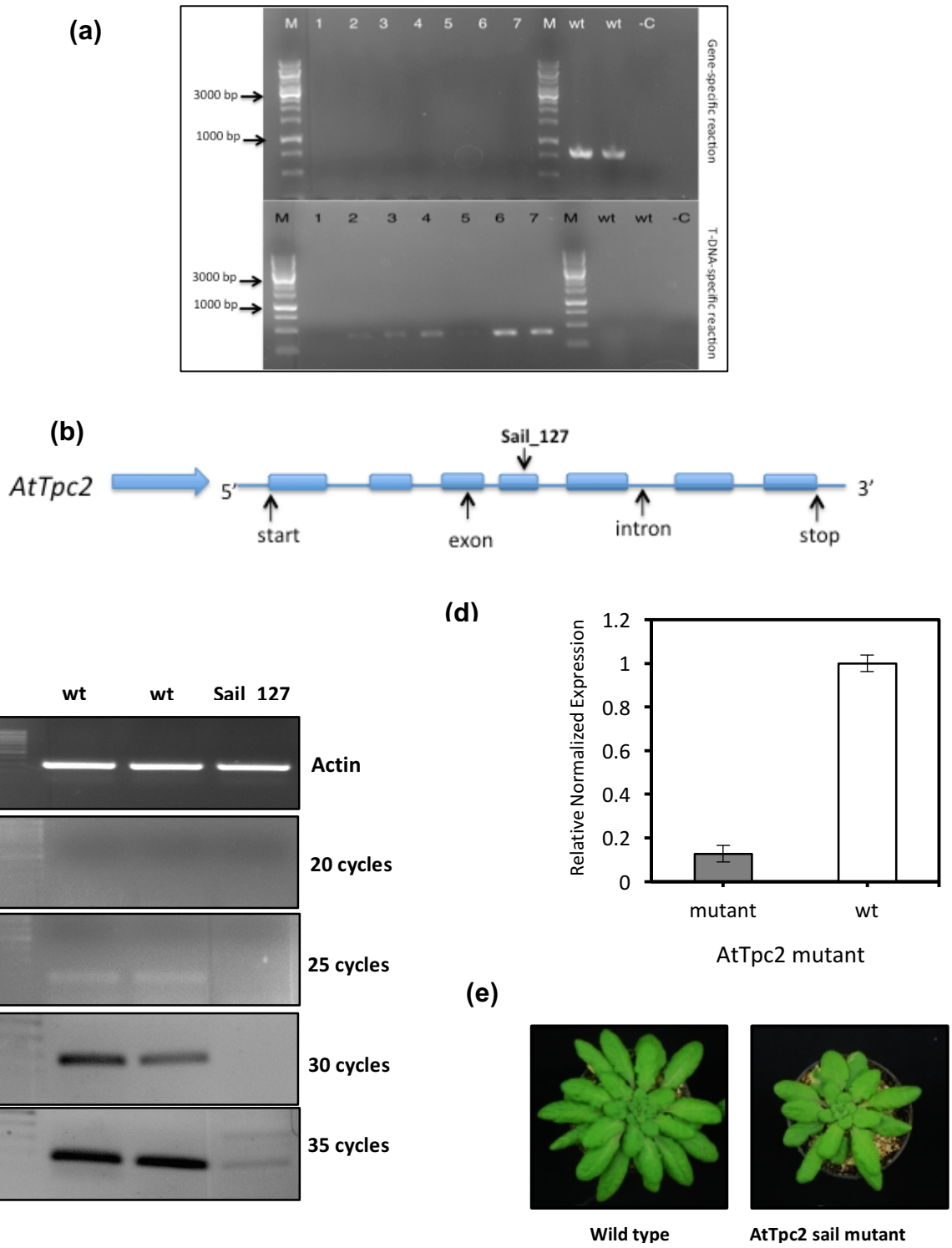

Figure 3.2: Analysis of SAIL_127_G03 mutant in *Arabidopsis* AtTpc2. (a) PCR analysis indicating plant genotypes that employ primer pairs specific to the T-DNA SAIL_127_G03 insertion. Molecular marker (M), wild type (wt), numbers indicate segregations. **(b)** Location sites of the T-DNA insertion mutant. **(c)** RT-PCR analysis: Actin was used as a control on the top, followed by a varying number of cycles to amplify the fragment of AtTpc2. **(d)** quantitative RT-PCR analysis: AtTpc2 mutant and wt samples were normalised against cyclophilin primers using the delta Ct method and showed a fold expression compared to wt values. Error bars indicate the standard deviation (SD) from three technical replicates as n = 1. **(e)** The phenotype of AtTpc2 mutant on plant growth at 7 weeks old.

The second mutant, GK-870B10-026116, was analysed by growing mutant seeds on an MS medium containing sulfadiazine, and resistant plants were clearly visible (Figure 3.3). To identify the homozygous lines for T-DNA insertion, resistant plants were screened by two PCR reactions. The first reaction was performed using specific primers to investigate the absence of GK T-DNA insertion. The second PCR reaction was performed using a combination of gene- and insert-specific primers to confirm the presence of GK T-DNA insertion (see Table 3.1 for primers and Figure 3.3 for PCR analysis). PCR amplification of homozygous lines was sequenced to determine the insertion site; the sequenced result confirmed that this insertion was placed in the second exon.

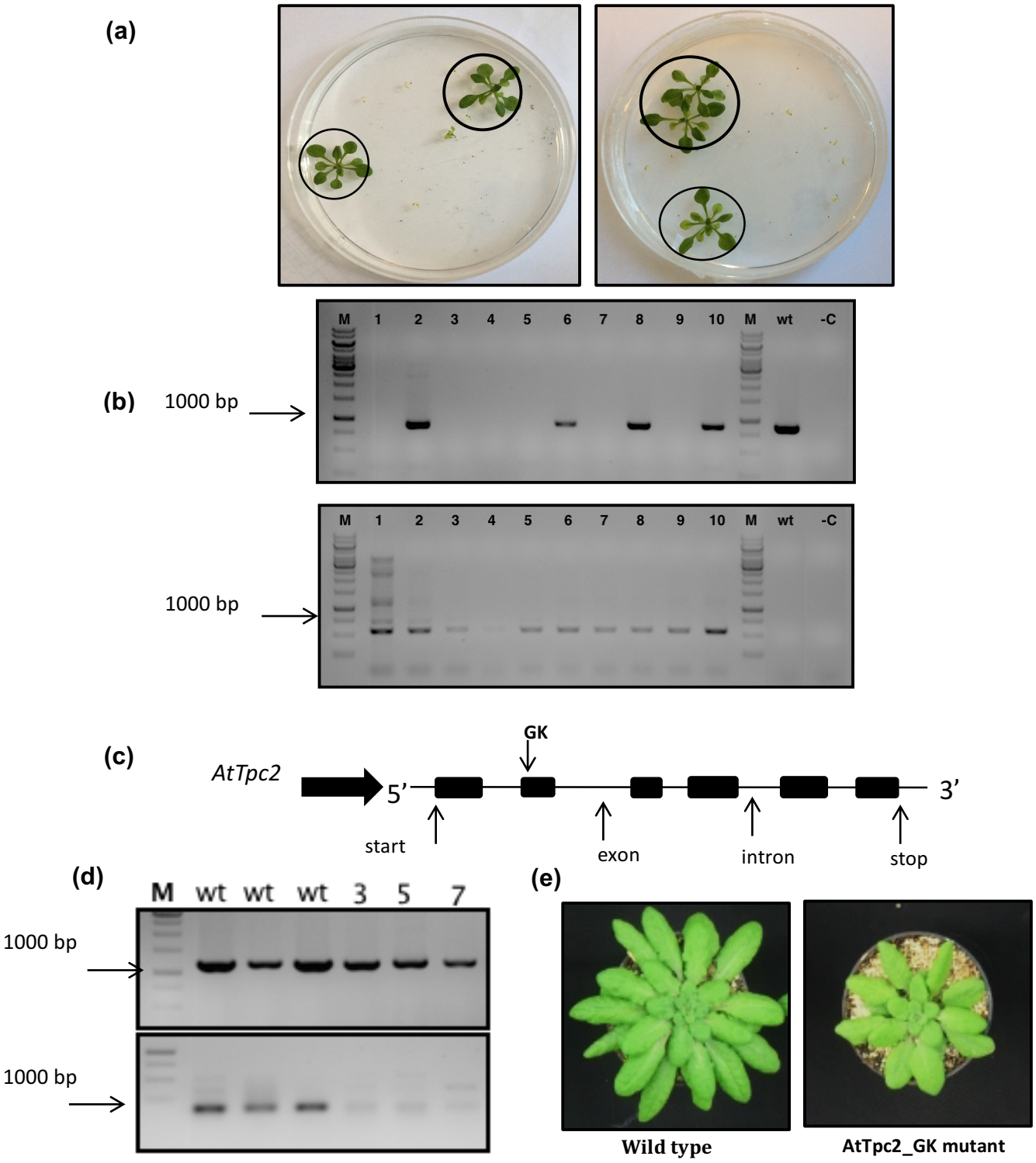

Figure 3.3: Analysis of GK-870B10-026116 mutant in *Arabidopsis* AtTpc2. (a) The sulfadiazine selection of the insertion mutant lines. **(b)** PCR analysis of sulfadiazine-resistance plants. Molecular marker (M), and wild type (wt). Numbers indicate mutant lines; homozygous lines are indicated by white numbers. **(c)** Location sites of the T-DNA GK insertion mutant. **(d)** RT-PCR of AtTpc2 mutant homozygous lines **(e)** The phenotype of AtTpc2 on plant growth at 7 weeks old.

3.2.2. Synthesis of RNAi constructs to inhibit AtTpc1 and AtTpc2

3.2.2.1. Preparation of the AtTpc1 and AtTpc2 constructs using Golden Gate cloning

Because suitable T-DNA mutants in the AtTpc1 transporter gene failed to be identified as homozygous mutant lines, the RNA interface (RNAi) technique was used as an alternative method to inhibit the AtTpc1 transporter to study the importance of AtTpc1 for plant growth. In contrast, the RNAi construct of AtTpc2 was designed to confirm the results of the AtTpc2 mutant analysis and determine the importance of AtTpc2 for plant growth.

Both RNAi constructs of AtTpc1 (AtTpc1::RNAi) and AtTpc2 AtTpc2::RNAi) were synthesised as described in Engler (2009). The target regions were selected in AtTpc1 and AtTpc2 cDNA sequences in the middle of the coding region. This selected region was in both AtTpc1 and AtTpc2, with 171 and 286 bp, respectively. The constructs were designed with antisense and sense orientation linked by an actin intron that consisted of 515 bp. Level 0 modules of both transporters were synthesised by Invitrogen. When both level 0 plasmids arrived, they were transferred into *E. coli* and plated on selective plates. A DNA concentration of 100 ng/µl was prepared for each assembly piece. Thus, the reaction mixture was set up separately for each construct. The reaction mixture included 100 ng of each the following: linearised vector level 1 backbone, p35S promoter, NOS terminator and the target sequence. Following this, 1 µl of each restriction enzyme – BsaI and NEB T4 ligase – was added to the reaction mixture with 1.5 µl of 10X NEB as a buffer. These restriction enzymes were used to assemble the p35S promoter, target sequence and NOS terminator to produce the level 1 acceptor. After adding dH_2O,

the total volume of the reaction was 15 µl. Once the preparation of the reaction was completed, the reaction assembly was performed in a thermocycler under the following conditions: 3 min at 37 °C and 4 min at 16 °C for 25 cycles, followed by 5 min at 50 °C and 5 min at 80 °C for one cycle. Then, 1–2 µl of the assembled reaction product was transferred into E. coli–competent cells and plated on an LB plate containing ampicillin, isopropyl β-D-1-thiogalactoside (IPTG) and 5-bromo-4-chloro-3-indolyl-β-D-galactopyranoside (X-gal). The positive colonies were selected by blue–white screening and checked by PCR using scr_pL1M_R primers. Finally, the level 1 modules of AtTpc1 and AtTpc2 were ready.

The reaction mixture of the level 2 module was set up as performed in level 1, with the linearised vector level 2 backbone used as an acceptor. The restriction enzyme in this reaction was the Bpil enzyme, and a 100 ng Hyg piece was added. The total volume was 15 µl, and the PCR conditions were performed as in the level 1 assembly reaction. The assembled reaction product was transferred into *E. coli*–competent cells and plated on an LB plate containing Kan as a selection marker. The positive colonies of each construct were identified by PCR and checked by the digestion enzyme HindIII to ensure that the insert was present. Finally, plasmids of each construct were transferred into *Agrobacterium* and then into plants (Figures 3.4, 3.5 and 3.6).

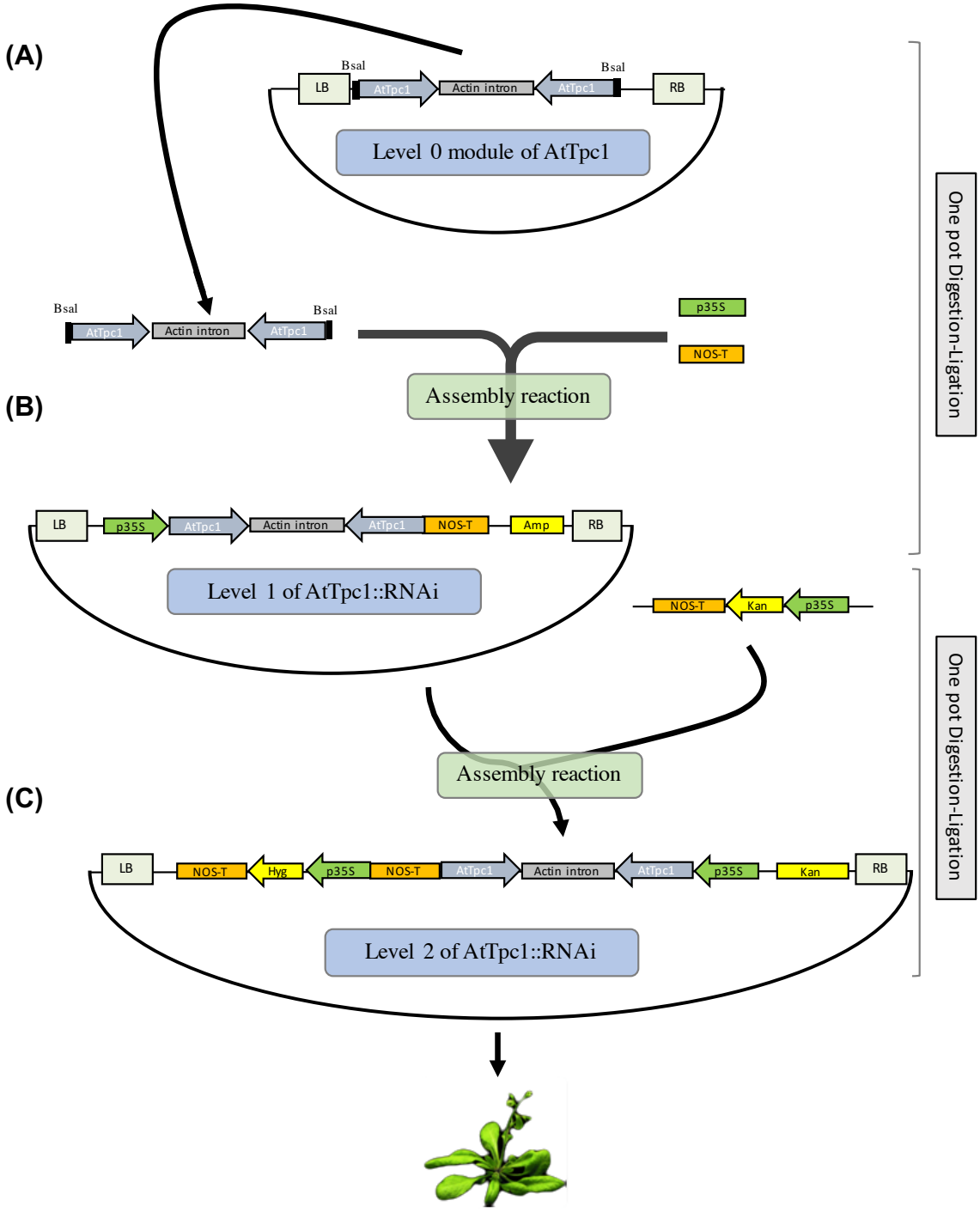

Figure 3.4: Scheme of designing the AtTpc1::RNAi construct for knocking out AtTpc1 in Arabidopsis. (A) Level 0 plasmid containing the actin intron between the target of antisense and sense orientation of the AtTpc1 coding sequence (AtTpc1), **(B)** which was digested and ligated with the 35S promoter (p35S) and NOS terminator (NOS-T) in one assembly reaction to generate the level 1 module of the AtTpc1::RNAi construct. **(C)** 35S::AtTpc1::intron::A.AtTpc1::NOS was digested from the level 1 plasmid and cloned into the level 2 vector with NOS-T::Hyg::p35S in one digestion–ligation reaction to generate the expression vector of AtTpc1::RNAi.

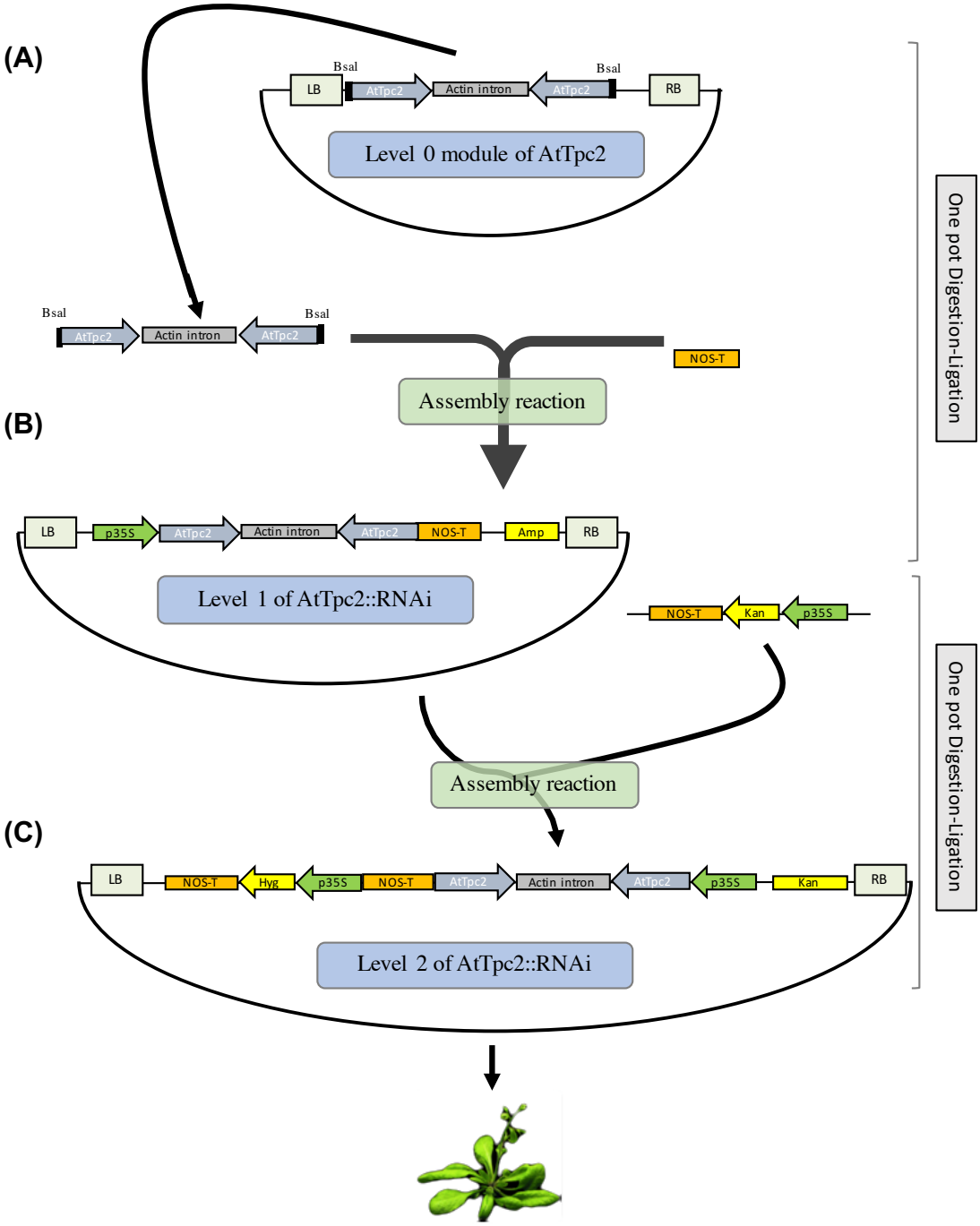

Figure 3.5: Building the AtTpc2::RNAi construct for knocking out AtTpc2 in plants. (A) Level 0 backbone containing the target region of antisense and sense orientation of AtTpc2 coding sequence (AtTpc2) linked by the actin intron. AtTpc2::intron::A.AtTpc2 were digested and ligated with the 35S promoter (p35S) and NOS terminator (NOS-T) in the level 1 backbone vector. The level 1 plasmid carry ampicillin resistance gene was identified as a selectable marker in bacteria. **(C)** 35S::AtTpc2::intron::A.AtTpc2::NOS and NOS-T::Hyg::p35S were cloned into the level 2 vector in one digestion–ligation reaction to generate the expression vector of AtTpc2::RNAi, which was transferred into plants.

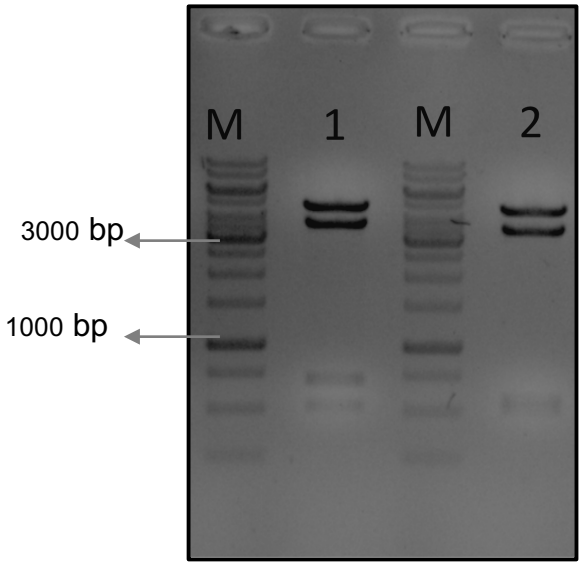

Figure 3.6: Screening level 2 of AtTpc1:RNAi and AtTpc2:RNAi by restriction digestion. Both constructs were digested using the *HindIII* enzyme. **(M)** marker, **(1)** digestion of AtTpc1, **(2)** digestion of AtTpc2.

3.2.2.2. Screening transgenic plants of AtTpc1::RNAi and AtTpc2::RNAi

To identify the transgenic plants of AtTpc1 and AtTpc2, T1 seeds of both plants were collected separately and sown on LB plates containing 10% hygromycin. The plates were incubated in a growth room under controlled conditions in a long-day chamber (16 h light, 8 h dark, 25 °C) for 2 weeks. Then, five AtTpc1 plants and six AtTpc2 plants resistant to hygromycin were transferred to soil. Following this, the selected plants were left in the growth room under the same controlled environment and watered regularly. Once the plants reached 4–5 weeks old, samples were collected to extract RNA and screen transcript expression level. The transcript expression of AtTpc1 and AtTpc2 was determined by qRT-PCR using suitable primers (see the appendix for primer sequences). The qRT-PCR results showed that the expressions of the majority of AtTpc1 lines were reduced by fourfold compared to AtTpc1 expression level in the WT (Figure 3.7), whereas AtTpc2 expression levels decreased more than 50% in transgenic lines (Figure 3.8).

The seeds of all T1 plants were collected and stored in the dark for 2 weeks before growing for further studies. Two independent lines of AtTpc1 and AtTpc2 T1 generations were grown directly in soil to study their importance in terms of plant growth.

(A)

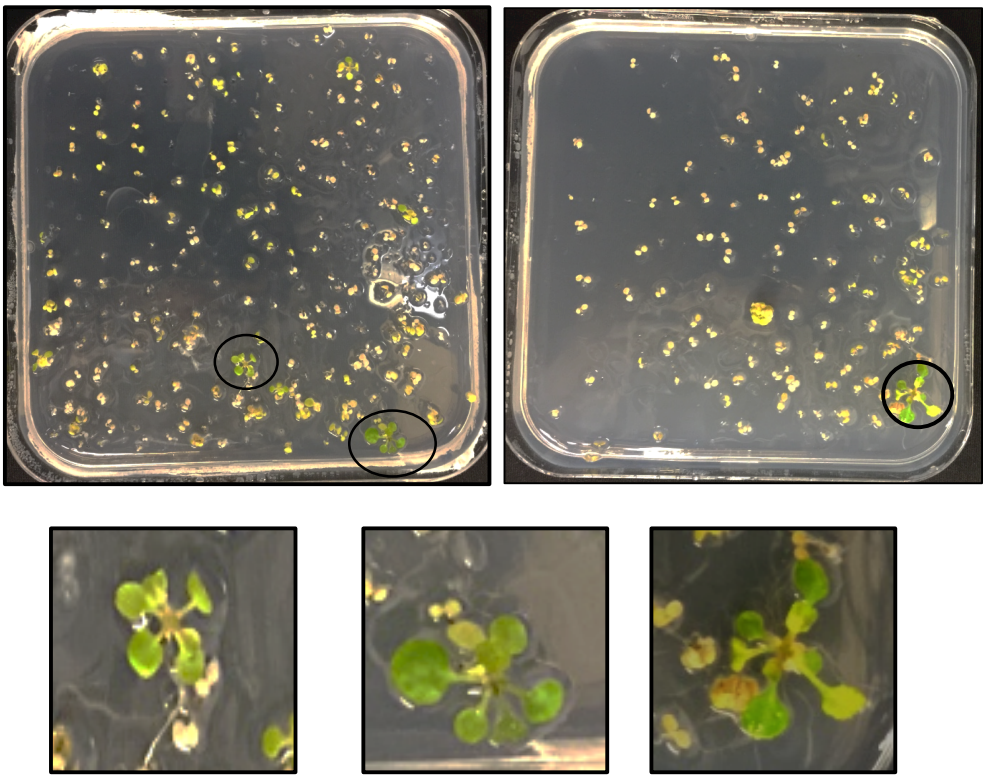

(B)

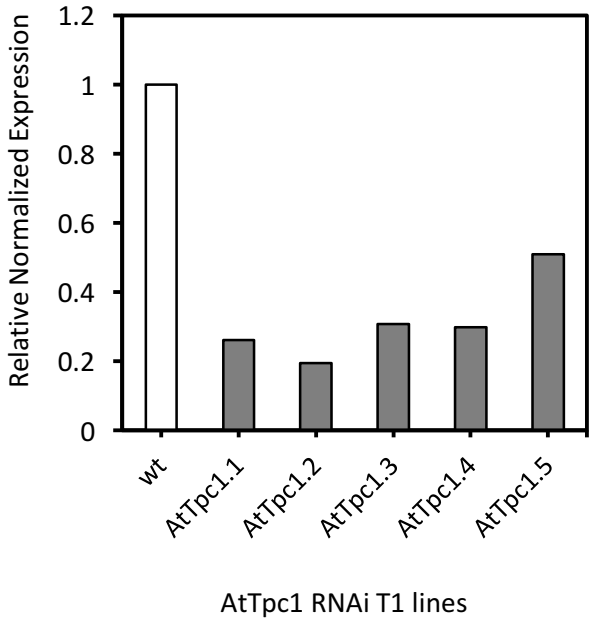

Figure 3.7: T1 screening of AtTpc1::RNAi plants. T1 plants were grown on selection plates with hygromycin and kept in long-day chambers to allow growth for 2 weeks before moving to soil. (**A)** Only five plants were resistant to hygromycin, and **(B)** the transcript expression was screened by qPCR. Expression levels were normalized against a reference gene (cyclophilin).

(A)

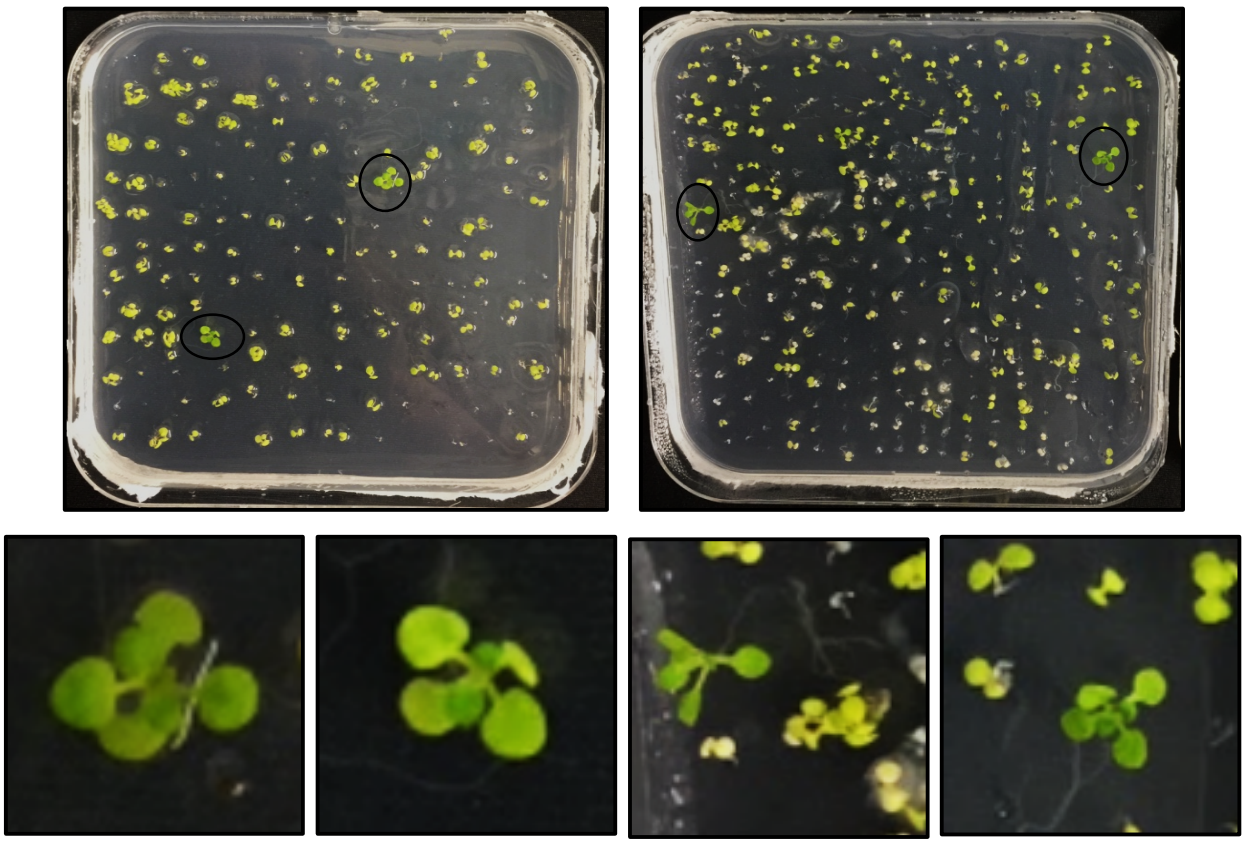

(B)

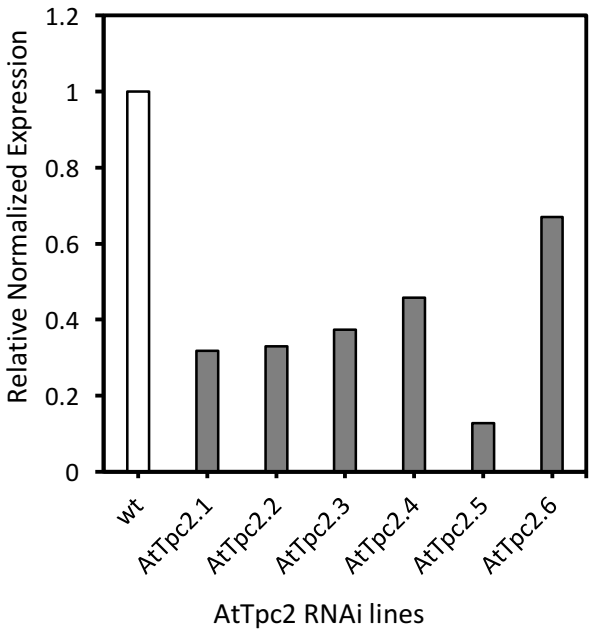

Figure 3.8: T1 screening of AtTpc2::RNAi plants. T1 plants were grown on selection plates with hygromycin and kept in a long-day chamber to allow growth for 2 weeks before moving to soil. **(A)** Six plants were resistant to hygromycin, and the transcript expression of AtTpc2::RNAi plants were screened by qPCR **(B)**. Expression levels were normalized against cyclophilin.

3.2.3. Growth analysis of mitochondrial TPP transporters (AtTpc1 and AtTpc2)

3.2.3.1. The importance of AtTpc1 in Arabidopsis growth

To study the importance of AtTpc1 in *Arabidopsis thaliana* growth, the two lowest expression lines (line 1 and line 2) of AtTpc1::RNAi were selected in T1. This experiment was set up on the Col_0 WT and the second generation of knockdown plants of AtTpc1 (T2 plants). These lines were grown directly on soil with triplicates of 10 plants. Seeds were allowed to grow under normal environmental conditions using a short day (8 h light, 16 h dark, 22 °C), and the measurement of the leaf area was initiated when the first four leaves were completely grown. The results from the measurements showed that the effect of the knockdown of AtTpc1 on the length of the main stem was limited and significant. The AtTpc1 plants were shorter than the WT; they were about 19 cm in line 1 and about 21 cm in line 2, whereas the WT plants were about 25 cm. The leaf area was slightly smaller than the that of the WT, but the difference was not significant. Not only was the leaf area not affected significantly, but the numbers of secondary stems and roots were also unaffected (Figures 3.9, 3.10, 3.11 and 3.12). These observations suggest that AtTpc1 has a limited effect on *Arabidopsis* growth, but it is important for plant growth, at least under normal conditions.

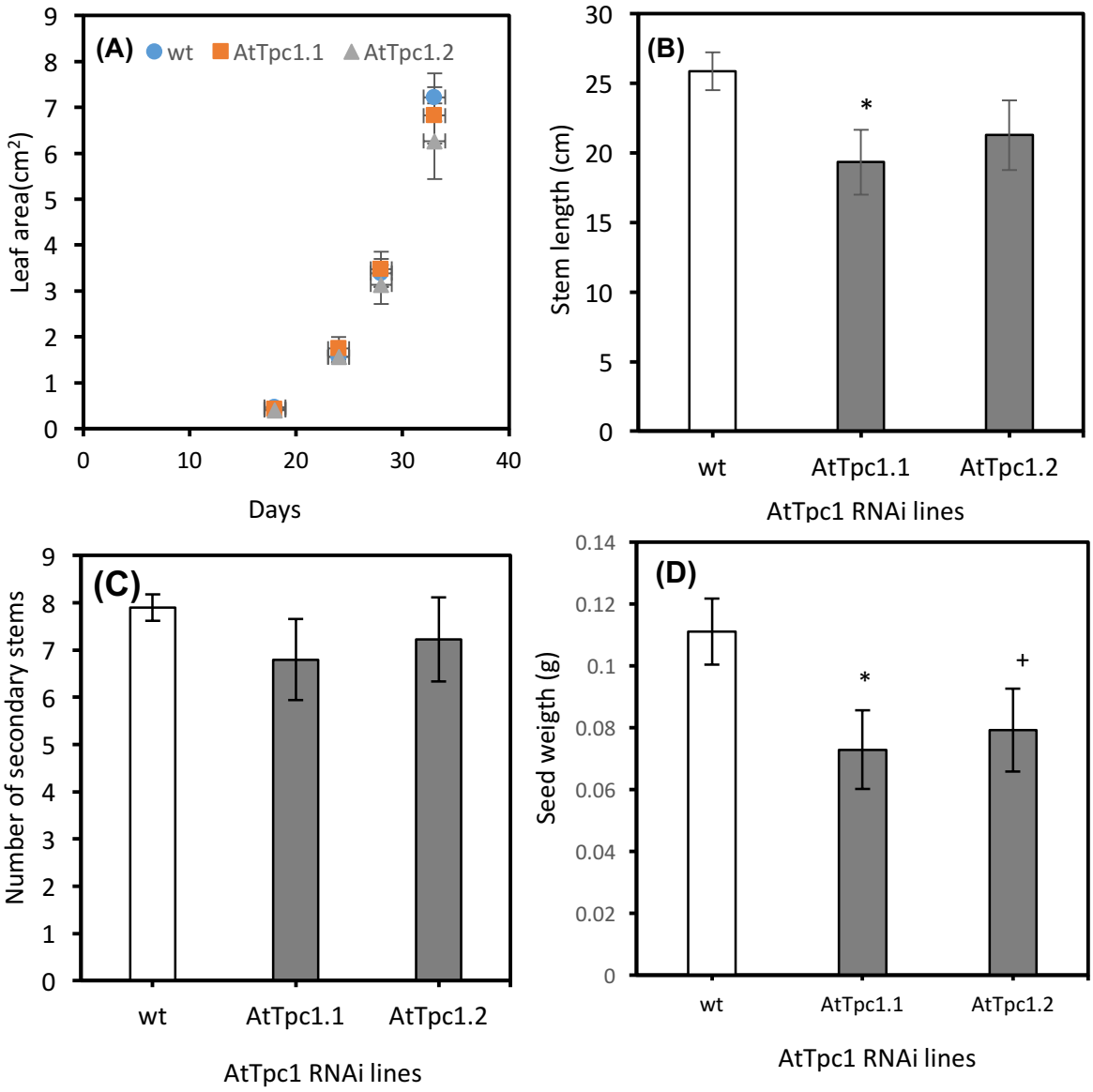

Figure 3.9: Growth analysis of the AtTpc1::RNAi and wild-type (WT) plants. Plants were grown directly in soil under a controlled environment in a short-day growth room. **(A)** The leaf area in two independent AtTpc1 RNAi lines. **(B)** The length of the main stem of the two independent AtTpc1 RNAi lines. **(C)** The number of secondary stems of the individual lines. **(D)** Seed weight from two AtTpc1 RNAi lines. Error bars indicate the standard error (SE) from 10 replicates. Significant changes to the WT were determined by one-way analysis of variance (ANOVA) for $p < 0.05$ and are indicated by an asterisk.

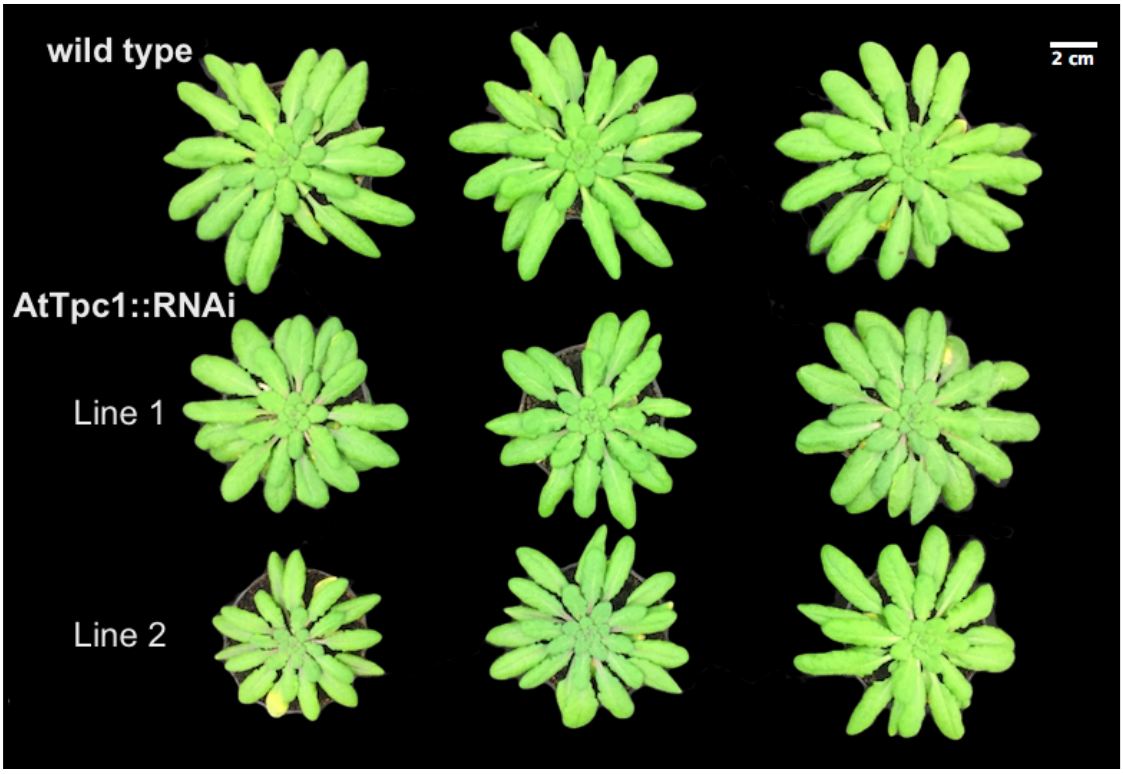

Figure 3.10: Phenotype of *Arabidopsis* AtTpc1. Plants were grown directly in soil under a controlled environment in short-day growth room (8 h light, 16 h dark, 22 °C). Wild-type plants (wt) are shown on the top, and two AtTpc1 independent lines are shown in the middle and on the bottom. Photos were taken when the plants were 53 days old.

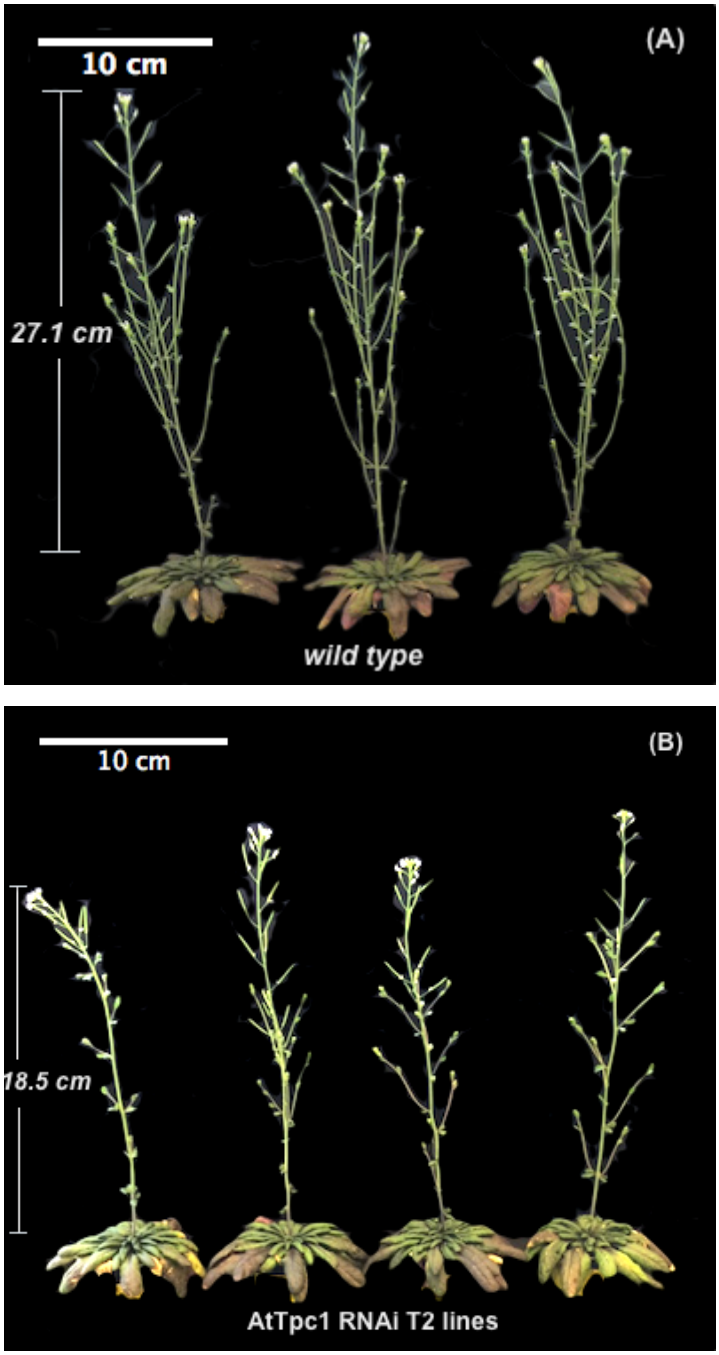

Figure 3.11: Comparison of the length of the main stem and the number of secondary stems between the wild type (WT) and the AtTpc1 RNAi plants. Both plants were grown directly in soil under a controlled environment in a short-day growth room (8 h light, 16 h dark, 22 °C). (A) wild type and (B) AtTpc1 RNAi lines.

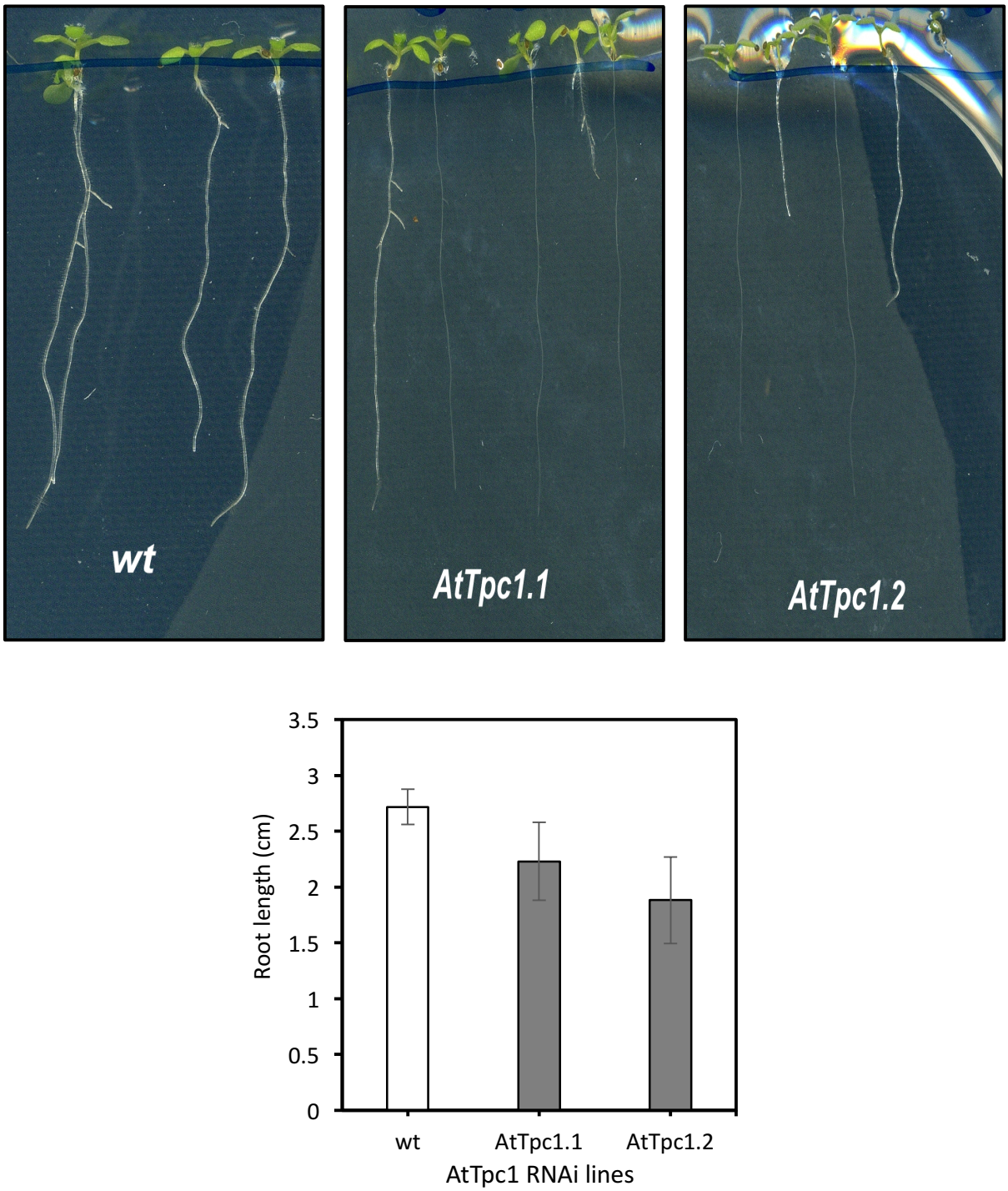

Figure 3.12: Comparison between the root length of AtTpc1 RNAi and the wild type (WT). Seeds were sterilised and planted at 4 °C for 2 days. Then, they were grown on half MS medium and allowed to grow in a long-day growth room. The photos were taken at 9 days. Measurements were carried out using the ImageJ program. The bar charts represent the root length at 9 days. Error bars indicate the standard error (SE) from 4–5 replicates. Significant changes to the WT were determined by one-way analysis of variance (ANOVA) for $p < 0.05$ and indicated by an asterisk.

3.2.3.2. The importance of AtTpc2 in *Arabidopsis* growth

To study the importance of AtTpc2 for plant growth, a new experiment was set up with two independent lines (line 2 and line 5) of AtTpc2 RNAi T1 plants and the WT. These lines were grown directly in soil with triplicates of 10 plants. Seeds were allowed to grow under normal environmental conditions under a short day (8 h light, 16 h dark, 22 °C). The measurement of the leaf area was initiated when the first four leaves were completely grown. The results showed that the leaf area average was 6.27 cm^2 in the AtTpc2 lines and 7.22 cm^2 in the WT when the plants reached 33 days. In the construct, the AtTpc2 plant length was 15.85 cm, whereas the length of the WT was about 25 cm. In addition, there were fewer secondary stems on the AtTpc2's main stem than there were in the WT, but the difference was not significant. From these results, the absence of AtTpc2 affected the leaf area and the length of main stem (Figures from 3.13 to 3.15). These data confirm that AtTpc2 affected plant growth under normal growth conditions.

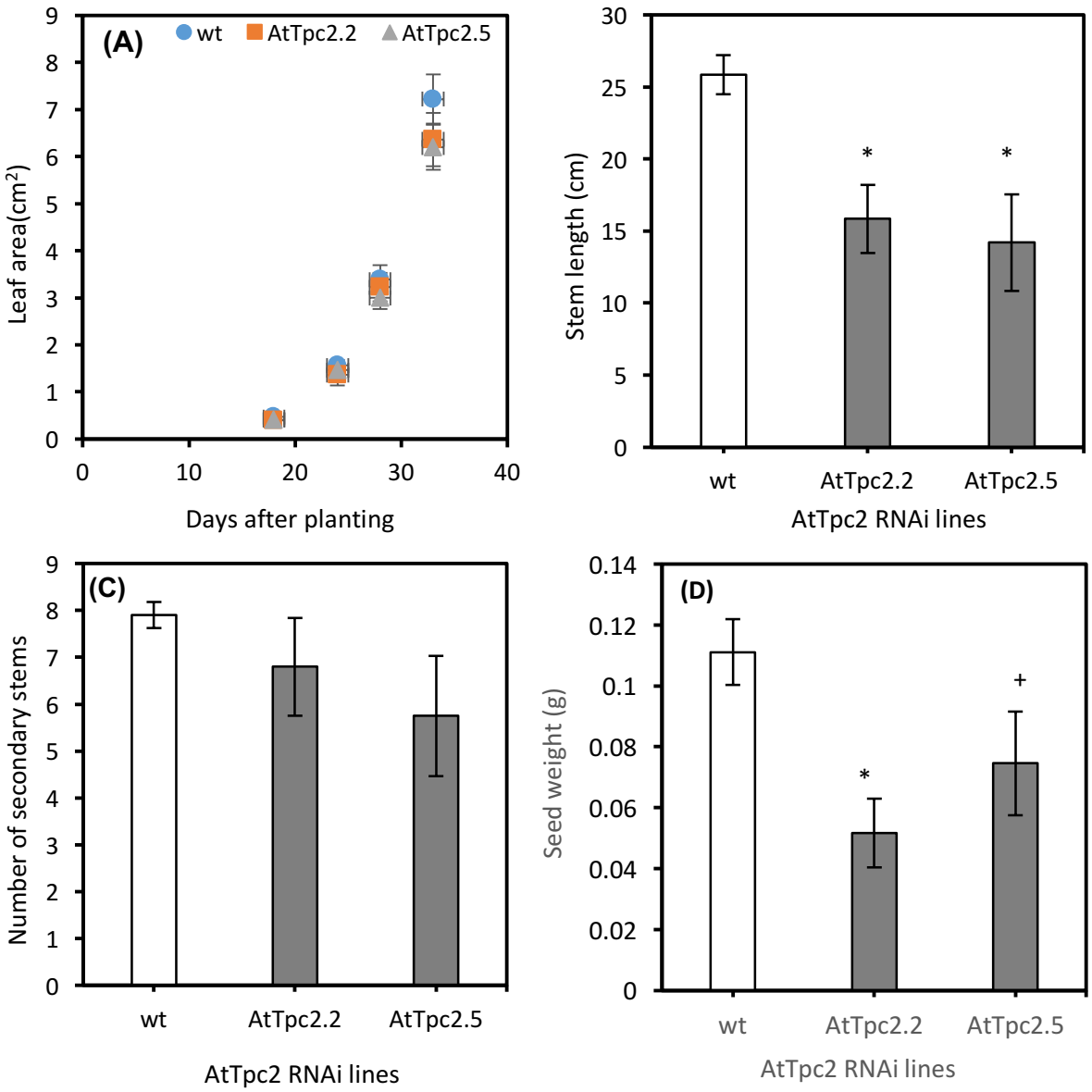

Figure 3.13: Growth analysis of AtTpc2::RNAi transgenic and wild type (WT) plants. Plants were grown directly in soil under a controlled environment in a short-day growth room. **(A)** The leaf area in two independent AtTpc2 lines. **(B)** the length of the main stem of the individual. **(C)** The number of secondary stems of the individual. **(D)** Seed weight from two AtTpc2 RNAi lines. Error bars indicate the standard error (SE) from 10 replicates. Significant changes to the WT were determined by a one-way analysis of variance (ANOVA) for $p < 0.05$ and

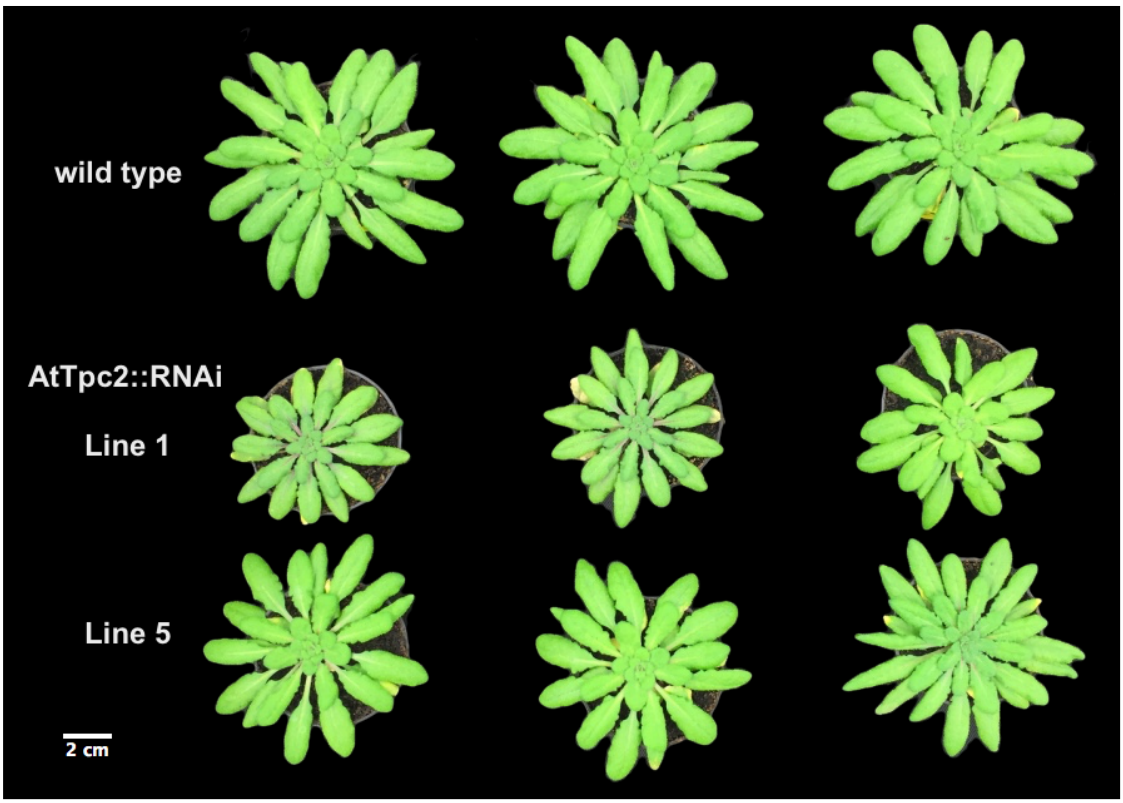

Figure 3.14: Phenotype of *Arabidopsis* AtTpc2 RNAi lines. Plants were grown directly in soil under a controlled environment in a short-day growth room (8 h light, 16 h dark, 22 °C). Wild-type plants (WT) are shown on the top, and two AtTpc2 independent lines are shown in the middle and on the bottom. Photos were taken when the plants were 53 days old.

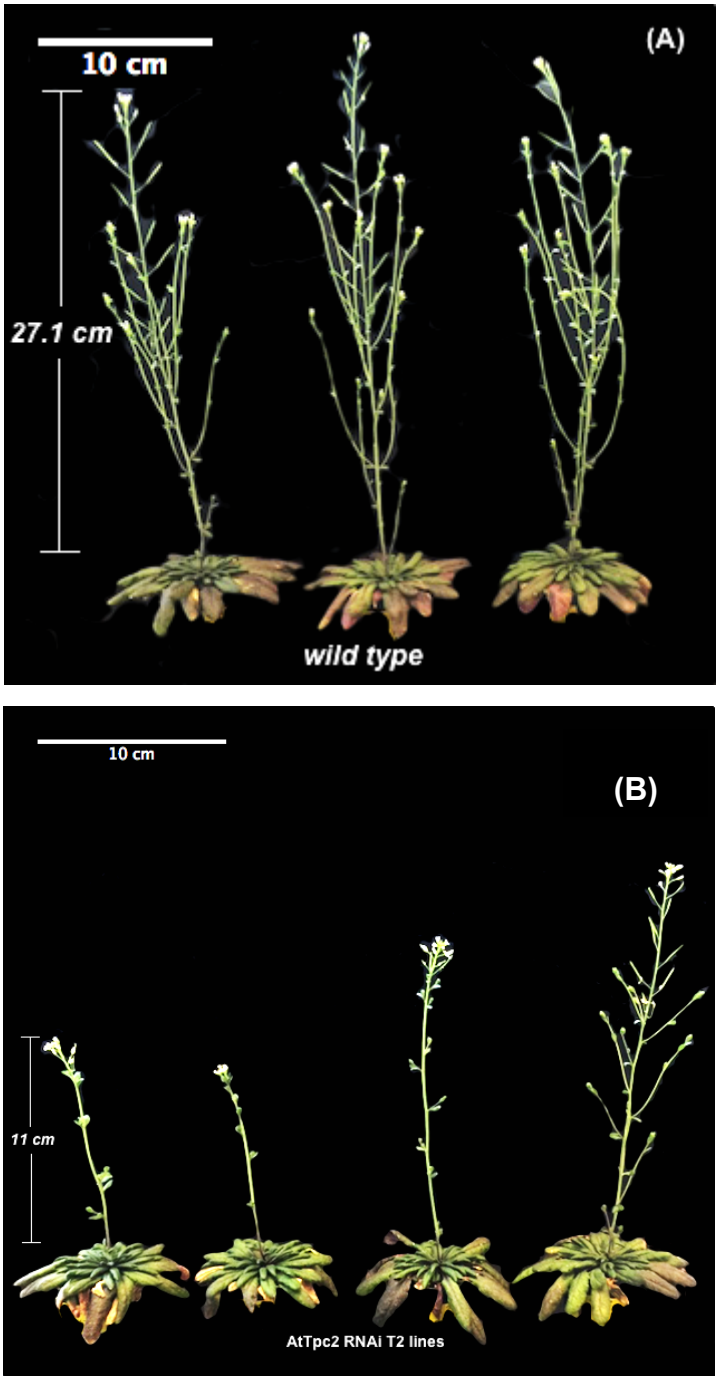

Figure 3.15: Comparison of the length of the main stem and the number of secondary stems between the wild type (WT) and the AtTpc2 RNAi lines. Both plants were grown directly in soil under a controlled environment in a short-day growth room (8 h light, 16 h dark, 22 °C). (A) wild type and (B) AtTpc2 RNAi lines.

3.2.3.3. Growth analysis of AtTpc2 T-DNA insertion mutants

The change in the transcription level of AtTpc2 Arabidopsis mutants was clear when compared to the WT. Therefore, an experiment was performed to evaluate the impact of this change on plant growth. This experiment included two different independent lines of AtTpc2 Arabidopsis mutants (SAIL_127_G03 and GK). It was set up on a short day (8 h light, 16 h dark, 22 °C), and seeds were grown directly in soil with triplicates of 18 plants each. After the first four leaves were fully formed, measurements of their surface area were initiated; measurements were taken until the plants reached 33 days old at four time points (19, 24, 29 and 33 days). The AtTpc2 mutant lines showed a slow growth phenotype compared to the WT. The smaller rosettes were significant in their later development in both AtTpc2 mutant lines. The AtTpc2 rosettes were smaller than those of the WT plants; the difference was about 20% at 33 days old (Figure 3.16 and 3.17).

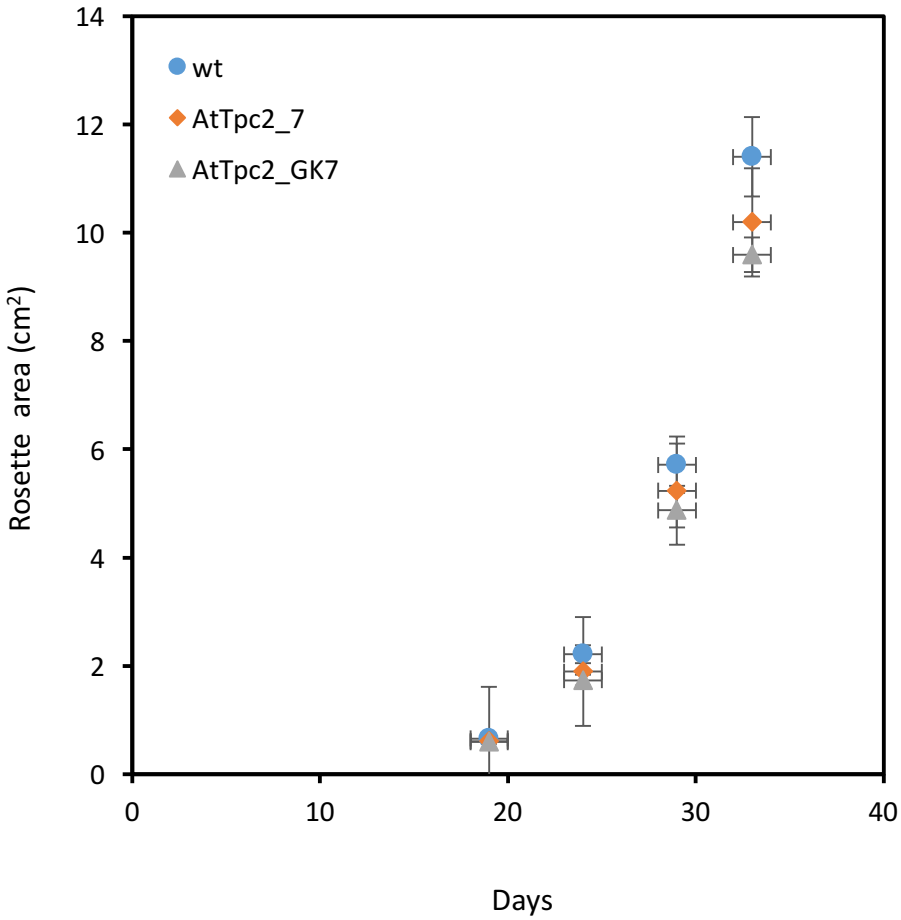

Figure 3.16: Comparison of rosette area between the wild type (WT) and the AtTpc2 mutant. Plants were grown directly in soil under a controlled environment in a short-day growth room (8 h light, 16 h dark, 22 °C). **(a)** Length of main stem. **(b)** Number of secondary stems. **(c)** Number of siliques on the main stem. Error bars indicate the standard error (S)E from 12 replicates. Significant changes to the WT were determined by one-way analysis of variance (ANOVA) for $p < 0.05$ and indicated by an asterisk.

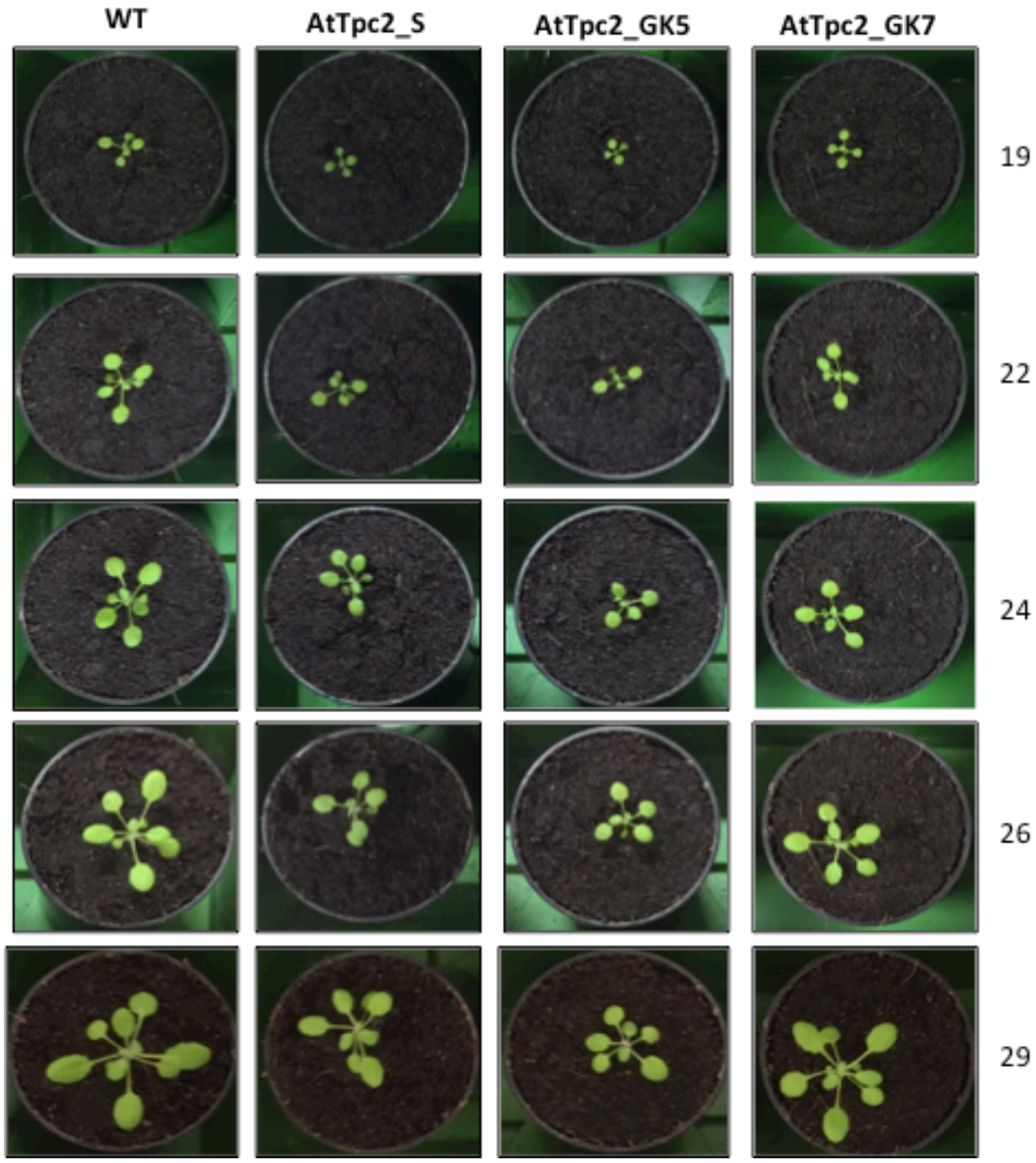

Figure 3.17: Phenotype of *Arabidopsis* AtTpc2 mutant lines. Plants were grown directly in soil under a controlled environment in a short-day growth room (8 h light, 16 h dark, 22 °C). Numbers indicate days of plant age. Wild type plants (wt) are shown on the left, and the different dependent lines of AtTpc2 are on the top. Photos were taken on different days are on the right.

It was considered that, since the knockout of AtTpc2 insertion mutant affected the plant growth, it could also affect the root growth. Accordingly, a new experiment was performed to study the importance of AtTpc2 for root growth. Seeds were grown on plates containing half MS medium without sucrose and placed in a long-day controlled-environment growth room (16 h light, 8 h dark, 22 °C). The seeds were allowed to germinate, and root measurements were carried out at 9 and 12 days. The AtTpc2 mutant roots clearly were shorter than the WT by about 35% (Figure 3.18).

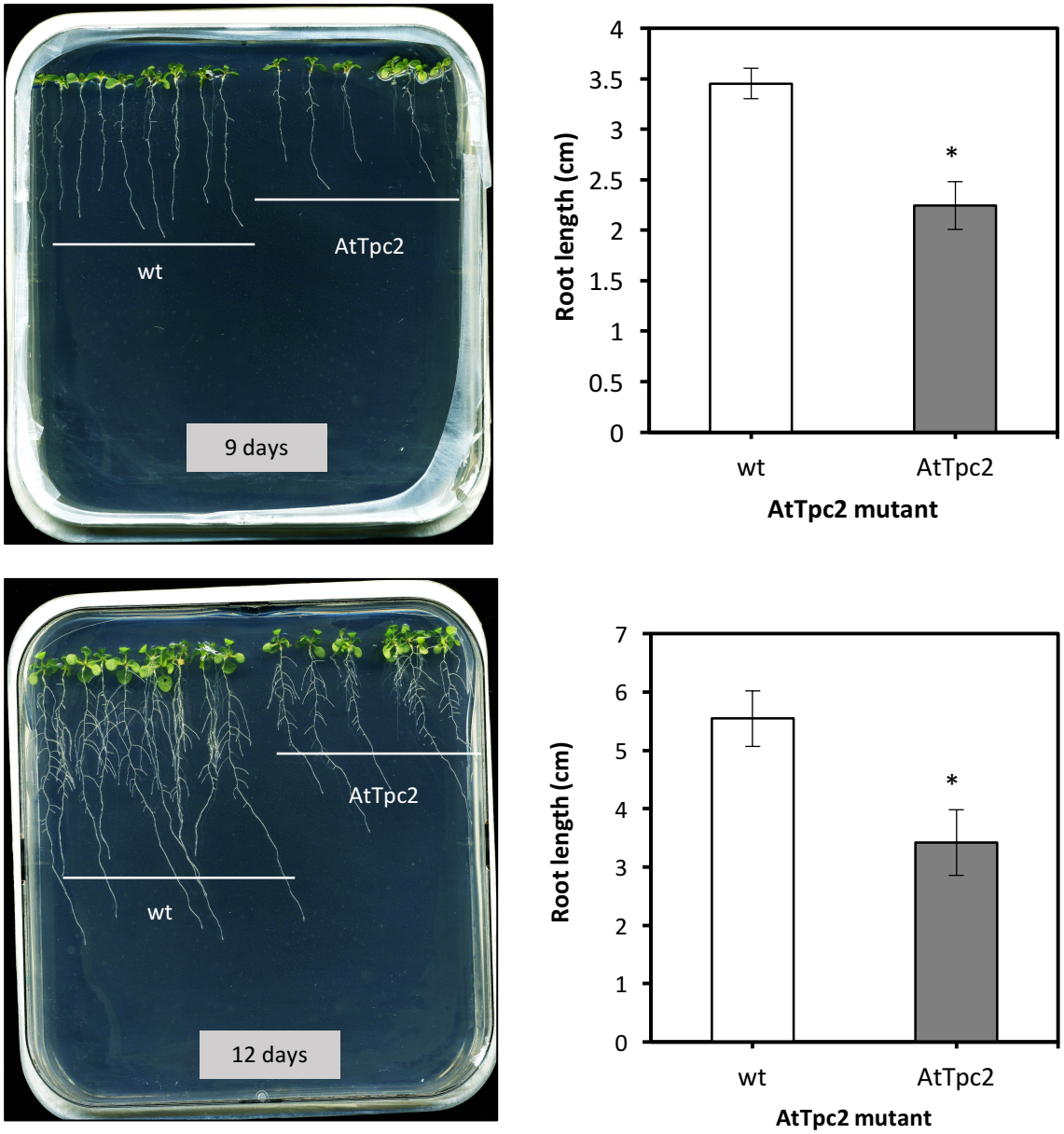

Figure 3.18: Comparison between the root length of AtTpc2 insertion mutant and the wild type (WT). Seeds were sterilised and planted at 4 °C for 2 days. Then, they were grown on half MS medium and allowed to grow in a long-day growth room. These photos were taken at 9 and 12 days. Measurements were carried out using the ImageJ program. The bar charts represent the root length at nine days **(top right)** and 12 days **(bottom right)**. Error bars indicate the standard error (SE) from 6–10 replicates. Significant changes to the WT were determined by one-way analysis of variance (ANOVA) for $p < 0.05$ and indicated by an asterisk.

3.3. Discussion

Arabidopsis AtTpc1 and AtTpc2 are members of MCF, and their localisation and function have recently been investigated (Palmieri et al., 2001; Frelin et al., 2012). The findings provide preliminary evidence that these proteins are mitochondrial TPP transporters. The study showed that both are located in mitochondria and furthermore, evidence for a role for AtTpc1 and AtTpc2 in transport of TPP was demonstrate in yeast cells that lack Tpc1, the mitochondrial TPP carrier in yeast (Frelin et al., 2012). However, no reports have yet considered the characterisation and analysis of AtTpc1 and AtTpc2 in plant and this study focussed on the importance of AtTpc1 and AtTpc2 for *Arabidopsis thaliana* growth.

The results of disrupting AtTpc1 in *Arabidopsis* showed that the leaf area was slightly smaller in the AtTpc1 plants than in the WT, and the secondary stems on the main stem were also a little smaller than on the WT, but this difference was not significant. In contrast, the length of the plants was significantly shorter than for the WT. These phenotypes may have emerged because AtTpc1 is one of the mitochondrial TPP transporters in *Arabidopsis* (Frelin et al., 2012), meaning that the quantity of mitochondrial TPP in the absence of AtTpc1 is not sufficient for plants to grow normally, at least under normal conditions. Similar phenotypes appeared on *Arabidopsis* growth when AtTpc2, a second mitochondrial TPP transporter, was inhibited by RNAi. This knocking out of AtTpc2 resulted in a significant effect on the length of the main stem and the seed yield. These phenotypes may be due to a reduction of TPP in the mitochondria, which would affect the activity of TPP-dependent enzymes in the mitochondria. In contrast, the difference between the influence of mitochondrial TPP transporters appeared in the root growth, where

disruption of AtTpc2 affected root growth, whereas AtTpc1 did not affect the root, and the plants grew normally. These findings could lead to the conclusion that AtTpc2 has an active function in the root. In conclusion, *Arabidopsis* requires both AtTpc1 and AtTpc2 to grow normally under normal conditions.

The results of growth analysis of the AtTpc2 mutant was different from the wild type, specifically, in the plant length and secondary stems. This may have caused some issues to arise in the growth environment, because none of the plants, including the WT, grew normally after flowering in AtTpc2 mutant study. Both experiments were carried out under the same conditions but at different times, so it would be interesting to conduct the analysis of AtTpc2 mutant and AtTpc2 RNAi at the same time under the same conditions. In addition, it will be interesting to knockout both AtTpc1 and AtTpc2 to investigate the impact on plant growth. This approach would also provide information on the possible presence of additional mitochondrial TPP transporters.

In summary, the limitation of this current study is that using only 2 independent lines does not provide sufficient evidence that the phenotype is due solely to a KO of the AtTpc genes, as a result, further analysis of additional independent lines is essential to provide convincing evidence of the role of AtTpc1 and AtTpc2 in plant growth. Complementation of AtTpc1 and AtTpc2 would be an alternative approach to this question. Another approach to address this problem would be to sequence the genome of AtTpc1 and AtTpc2 transgenic plants.

Chapter 4:

Identifying potential chloroplast TPP transporter(s)

4.1. Introduction

As described in previous chapters, TPP is synthesised in the cytosol through the action of TPK, which catalyses the conversion of free thiamine to TPP. Consequently, both the chloroplast and mitochondria must import TPP because both contain TPP-dependent enzymes (Goyer, 2010, Rapala-Kozik et al., 2008, Ajjawi et al., 2007). Recently, it has been shown that it is TMP that is transported from the chloroplast and that free thiamine is produced in the cytosol, catalyzed by TMP phosphatase (Mimura et al., 2016). Mitochondrial TPP transporters were identified and reported in various organisms: humans, yeast and drosophila (Lindhurst et al., 2006; Marobbio et al., 2002). Later, phylogenetic analyses and complementation assays were carried out, which resulted in the identification of mitochondrial TPP carriers in plants, with two in *Arabidopsis* (AtTPC1 and AtTPC2) and two in maize (GRMZM2G118515 and GRMZM2G124911) (Frelin et al., 2012). However, chloroplast TPP transporters have not yet been identified.

All known TPP transporters belong to the MCF, and this could lead to the suggestion that chloroplast TPP transporters may also be MFC members, particularly since it has been shown that some MCF members are targeted to the chloroplast, such as the Arabidopsis folate carrier (AtFolt1). The localization of AtFolt1 was reported by Bedhomme et al., (2005), and the findings showed that it is located on the chloroplast membrane. AtFolt1 has a homology with known folate transporters and is located in the chloroplast. In addition, AtFolt1 is able to take up exogenous folic acid when it is expressed in *Escherichia coli*. However, the folate content in chloroplasts was not affected in the absence of AtFolt1 activity (Bedhomme et al., 2005).

Phylogenetic analysis is an approach that allows the relationship between known TPP carriers in different organisms to be determined, and it can be used to identify putative chloroplast TPP carriers in plants. In addition, to study the relationships in the primary protein sequence, a 3D modeling approach can provide additional information to support the results obtained from the sequence similarities. The aim of the work in this chapter was to adopt a bioinformatic approach in order to identify putative chloroplast TPP transports based on homology with known TPP transporters.

4.2. Results

4.2.1. Building a phylogenetic tree of plant transporters

To carry out phylogenetic analysis, the phylogenetic tree was built as follows. Thiamine transporter sequences from yeast, bacteria and plants were obtained from the Universal Protein Resource (UniProt, 2013; http://www.uniprot.org/, 2013), and all sequences were aligned using ClustalW to obtain the conserved sequences of TPP transporters in different known TPP transporter proteins (Larkin et al., 2007). Then, the conserved sequences were blasted against the *Arabidopsis* proteome to select similar sequences that may target the chloroplast. Chloroplastic inner membrane sequences were added to these selected sequences in TPP transporters, which were aligned using ClustalW. A phylogenetic tree was constructed using different methods by MEGA5 (Tamura et al., 2011), wherein a bootstrap test was conducted based on 1000 re-samplings. Through a phylogenetic tree analysis of known TPP mitochondrial transporters in different organisms and in chloroplast membrane proteins, we identified five proteins located close to TPP carriers on the same node. These proteins are AT5G66380 (AtFolt1), AT3G51870 (CTT), AT3G54110, AT5G42130 and AT4G30580 (Figure 4.1). AtFolt1, CTT and AT3G54110 are the closest to TPP carriers except for yeast (Tpc1), which was located on a separate clade (Figure 4.1). The reason for low bootstrap values is due the presence of proteins from different transporter families.

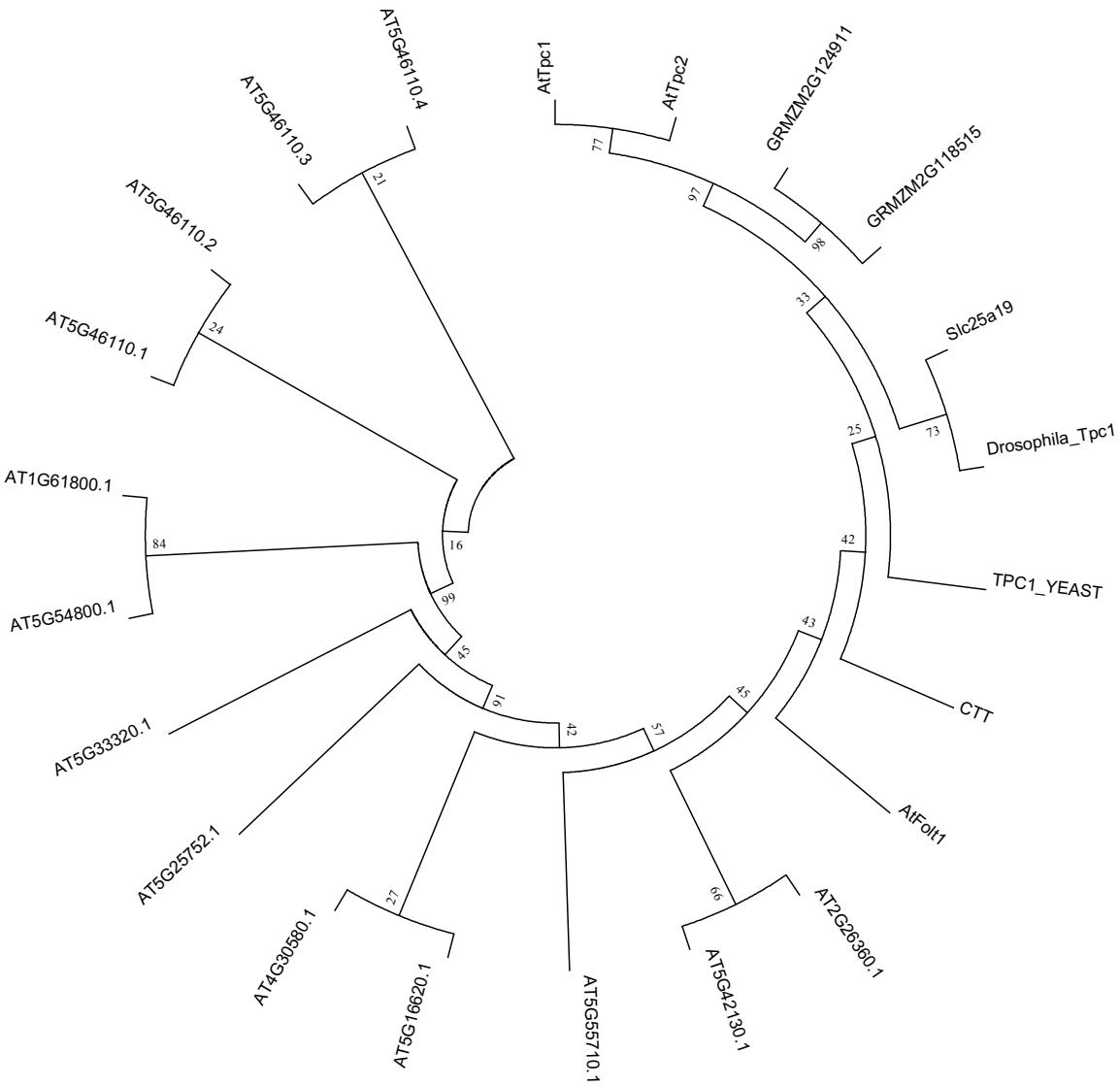

Figure 4.1a: Phylogenetic analysis of the known TPP transporters from yeast, humans and other chloroplast membranes. Sequences were aligned using ClustalW; the tree was constructed using the maximum likelihood method of MEGA5. The bootstrap values (%) for 1000 replicates are shown next to the nodes. Only the tree's topology is shown; the branch lengths are not proportional to the estimated number of amino acid substitutions. The red squares indicate the known TPP carriers, and the blue squares indicate the putative chloroplast transporters. Mitochondrial TPP carrier in humans **(SLC25A19**), mitochondrial TPP carrier 1 in yeast **(TPC1_yeast)**, mitochondrial TPP carrier in Drosophila **(TPC1_Drosophila)**, Arabidopsis mitochondrial TPP transporters (AtTpc1 and AtTpc2), Zea mays mitochondrial TPP transporters **(GRMZM2G118515 and GRMZM2G124911)** and plant mitochondrial TPP transporter, AtTpc1 and AtTpc2. **AT3G51870** is Arabidopsis unknown protein and **AT5G66380** is Arabidopsis folate transporter.

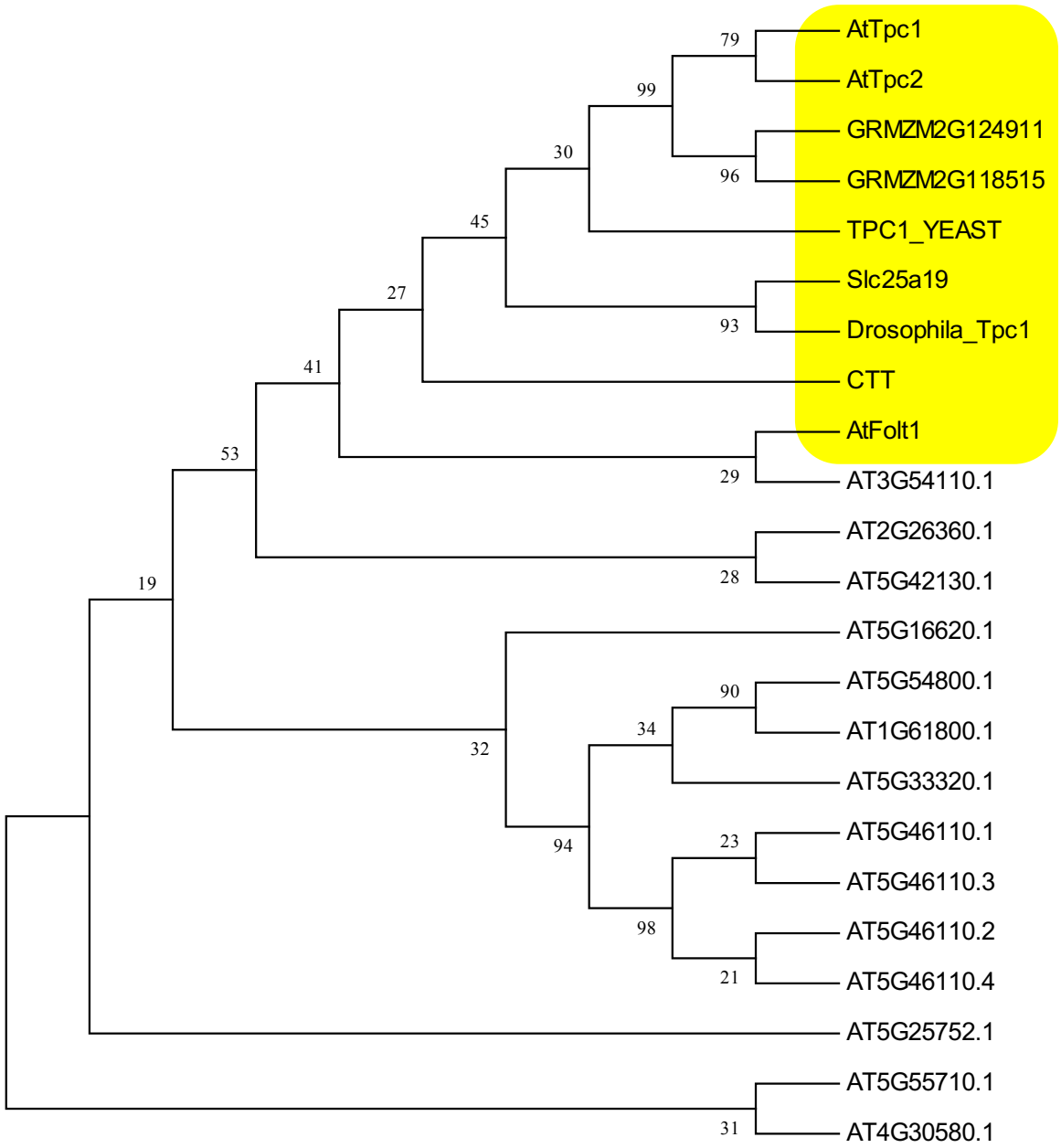

Figure 4.1b: Phylogenetic analysis of the known TPP transporters from yeast, humans and other chloroplast membranes. Sequences were aligned using ClustalW; the tree was constructed using the maximum likelihood method of MEGA5. The bootstrap values (%) for 1000 replicates are shown next to the nodes. Only the tree's topology is shown; the branch lengths are not proportional to the estimated number of amino acid substitutions. The red squares indicate the known TPP carriers, and the blue squares indicate the putative chloroplast transporters. Mitochondrial TPP carrier in humans **(SLC25A19**), mitochondrial TPP carrier 1 in yeast **(TPC1_yeast)**, mitochondrial TPP carrier in Drosophila **(TPC1_Drosophila)**, Arabidopsis mitochondrial TPP transporters (AtTpc1 and AtTpc2), Zea mays mitochondrial TPP transporters **(GRMZM2G118515 and GRMZM2G124911)** and plant mitochondrial TPP transporter, AtTpc1 and AtTpc2. **AT3G51870** is Arabidopsis unknown protein and **AT5G66380** is Arabidopsis folate transporter.

4.2.2. Sequence analysis of plant TPP candidates

To proceed with the investigation of the putative TPP transporter candidates, the five protein sequences (AtFolt1, CTT, AT3G54110, AT5G42130 and AT4G30580) were screened to identify any shared motifs with the known TPP transporter proteins. Motifs were discovered using the Multiple EM for Motif Elicitation (MEME) Suite (Bailey and Elkan, 1994). The analysis showed that there were five shared motifs between TPP carriers and two candidates, AtFolt1 and CTT. In contrast, to the other three proteins, two – namely AT3G54110 and AT5G42130 – had four shared motifs with TPP carriers, whereas AT4G30580 did not have any conserved motif (Figures 4.2 and 4.3). Consequently, AtFolt1 and CTT could be putative chloroplast TPP transporters.

A sequence alignment analysis of AtFolt1, CTT and *Arabidopsis* mitochondrial TPP carriers (AtTpc1 and AtTpc2) was conducted using ClustalW. The findings showed that AtFolt1 and the plant mitochondrial TPP transporters shared 27% amino acids identity and 35% similarity (Figure 4.4). Furthermore, CTT shared 25% of its amino acids with plant mitochondrial TPP transporters (Figure 4.5). Interestingly, the alignment showed that these proteins have a highly conserved region in the C-terminus that is shared with mitochondrial TPP transporter proteins and they also have additional shared motifs (Figure 4.2, 4.3 and 4.6).

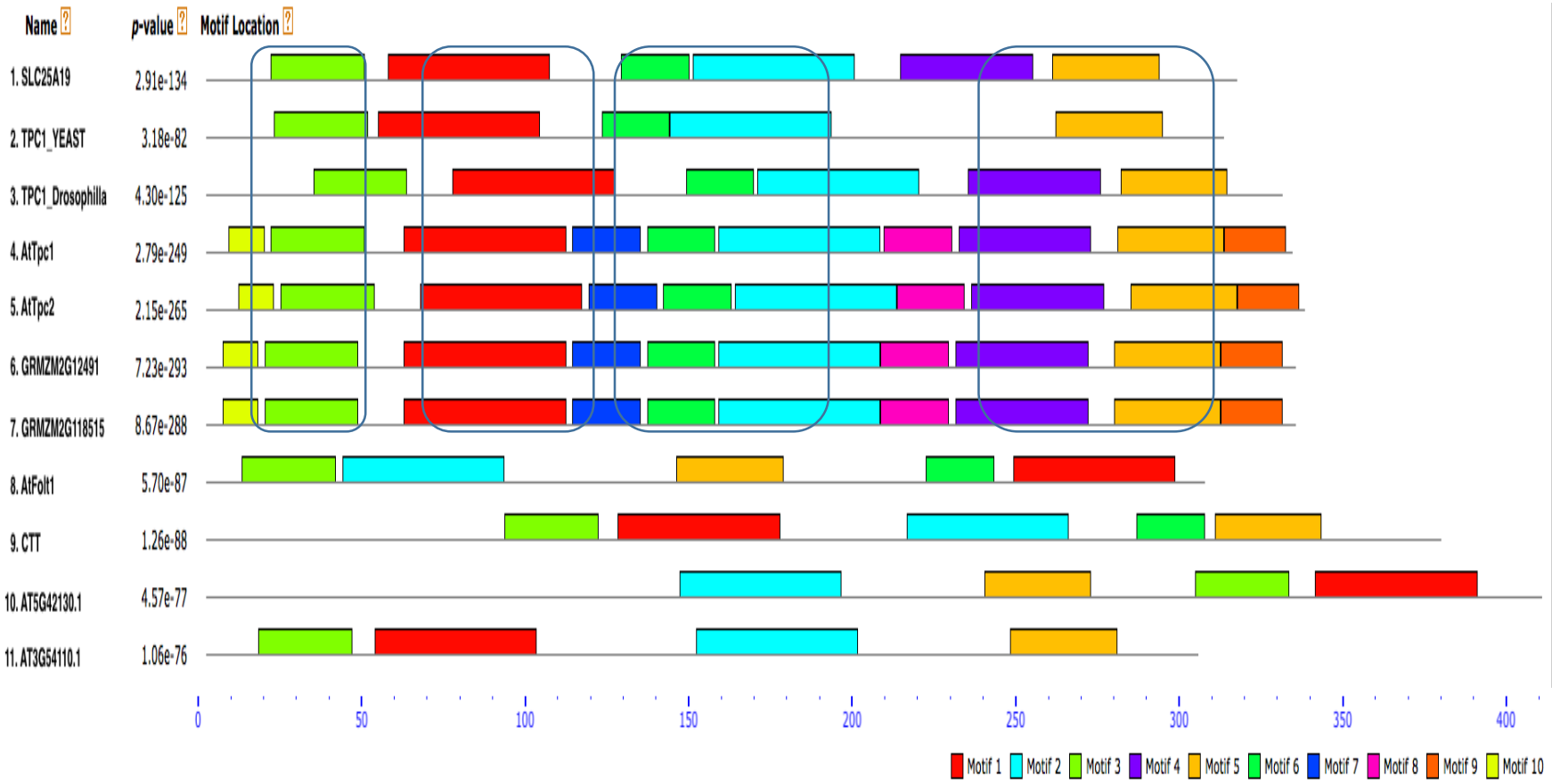

Figure 4.2: Comparison of conserved motifs among TPP transporters. The motifs were identified by the MEME search tool. Each motif is represented by a coloured box and defined at the top right of the figure. The length of the box corresponds to the length of the motif. The scale represents the length of sequences. Mitochondrial TPP carrier in humans (SLC25A19), mitochondrial TPP carrier 1 (TPC1_yeast), mitochondrial TPP carrier in *Drosophila* (TPC1_Drosophila), *Arabidopsis* mitochondrial TPP transporters (AtTpc1 and AtTpc2), *Zea mays* mitochondrial TPP transporters (GRMZM2G118515 and GRMZM2G124911) and plant transporters (AtFolt1, CTT, AT3G54110 and AT5G42130). Boxes represent the conserved regains in TPP transporters.

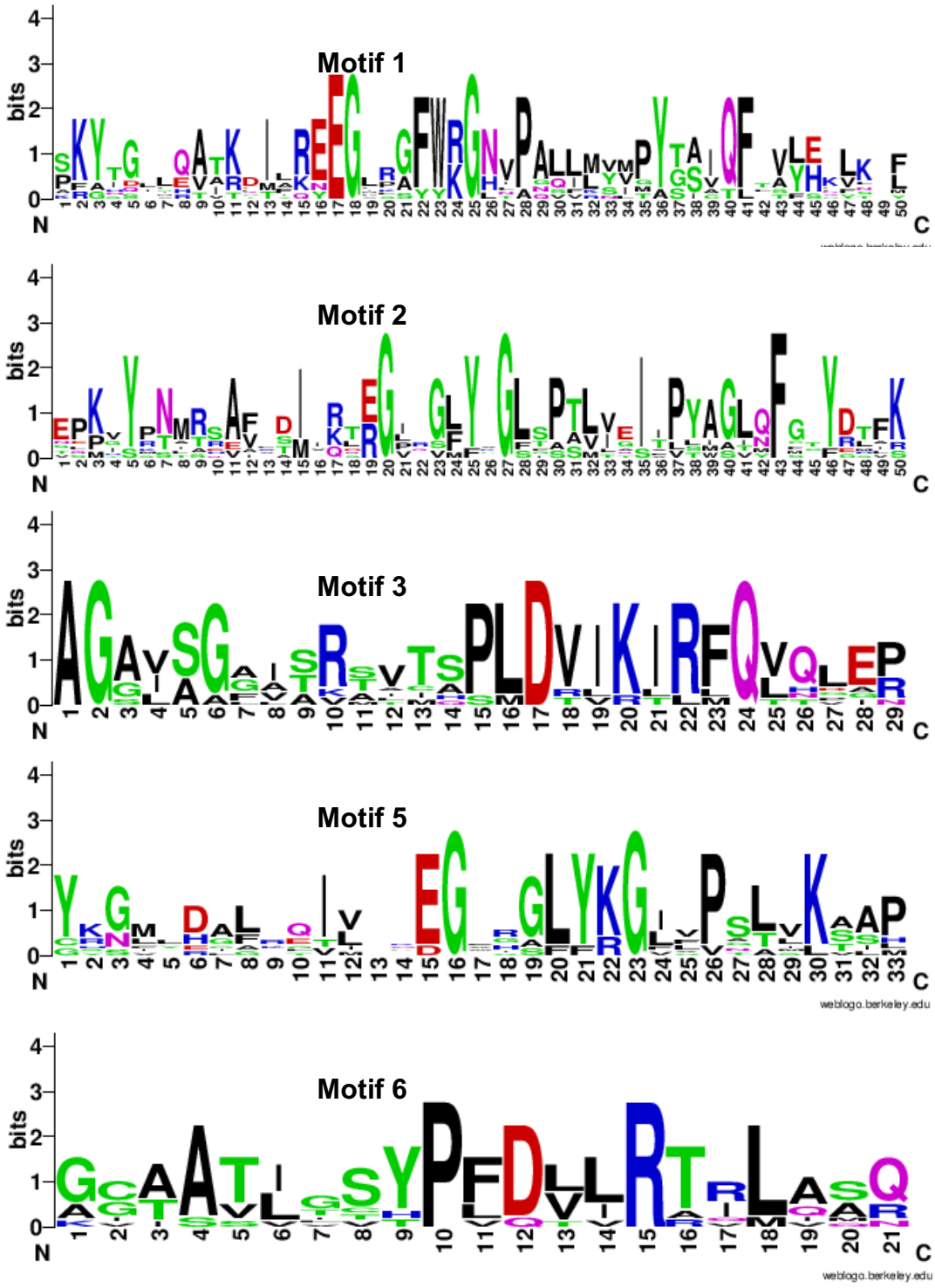

Figure 4.3: Conserved motifs shared between TPP carriers, CTT and AtFolt1. Motifs were discovered using the MEME search tool. The graphical logo of motifs was created by the WebLogo tool. The numbers represent the length of the motif.

Figure 4.4: Alignment of Arabidopsis TPP carriers and AtFolt1. Protein sequences were obtained from the *Arabidopsis* Information Resource (TAIR). AtFolt1 was aligned with plant mitochondrial TPP transporters using ClustalW. **(AtFolt1)** is putative chloroplast TPP transporter and **(AtTpc1 and AtTpc2)** the plant mitochondrial TPP transporters.

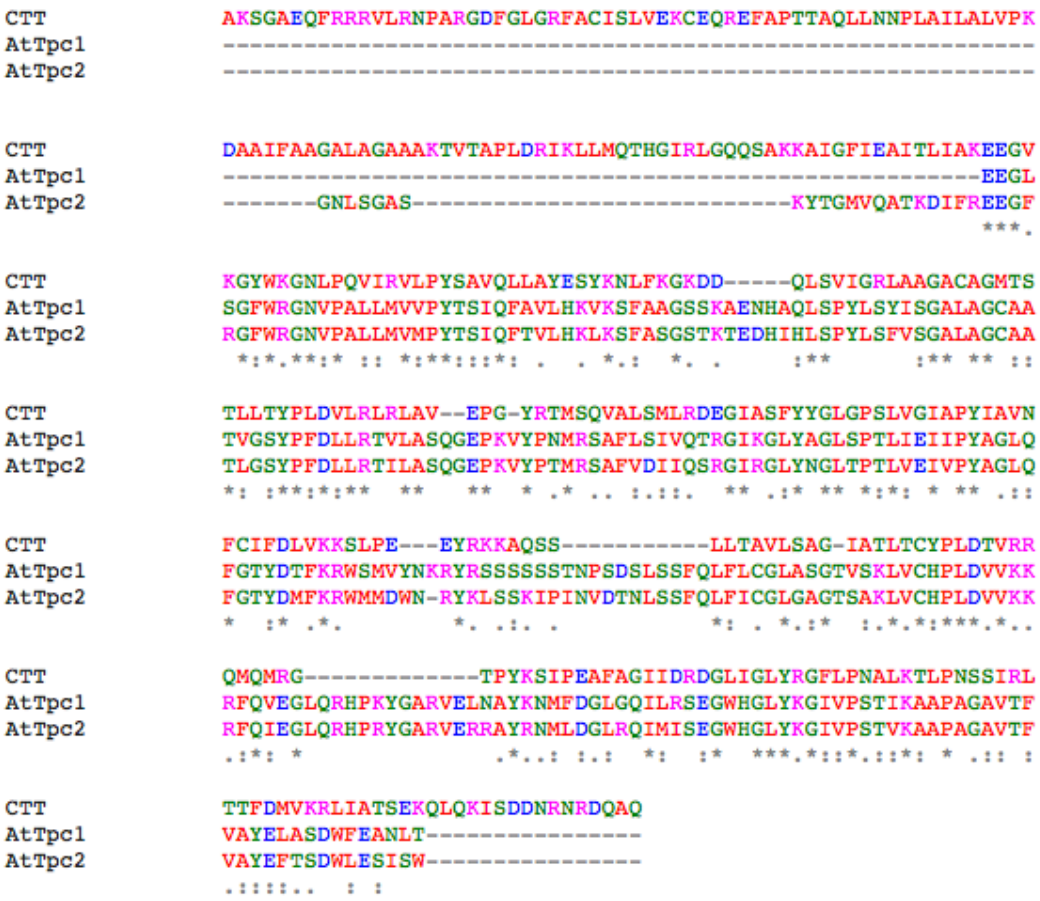

Figure 4.5: Alignment of Tpc and CTT sequences. Protein sequences were obtained from the *Arabidopsis* Information Resource (TAIR). CTT was aligned with plant mitochondrial TPP transporters using ClustalW.

Figure 4.6: Alignment of AtTpc, CTT and AtFolt1. Protein sequences were obtained from the *Arabidopsis* Information Resource (TAIR). The alignment was conducted by ClustalW. A shared highly conserved region appeared in the C-terminal region.

4.2.3. Producing a predicted 3D structure for the TPP transporter

To investigate the function of CTT and AtFolt1, it is important to first study the protein structure. The functions of *AtTpc1* and *AtTpc2* have been demonstrated; they have been shown to be responsible for transferring TPP from the cytosol to mitochondria in plants (Frelin et al., 2012). Mitochondrial TPP transporter proteins were compared with CTT and AtFolt1 protein structures. Unfortunately, none of these transporters has a crystallised structure in the Protein Data Bank (PDB); therefore, a 3D structure had to be predicted to conduct a comparison between Arabidopsis mitochondrial TPP transporter proteins (*AtTpc1* and *AtTpc2*) and putative chloroplast TPP transporters (*CTT* and *AtFolt1*). In addition, the predicted structure of the folate carrier in humans (*SLC19A1*) was produce to determine whether it is the same as that of a plant folate carrier (AtFolt1). All protein sequences were obtained from TAIR and UniProt; the sequence alignment was carried out using ClustalW. After alignment, the protein sequences were used to produce the predicted 3D structures with the aid of the Phyre2 server (Kelley and Sternberg, 2009), and the structure photos were created using PyMol software (Version 1.7.4.4; Schrödinger (2015). The results showed that AtFolt1 is different from S*LC19A1*. In contrast, *CTT* and *AtFolt1* are highly similar to mitochondrial TPP transporters (Figures 4.7 and 4.8).

The sequence alignment of *CTT* and *AtFolt1* was analysed, and the findings showed that they have low similarity (under 40%), whereas they have a highly conserved homology in the C-terminal region (Figure 4.9). To deepen our analysis and determine the extent of the similarity between mitochondrial TPP transporters and the CTT and AtFolt1 transporters, a structural alignment was carried out to

perform compression and identify the implicit evolutionary relationships between these proteins. PyMol software was used to conduct this compression with the aid of root mean square deviation (RMSD). Put simply, RMSD measures the difference between the aligned residues in two proteins to define how well the submitted structures match each other. The RMSD value is 0.0 if the two proteins are identical. In our analysis, the RMSD value of the predicted structures of the mitochondrial TPP transporters was 0.506, and both had the same function as that described by Frelin et al. (2012). The results of the structural alignment of CTT and AtFolt1 with AtTpc1 and AtTpc2 showed that they have high similarity; the RMSD value between AtTpc1 and AtTpc2 was 0.506 with a known function (Figure 4.10 and 4.11).

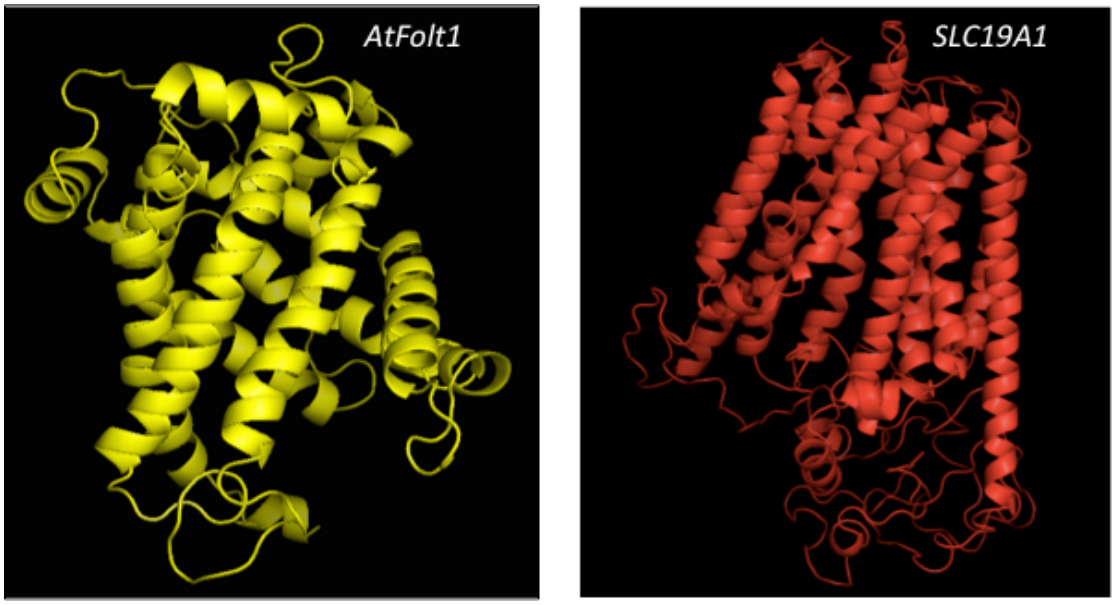

Figure 4.7: Prediction of folate transporter protein structures. 3D prediction models were obtained using the Phyre2 server. The left model is the plant folate transporter protein (ATFOLT1) and the right model is the folate transporter protein in humans (SLC19A1).

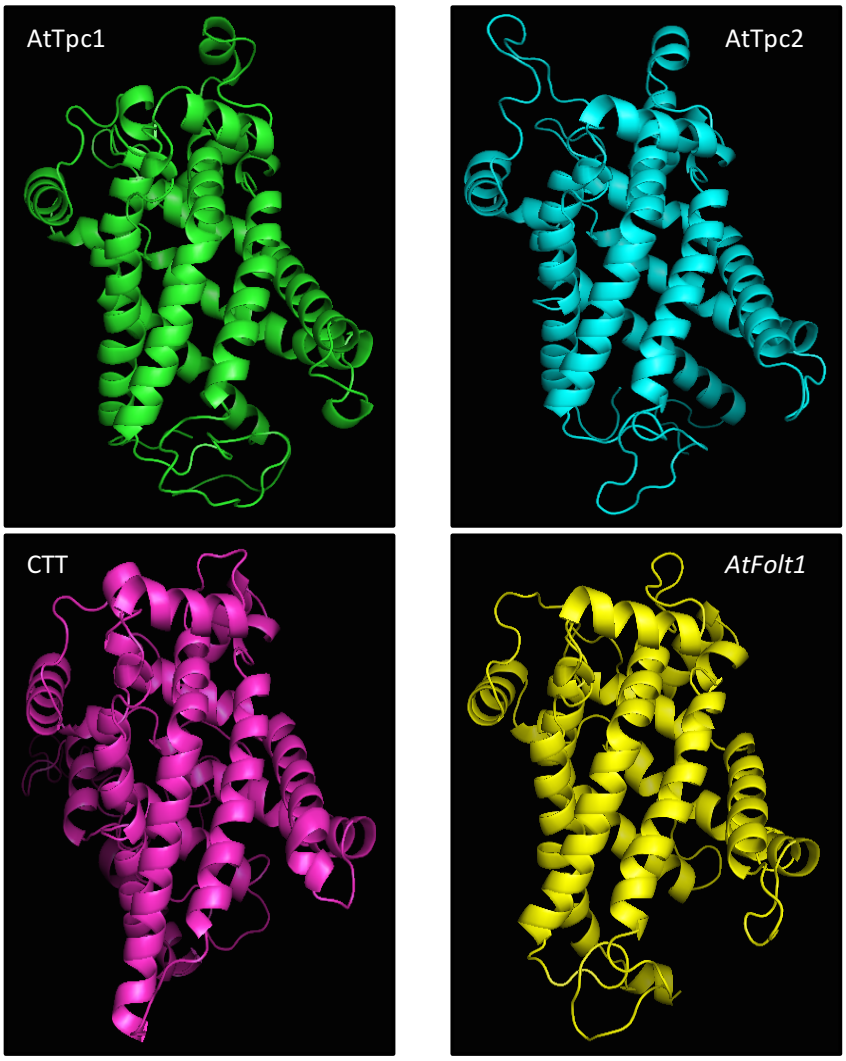

Figure 4.8: Prediction of TPP transporter protein structures. 3D prediction models were obtained using the Phyre2 server. The top models are the plant mitochondrial TPP transporter proteins; the bottom models are the CTT and AtFolt1 transporter proteins.

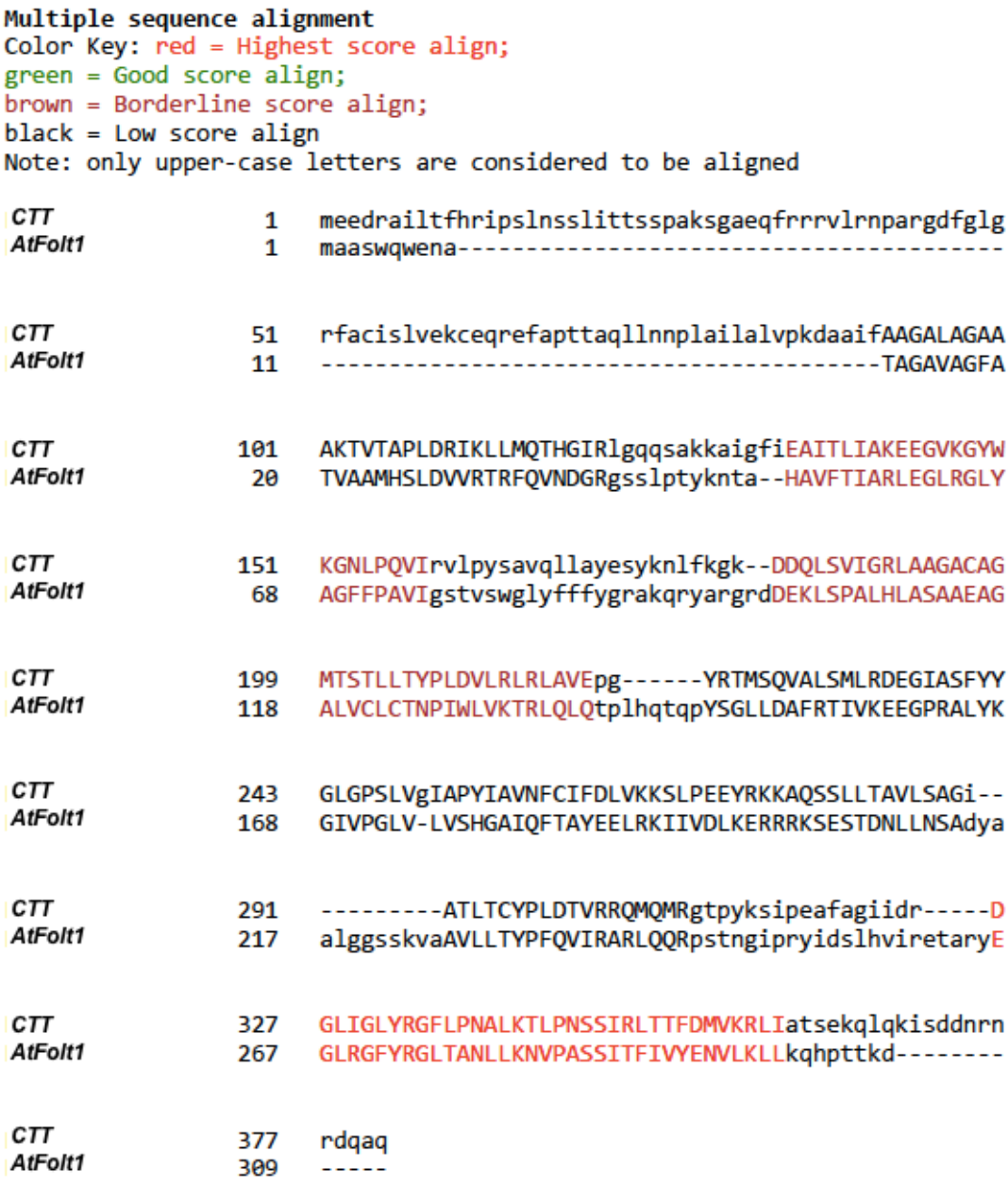

Figure 4.9: Alignment of CTT and AtFolt1 sequences. Protein sequences were obtained from the *Arabidopsis* Information Resource (TAIR). The alignment was conducted by ClustalW.

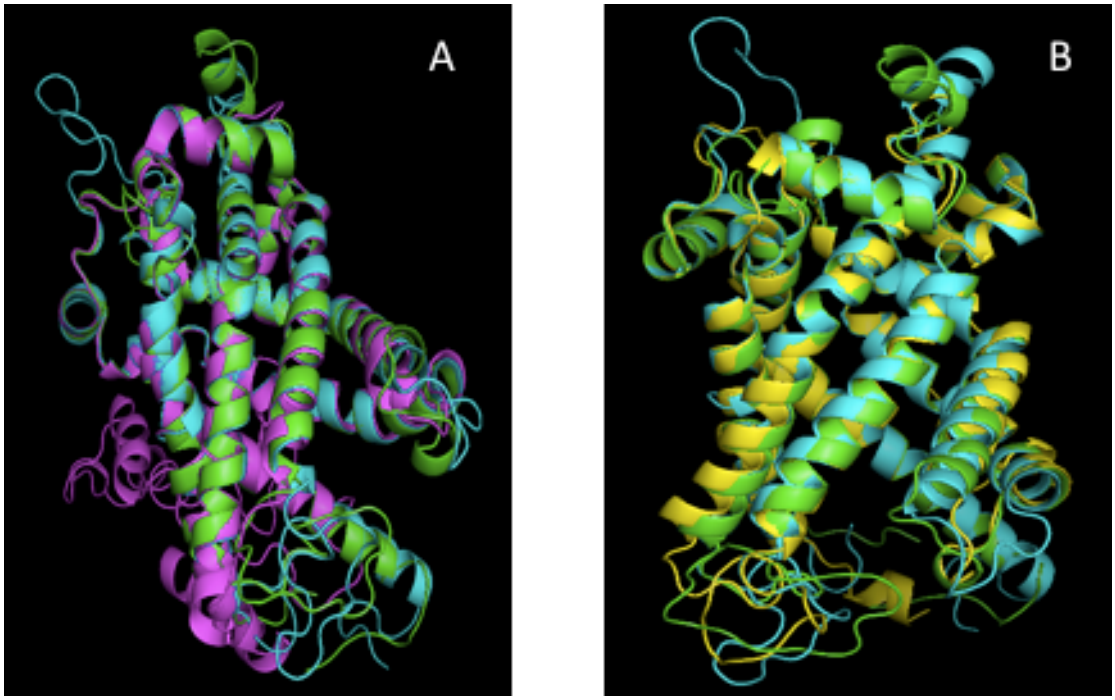

Figure 4.10: Structural alignment of CTT and AtFolt1 with mitochondrial TPP protein carriers. (A) CTT protein structure (magenta) was aligned with mitochondrial TPP carrier structures (AtTpc1 is green and AtTpc2 is cyan). **(B)** AtFolt1 protein structure (yellow) was aligned with AtTpc1 and AtTpc2. The alignment was carried out using PyMol software. **(C)** Table showing the RMSD values.

Proteins	RMSD	Proteins	RMSD
AtTpc1 vs. AtTpc2	0.506	**AtFolt1 vs. Slc25a19**	0.602
AtTpc1 vs. CTT	0.419	**AtFolt1 vs. Tpc1**	1.219
AtTpc2 vs. CTT	0.500	**CTT vs. Slc25a19**	0.853
AtTpc1 vs. AtFolt1	0.646	**CTT vs. Tpc1**	0.574
AtTpc2 vs. AtFolt1	0.695		

Table 4.11: The compression alignment of putative and TPP transporters. Table showing the RMSD values came out of models alignment which were carried out using PyMol. AtTpc1 and 2 are Arabidopsis mitochondrial TPP transporters, AtFolt1 and CTT are putative chloroplast TPP transporters, **Slc25a19 is a *human* TPP transporter, and Tpc1 is a *yeast* TPP transporter.**

4.2.4. Studying the localisation of CTT

AtFolt1 was shown previously to be a chloroplastic protein and contains a chloroplastic transit peptide with 11 residues (Bedhomme et al., 2005); however, the subcellular localisation of CTT is as yet unknown. To study the localisation of CTT, several servers were utilised to analyse its sequence. In silico sequencing analysis of CTT using different servers showed that it is located in chloroplasts or mitochondria. However, the prediction results from the ChloroP and TargetP prediction servers, which are widely used with plants (Emanuelsson et al. (1999); Emanuelsson et al. (2000), indicated that CTT contains a cTP, where the length was predicted to be 26 residues with a score of 0.510 (Figure 4.12).

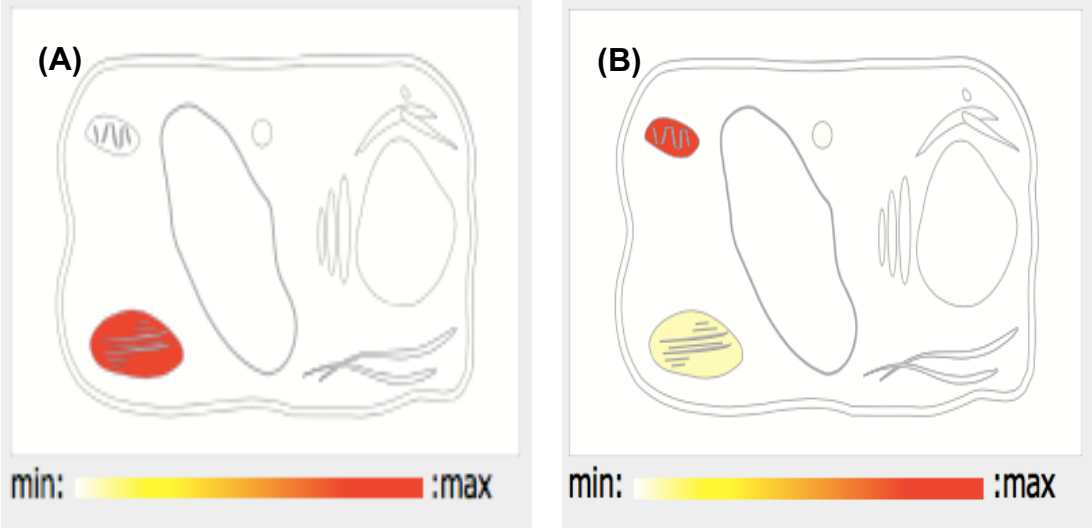

Predictor	Predicted location	Predictor	Predicted location
AdaBoost	Mitochondrion	SLPFA	Mitochondrion
BaCelLo	Plastid	SLP-Local	Mitochondrion
ChloroP	Plastid	SubLoc	Mitochondrion
MitoPred	Mitochondrion	TargetP	Plastid
MultiLoc	Plastid	WoLF PSORT	Nucleus
Plant-mPloc	Mitochondrion	YLoc	Mitochondrion
PProwler	Plastid		

Figure 4.12: The prediction of subcellular localisation for CTT. (A) The cell map shows where AtFolt1 is expressed in the plastid (red). **(B)** The cell map shows that CTT may be expressed in mitochondria (red) or in the plastid (yellow). At the bottom is the list of servers used to predict the subcellular localisation of CTT. The predictions were obtained using the SUBA3 tool (Hooper et al. (2014).

4.2.4.1. Building CTT::YFP fusion constructs

To study the subcellular localisation of the CTT gene, a YFP construct was designed using the *Arabidopsis* CTT coding region. The The pGWB41 plasmid contained the coding region of the enhanced yellow fluorescent gene (YFP) in the C-terminal region. After removing the stop codon from the coding region sequence of CTT because of its existence in the a The pGWB41 vector, specific primers were utilised to amplify 1146 bp of CTT. The target fragment was amplified using the Phusion enzyme by PCR, and a blunt-end product was cloned into the pENTR/D-TOPO vector. The *E. coli* colonies were screened by PCR using M13 primers (the M13 forward: 5'-GTA AAA CGA CGG CCA G-3' and the M13 reverse: 5'-CAG GAA ACA GCT ATG AC-3') to identify positive colonies, confirming that the target fragment had been transformed successfully into the entry vector. The positive colonies were sequenced to confirm that the insert was placed in the correct position before being transferred to the The pGWB41 destination vector. Then, the LR reaction was performed to transfer the target fragment to the destination vector using LR Clonase™ II enzyme mix, as described in Chapter 2 (Figures 4.13 and 4.14).

4.2.4.2. Agrobacterium transformation into *Arabidopsis* and bacterial PCR

The CTT::YFP gene construct in The pGWB41 was transferred into *Agrobacterium*-competent cells using the electroporation method. PCR analysis was performed for kan-resistant colonies using a combination of the promoter primer and a YFP primer to confirm the presence of the target fragment–tagging YFP in the

Agrobacterium. PCR products were loaded onto agarose gel to confirm the correct size of the target fragment.

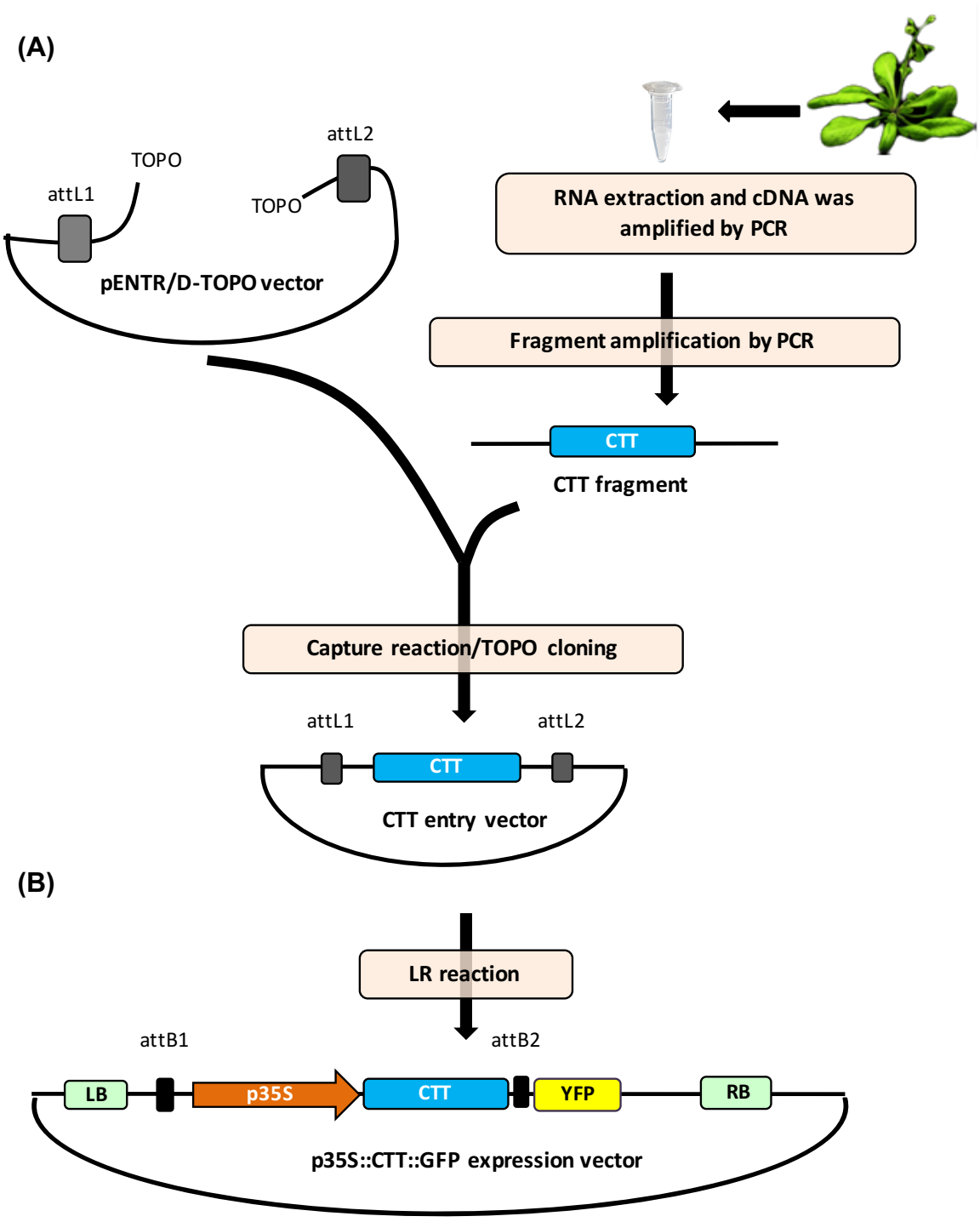

Figure 4.13: Scheme for designing the CTT::YFP construct for identifying the localisation of CTT in plant cells. RNA was extracted from leaves and cDNA was synthesised. The coding region of CTT was amplified using the specific primers. **(A)** The TOPO reaction; the CTT coding region was insert into a pENRY vector to produce the CTT entry vector. **(B)** LR reaction was performed to place the target region in the expression vector.

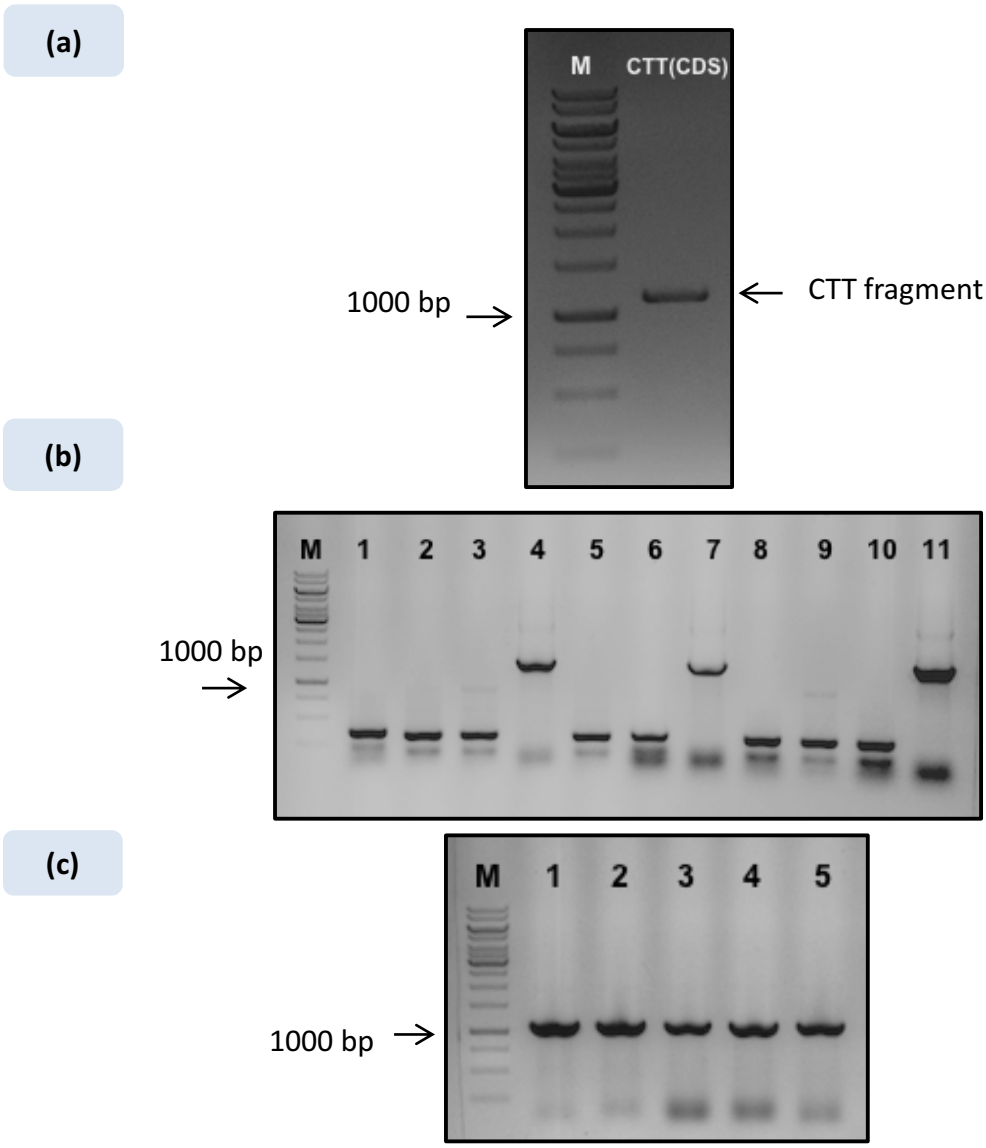

Figure 4.14: Building a CTT::YFP expression vector to study the localisation of CTT in plants. (a) Production of a blunt-end CTT using specific primers. **(b)** Colony PCR of CTT entry into kanamycin-resistant *E. coli* colonies. **(c)** *E. coli* colonies' PCR from the LR reaction plate. Rows indicate the marker and the insert. The PCR reaction was 20 µl and the PCR products were run on 1% gel agarose for 35 min at 100 V. The ladder was the GeneRuler 1 kb DNA ladder.

4.2.4.3. Studying the localization of CTT using transit assay

To identify the localization of CTT, the positive construct was transferred into the leaf *N. benthamiana* and screened under a confocal microscope. However, no expression of CTT::YFP was appeared and the result is unknown.

4.3. Discussion

CTT and AtFolt1 proteins were defined as members of MCF, as they have MCF properties (Belenkiy et al., 2000, Palmieri, 1994). TPP carriers in different organisms also belong to MCF (Marobbio et al., 2002; Lindhurst et al., 2006; Iacopetta et al., 2010). Our phylogenetic and sequence analyses showed that CTT and AtFolt1 are located on the same node as TPP carriers; in addition, AtFolt1 and CTT shared five conserved motifs with TPP carriers. Furthermore, a highly conserved region appeared in the C-terminus when aligning AtFolt1 and CTT with *Arabidopsis* TPP carriers. These data imply that AtFolt1 and CTT may have a function as TPP carriers.

AtFolt1 was found to be homologous to the mitochondrial folate transporters in mammalian cells (Bedhomme et al., 2005); it functions as a folate transporter in the Chinese hamster, and it is able to take up exogenous folic acid when it is expressed in *E. coli*. In plants, a localisation study using transient expression analysis of the full-length *AtFolt1* protein tagged with YFP and western blot analysis showed that the AtFolt1 protein is located in the chloroplast envelope (Bedhomme et al., 2005). Interestingly, the absence of AtFolt1 in *Arabidopsis* does not alter the level of folate in chloroplasts (Bedhomme et al., 2005). This means that there may be an alternative mechanism for folate transport. It was interesting to take this result a step further and compare the human folate carrier structure (SLC19A1) with that of AtFolt1. The findings of predicted 3D structures were interesting, as the structure was different, and this means that they could have different functions. Consequently, before moving to an experimental analysis, the predicted structures of known TPP structures and CTT were produced and compared; AtFolt1 and CTT

seem to be very similar to all known predicted structures of TPP carriers in different organisms. However, the limitation of this analysis is that none of the TPP carriers have been crystallised to allow confirmation of the predictions based on modelling. Another point is that we do not know the TPP binding site which will allow to study the docking of putative TPP transporters with TPP.

Thiamine or thiamine monophosphate is transported from chloroplast to cytosol to generate TPP, and chloroplast and mitochondria import TPP from cytosol (Goyer, 2010; Ajjawi et al., 2007a). According to this, two hypotheses were suggested, as follows: firstly, AtFolt1 and CTT could have a function as TPP carriers, and they may be responsible for transferring TPP from cytosol to chloroplast; and secondly, it may be that one of them could responsible for transferring TPP from cytosol to chloroplast, with the other working as a thiamine or thiamine monophosphate transporter to transport thiamine or thiamine monophosphate from chloroplast to cytosol. To investigate this, first, we needed to investigate the localisation of CTT. Our sequence analysis showed that CTT contains transit peptide consist of 26 residues; thus, CTT was tagged using YFP, and a construct was designed successfully and transferred into *Nicotiana benthamiana* to identify the localisation of CTT. However, our construct did not show any expression under a confocal microscope. The experiment was repeated several times, the localisation of CTT could not be identified experimentally; the reason for this might be that CTT did not express or the flag tag was not in frame with the coding sequence of the CTT protein and therefore expression could not be detected. In future, stable transformation should be considered and screen the flag existing before screen the CTT under the microscope.

In conclusion, the in silico findings support the hypothesis that AtFolt1 and/or CTT may serve as chloroplast TPP transporters. As a result, AtFolt1 and CTT functional studies should be carried out to provide evidence to support this this hypothesis.

Chapter 5:

Characterisation and analysis of the putative *Arabidopsis* chloroplast transporters

5.1. Introduction

As described in the previous chapter, our phylogenetic analysis focussed on putative chloroplast TPP carriers. One of these transporters is known as AtFolt1 (At5g66380). The second protein is unnamed, but we have called it CTT (At5g51870). These putative TPP transporters have homology with *Arabidopsis* mitochondrial TPP transporters (AtTpc1 and AtTpc2) in the C-terminal region. In addition, they share five conserved motifs with TPP transporters, as shown in the previous chapter (Figures 4.2 and 4.3).

The function of CTT has not yet been determined. However, CTT was identified as being related to 45 proteins that also belong to the MCF based on its homology with MCF members in yeast and humans, as reported by Millar and Heazlewood (2003). MCF is a large group of proteins located in the inner mitochondrial membrane, chloroplast or peroxisomes in the eukaryote (Bernhardt et al., 2012, Gennaro et al., 2011, Haferkamp, 2007, Bedhomme et al., 2005, Palmieri et al., 2001). The coding region of the CTT gene consists of 1146 bp and produces a protein consisting of 381 amino acid residues. In addition to the unknown physiological function of CTT, its importance in terms of plant growth remains a mystery. Our results from Chapter 3 show that CTT has a transit chloroplast peptide and that its predicted 3D structure is highly similar to those of mitochondrial TPP transporters.

The AtFolt1 transporter protein is a 34-kDa protein; it was identified as belonging to the MCF based on its structure (Palmieri, 2004). It is homologous to the mitochondrial folate transporters in mammalian cells (Bedhomme et al., 2005). However, in plants, a localisation study using transient expression analysis of the

full-length *AtFolt1* protein tagged with YFP and western blot analysis showed that this protein is located in the chloroplast envelope. In addition, the disruption of *Arabidopsis* AtFolt1 did not affect the folate level in the chloroplast, and this remained at the WT level (Bedhomme et al., 2005).

This chapter presents data on the analysis of plants where the function of AtFolt1 and CTT was disrupted in *Arabidopsis* using insertion mutant analysis and RNAi technology. Growth analysis is presented, along with a study of the effect of both AtFolt1 and CTT on TPP levels by measuring TPP in transgenic *Arabidopsis* plants.

5.2. Results

5.2.1. Identification and characterisation of *Arabidopsis* CTT insertion lines

To investigate CTT and AtFolt1 in *Arabidopsis*, two criteria were considered. The first was the type of insertion, which was T-DNA; the second condition was the location of the insertion, which was to be in the exon or very close to the exon to maximise the change and identify a knockout mutant.

5.2.1.1. Determining the homozygous mutant lines of CTT

To investigate the function of CTT, two T-DNA insertion mutants, SALK_760 and SALK_353, were selected after searching the Salk Institute Genomic Analysis Laboratory database and the TAIR database. These two mutants were chosen using the aforementioned criteria. Both mutant seeds were supplied by NASC. DNA was extracted from the first generation of seed stock and amplified by PCR using specific primers in a gene-specific reaction, as shown in Table 5.1. To look for homozygous lines for the T-DNA insertion, a T-DNA-specific reaction was performed. The reaction showed that the right border primer was specific, whereas the left border primer was LBb1.3, which is the reverse primer of T-DNA for SALK lines. Once homozygous lines were selected, DNA samples from homozygous plants for each mutant were sequenced at the Source Bioscience Company (http://www.lifesciences.sourcebioscience.com/overview/). The insertion site was determined, with the results showing that SALK_760 was inserted at 198 bp, where it was in the first exon after the start codon of CTT. Conversely, SALK_353 was inserted after the stop codon in the UTR (Figure 5.1). The next generation of

homozygous lines was grown, and three plants from SALK_760 lines of this generation were screened with PCR to ensure that the insertion still existed before beginning the study (Figure 5.1).

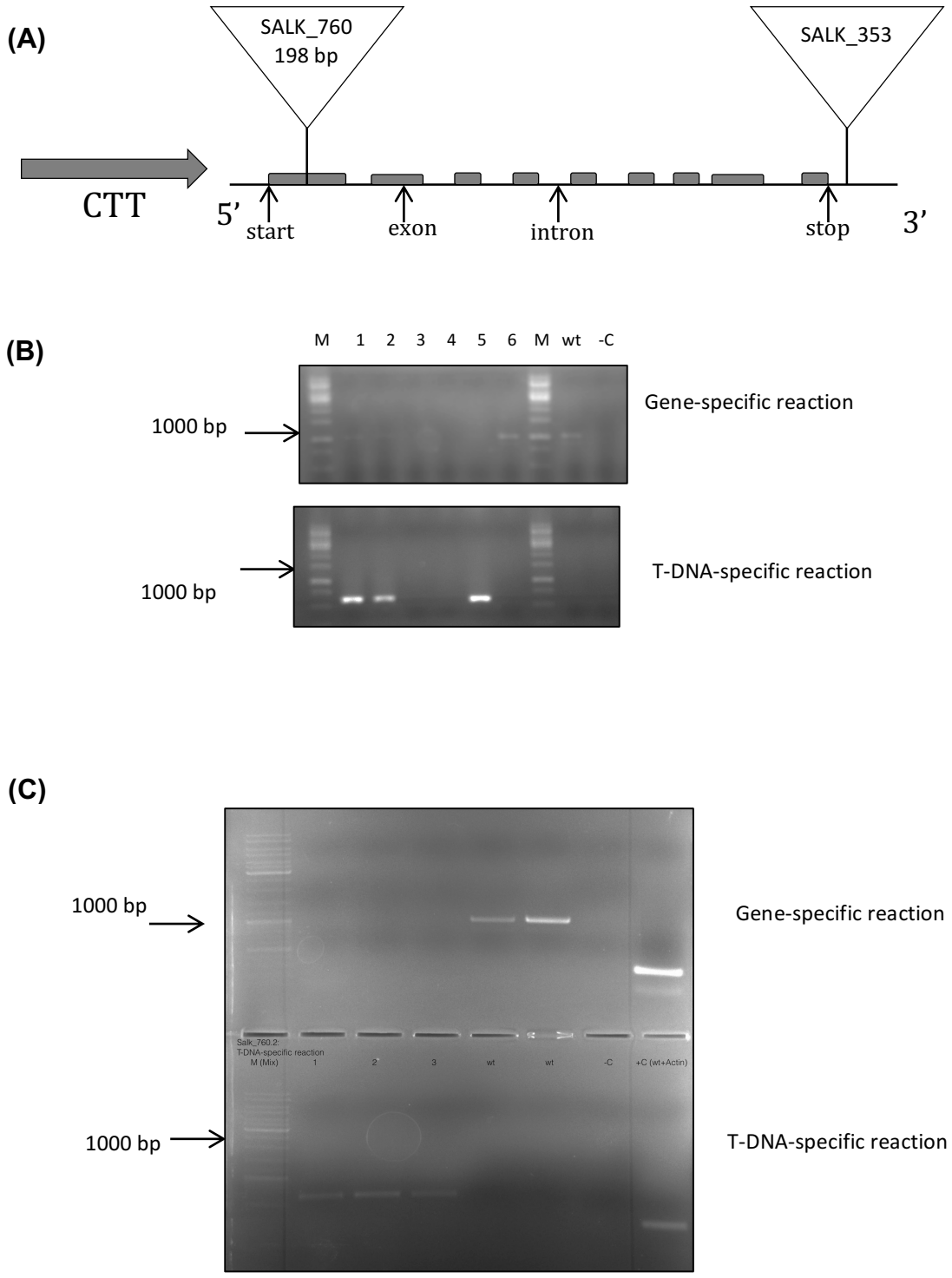

Figure 5.1: Selection of the homozygous SALK_760 lines. (A) Location sites of T-DNA insertion mutants in the CTT gene; exon–intron structure of Arabidopsis CTT, indicating the location of SALK_760 and SALK_353 insertions. **(B)** PCR analysis indicated plant genotypes that employ primer pairs specific to the T-DNA SALK_760 insertions into CTT. **(C)** Screening the segregation from plant 5. Molecular marker (M), wild type (wt), negative control (-C) and homozygous segregation, which was selected to screen the next generation (5); numbers indicate mutant plants.

5.2.1.2. Screening the transcript expression of the CTT insertion mutant line

Expression analysis of the CTT mutant was performed using semi-quantitative RT-PCR analysis with DNA samples taken from leaves. The investigation was carried out to assess the transcript expression level of CTT line 3. RNA samples were isolated from frozen leaf tissue of homozygous lines for the T-DNA SALK_760 insertion mutants in the *Arabidopsis* CTT gene, and one microgram of RNA was used to synthesise cDNA for the semi-quantitative RT-PCR analysis. Prior to this, the RNA quality was checked using NanoDrop. The primers used in this study are shown in Table 5.1; the actin primers (forward primer: CGT CTT CCC CTC CAT CG and reverse primer: CTC GTT AAT GTC ACG CAC) were used as control primers throughout the RT-PCR analysis. The PCR reaction was run under various PCR conditions; the only change was in the PCR cycles. The different range of these cycles was used to ensure that the expression was detected. The numbers of cycles used were 20, 25 and 30, and the PCR products were resolved using agarose gel electrophoresis. The results showed that there was no signal of amplification at 20 cycles; a low detection level of the WT sample was observed at 25 cycles; and no amplification was found in the third plant of SALK_760 line 5 at 25 cycles. At 30 cycles, a low detection level was observed in line 3 with a nonspecific band. Therefore, all transcript analyses found evidence of expression in the WT at 25 cycles; however, CTT mutant expression began to be observed at 30 cycles and showed a similar level to the WT. Consequently, RNAi constructs were designed to knock out CTT (Figure 5.2).

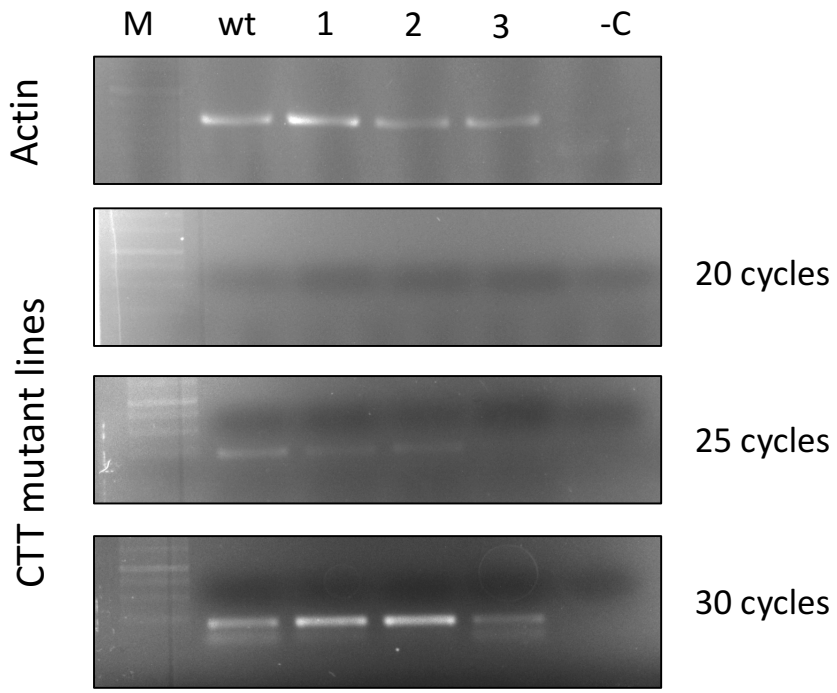

Figure 5.2: RT-PCR analysis of CTT lines. Plants were grown in soil. RNA was extracted from leaves to synthesise cDNA, which was used as a product in the RT-PCR analysis. WT and CTT fragments were amplified using different numbers of cycles, specifically, 20, 25, and 30 cycles. The control was actin, which was amplified with 35 cycles. Samples were run on 1% agarose for 35 min.

5.2.2. Synthesis of RNAi constructs to knock out CTT and AtFolt1

5.2.2.1. Creating the AtFolt1 and CTT constructs using Golden Gate cloning

Because suitable T-DNA mutants in the *AtFolt1* transporter gene were not available and only the homozygous line of the CTT mutant did not affect the expression level, the RNAi technique was used as an alternative method to inhibit the AtFolt1 and CTT transporter genes to investigate the effect of the absence of both genes on Arabidopsis growth and TPP levels. RNAi constructs of AtFolt1 and CTT were synthesised as described in Engler (2009). The target regions were selected in the AtFolt1 and CTT cDNA sequences based on the following criteria: The selected region was found in both AtFolt1 and CTT, with 303 and 252 bp, respectively. The constructs were designed with antisense and sense orientations linked by an actin intron consisting of 515 bp. Both constructs were sent to Invitrogen for synthesis level 0. When level 0 plasmids of AtFolt1 and CTT arrived, a DNA concentration of 100 ng/µl was prepared for each assembly piece. Thus, the reaction was set up separately for each construct. The reaction mixture was 100 ng each of linearised vector level 1 backbone, p35S promoter, NOS terminator and the target sequence; in addition, 1 µl each of restriction enzymes BsaI and NEB T4 ligase were added to the reaction mixture with 1.5 µl 10X NEB buffer. These restriction enzymes were used to assemble the p35S promoter, target sequence and NOS terminator to produce the level 1 acceptor. After adding dH_2O, the total volume of the reaction was 15 µl. One preparation of the reaction was completed and the reaction assembly was performed in a thermocycler under the following conditions: 3 min at 37 °C and 4 min at 16 °C for 25 cycles, followed by 5 min at

50 °C and 5 min at 80 °C for one cycle. Then, 1–2 µl of the assembled reaction product was transferred into *E. coli*–competent cells and plated on an LB plate containing ampicillin, IPTG (200 mg/ml) and X-gal (50 mg/ml). The level 1 acceptor contained a lacZ cassette, so IPTG was used to induce β-galactosidase (β-gal) expression, as β-gal will hydrolyse X-gal to create 5,5'-dibromo-4,4'-dichloro-indigo (blue product). When the insert is present, it will disrupt this reaction and the colony will be white. This is known as blue–white screening, and it is used to identify the presence of inserts in colonies. Depending on this technique, five positive colonies (white colonies) were selected and checked by PCR using scr_pL1M_R primers (Table 5.1). Finally, the positive colonies were cultured, and the plasmid was extracted using a MiniPrep kit; thus, the level 1 acceptors of AtFolt1 and CTT were ready for use as a target module to produce level 2.

To generate level 2 (the expression vector), the reaction mixture was set up as carried out in level 1 with the following modifications: The linearised vector level 2 backbone was used as the acceptor instead of the linearised vector level 1 backbone; the restriction enzyme was replaced with the BpiI enzyme; and a 100-ng hygromycin piece was added. The total volume was 15 µl, and the PCR conditions were performed as in the assembly reaction of the level 1 module. The assembled reaction product was transferred into *E. coli*–competent cells and plated on an LB plate containing kan as a selection marker. The positive colonies of each construct were selected by PCR and transferred into *Agrobacterium* and checked by the digestion enzyme HindIII to make sure the insert was still present. Finally, the expression modules of AtFolt1 and CTT were transferred into plants (Figures 5.3, 5.4 and 5.5).

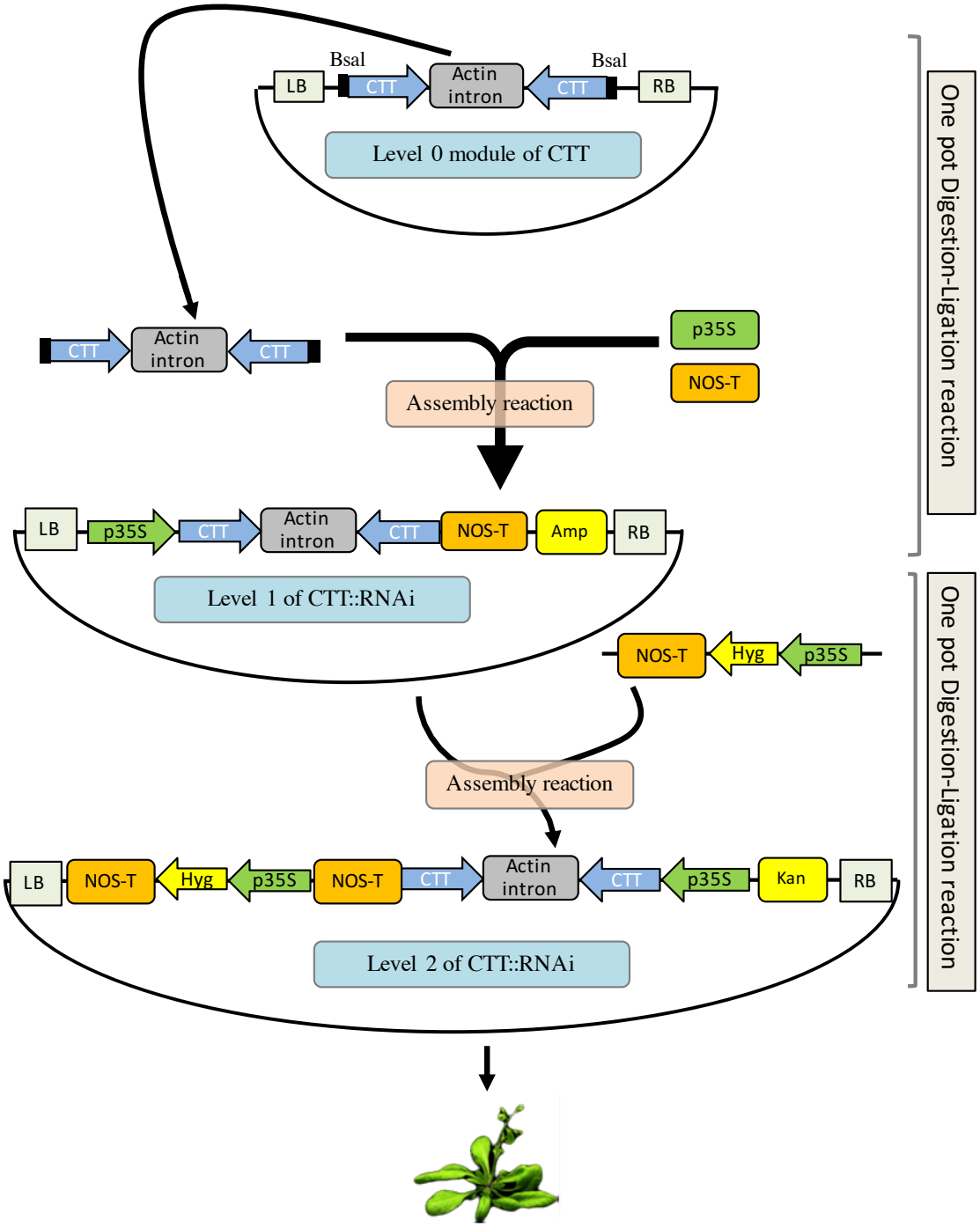

Figure 5.3: Scheme of designing the CTT::RNAi construct for knocking out CTT in plants. (A) Level 0 backbone containing the actin intron between the target of antisense and sense orientation of the CTT coding sequence (CTT), which was digested and ligated with 35S promoter (p35S) and NOS terminator (NOS-T) in the level 1 backbone vector. **(B)** 35S::CTT::intron::A.CTT::NOS was digested from the level 1 plasmid and cloned into the level 2 vector with a hygromycin piece added in one digestion–ligation reaction to generate the expression vector.

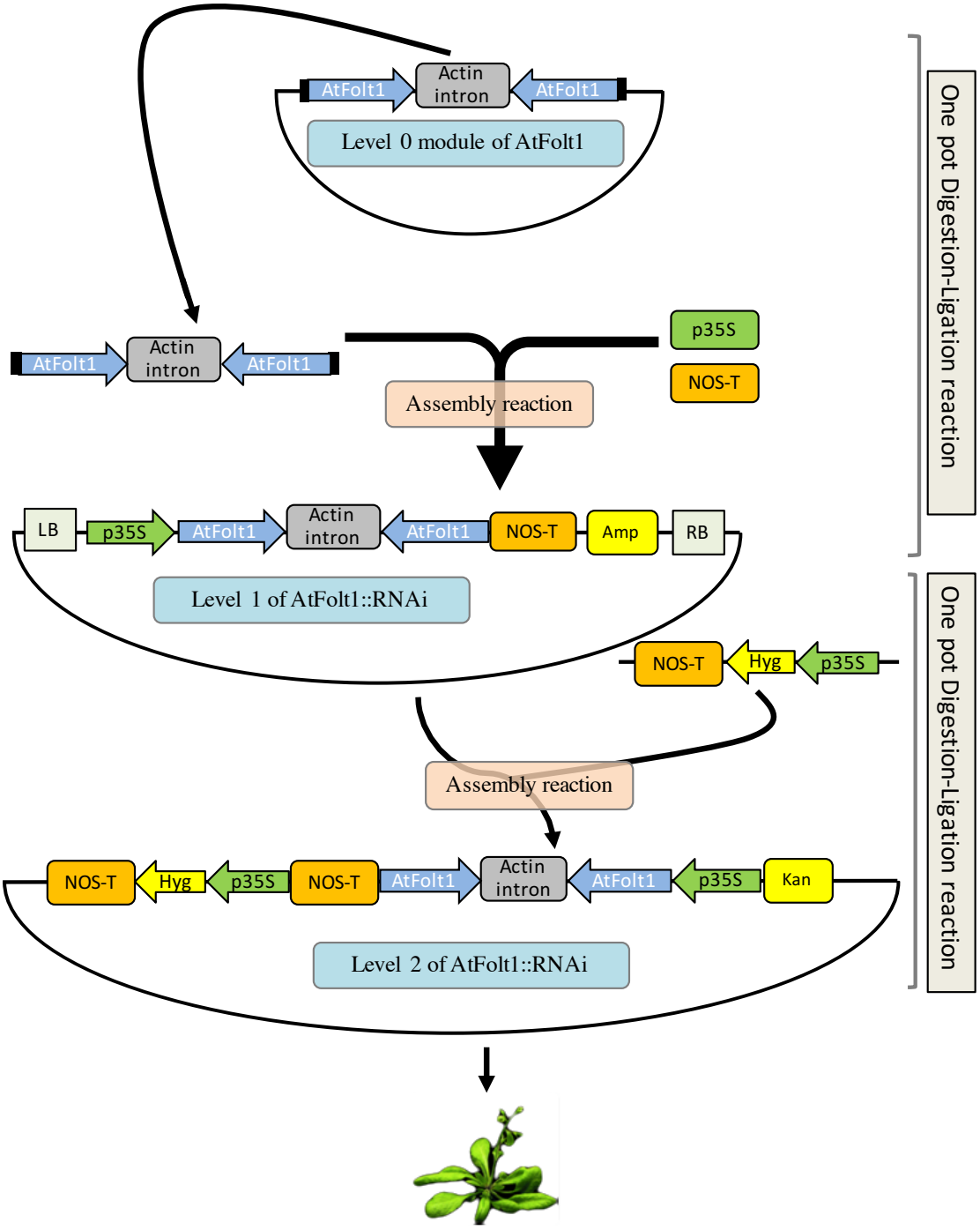

Figure 5.4: Building the AtFolt1::RNAi construct for knocking out AtFolt1 in plants. (A) Level 0 backbone containing the target of antisense and sense orientation of AtFolt1 coding sequence (AtFolt1) linked by the actin intron, which was digested and ligated with the 35S promoter (p35S) and NOS terminator (NOS-T) in the level 1 backbone vector. The level 1 plasmid carries the ampicillin resistance gene as a selectable marker in bacteria. **(B)** 35S::Folt1::intron::A.Folt1::NOS was digested from the level 1 plasmid and cloned into the level 2 vector with the addition of hygromycin in one digestion–ligation reaction to generate the expression vector.

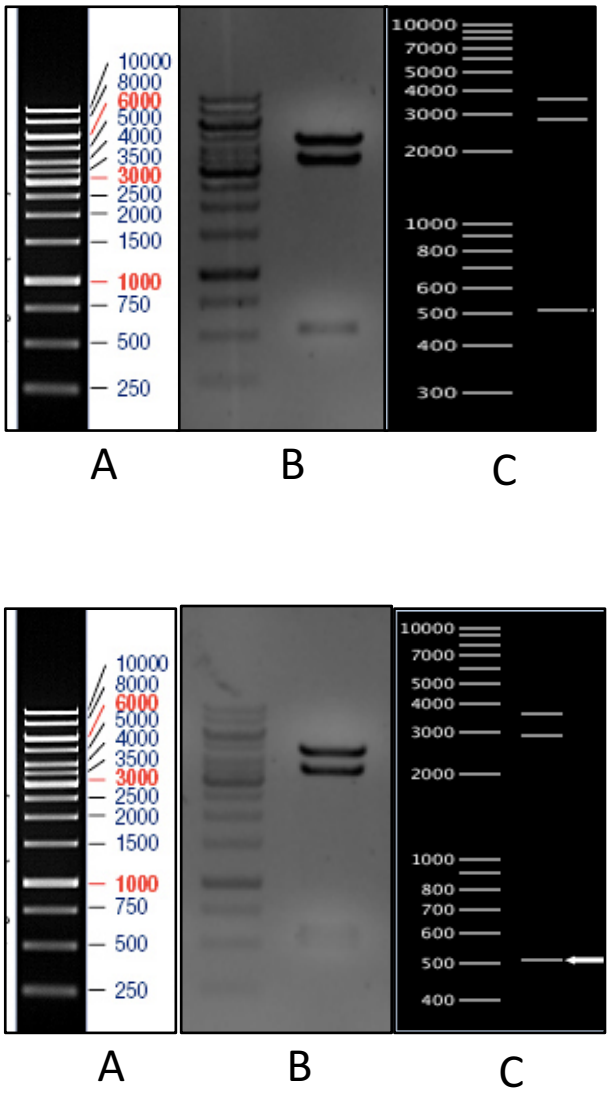

Figure 5.5: Screening level 2 of CTTi:RNAi and AtFolt1:RNAi by restriction digestion. (Top) Digestion of CTT:RNAi; **(bottom)** digestion of AtFolt1:RNAi. Both constructs were digested using HindIII enzyme. **(A)** marker, **(B)** digestion of the target, **(C)** the expected digestion.

5.2.2.2. Screening transgenic plants of AtFolt1 and CTT

AtFolt1 and CTT plants were screened using a hygromycin selection marker in the expression vector (level 2 backbone) to identify transgenic plants. T1 seeds were sown on LB plates containing 10% hygromycin and incubated in a growth room under controlled conditions (25 °C, 16 h light, 8 h dark) for 2 weeks. Then, the hygromycin-resistant plants were transferred to soil and moved back to the growth room under the same controlled environment. The plants were watered regularly three times a week. Once the plants reached 4–5 weeks old, samples were collected to extract RNA and screen the transcript expression level. The qRT-PCR results showed that the expression of the CTT transcript was reduced by about fivefold compared to the WT, whereas the transcript expression of AtFolt1 was reduced by more than 50% (Figures 5.6 and 5.7).

The seeds of the T1 plants were collected and stored in the dark for 2 weeks before growing them to conduct an analysis of the next generation. Some of the transgenic seeds of AtFolt1 and CTT T1 plants were grown on plates containing 10% hygromycin verify that the insert still existed in the T2 plants.

(A)

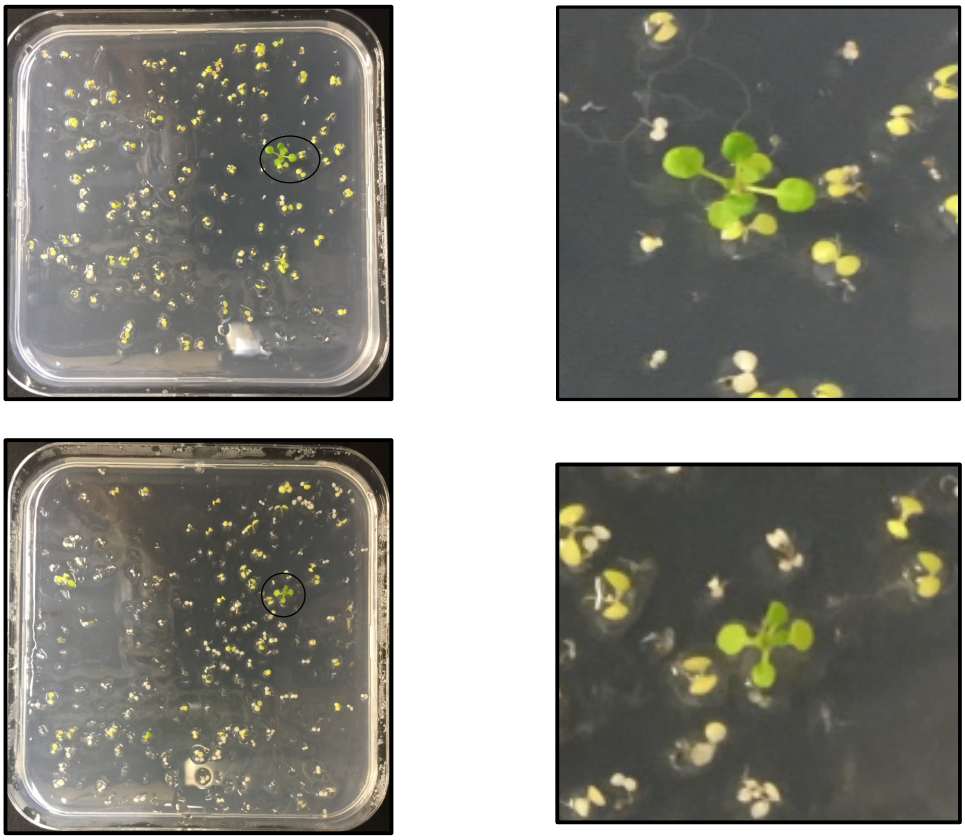

(B)

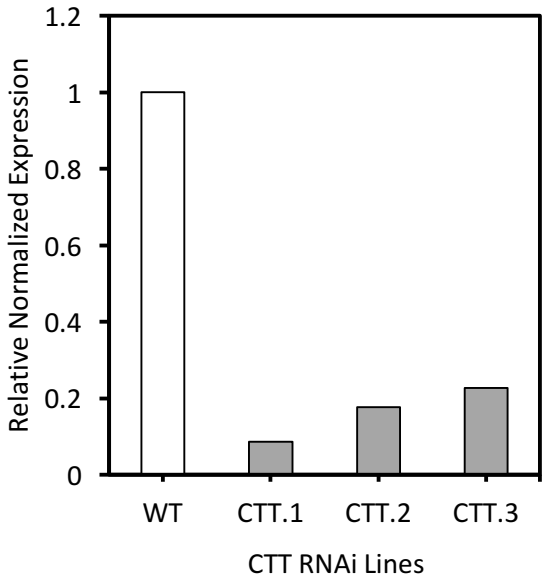

Figure 5.6: Screening of T1 progeny of CTT::RNAi plants. (A) T1 plants were grown on selection plates with hygromycin and kept in a long-day growth room to allow growth for 2 weeks before moving to soil. **(B)** Only three plants were resistant to hygromycin, and the transcript expression was screened by qPCR.

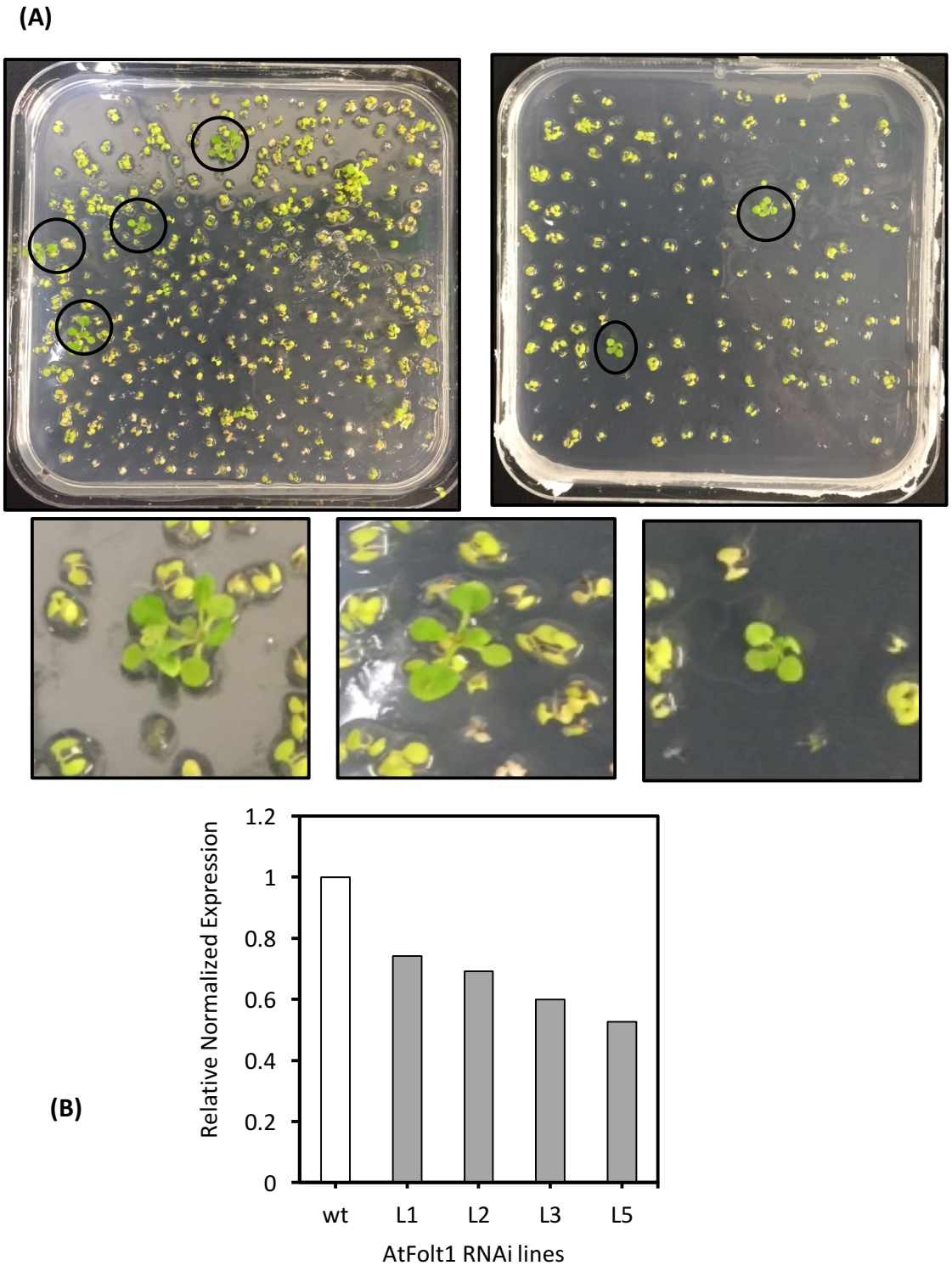

Figure 5.7: T1 screening of AtFolt1::RNAi plants. (A) T1 generation plants were grown on hygromycin plates and stored in a growth room for 2 weeks. Then, resistant plants were moved to soil. **(B)** Plants resistant to hygromycin were screened by qRT-PCR. AtFolt1 RNAi lines are indicated by (L(n)).

5.2.3. Growth analysis of CTT::RNAi and AtFolt1::RNAi

5.2.3.1. The effect of CTT::RNAi on plant growth

The effect of CTT on plant growth was presented previously depending on the mutant analysis results. Here, the results will be introduced after CTT is knocked out, using RNAi to confirm the results obtained via two different techniques. After positive lines of CTT were selected in T1 plants, a new experiment was set up on the Col_0 WT and the second generation of knockout CTT plants (T2 plants). Two independent lines of seeds, obtained from T1 CTT plants, were grown directly in soil with triplicates of 10 plants. Seeds were allowed to grow under normal environmental conditions over a short day (8 h light, 16 h dark, 22 °C), and the measurement of the leaf area was initiated when the first four leaves were completely developed. The results of the measurements showed that the leaf area was significantly smaller than that of the wild type by about 25%. This phenotype of the leaf area did not appear when the plant was small, but started to appear after 24 days, and it was clear when the plants reached 33 days old. Interestingly, not only was the leaf area affected, but the leaf shape was also altered; the leaves were observed to be wavy on the leaf border. This did not affect the leaves when the plant was younger; rather, it only became apparent after the plant developed (Figures 4.8c and 4.8d). The stem length of CTT::RNAi lines seem to be slightly shorter than the WT, but the difference was not significant. The length of the CTT was 24.6 cm, whereas that of the WT was 25.8 cm. However, the number of secondary stems on the main stem was 6.2 in the CTT and 7.9 in the WT. This represented a small but significant difference (Figures 5.8–5.12). These

observations suggest that CTT has a limited effect on *Arabidopsis* growth, and it is important for plant productions, at least in *Arabidopsis*.

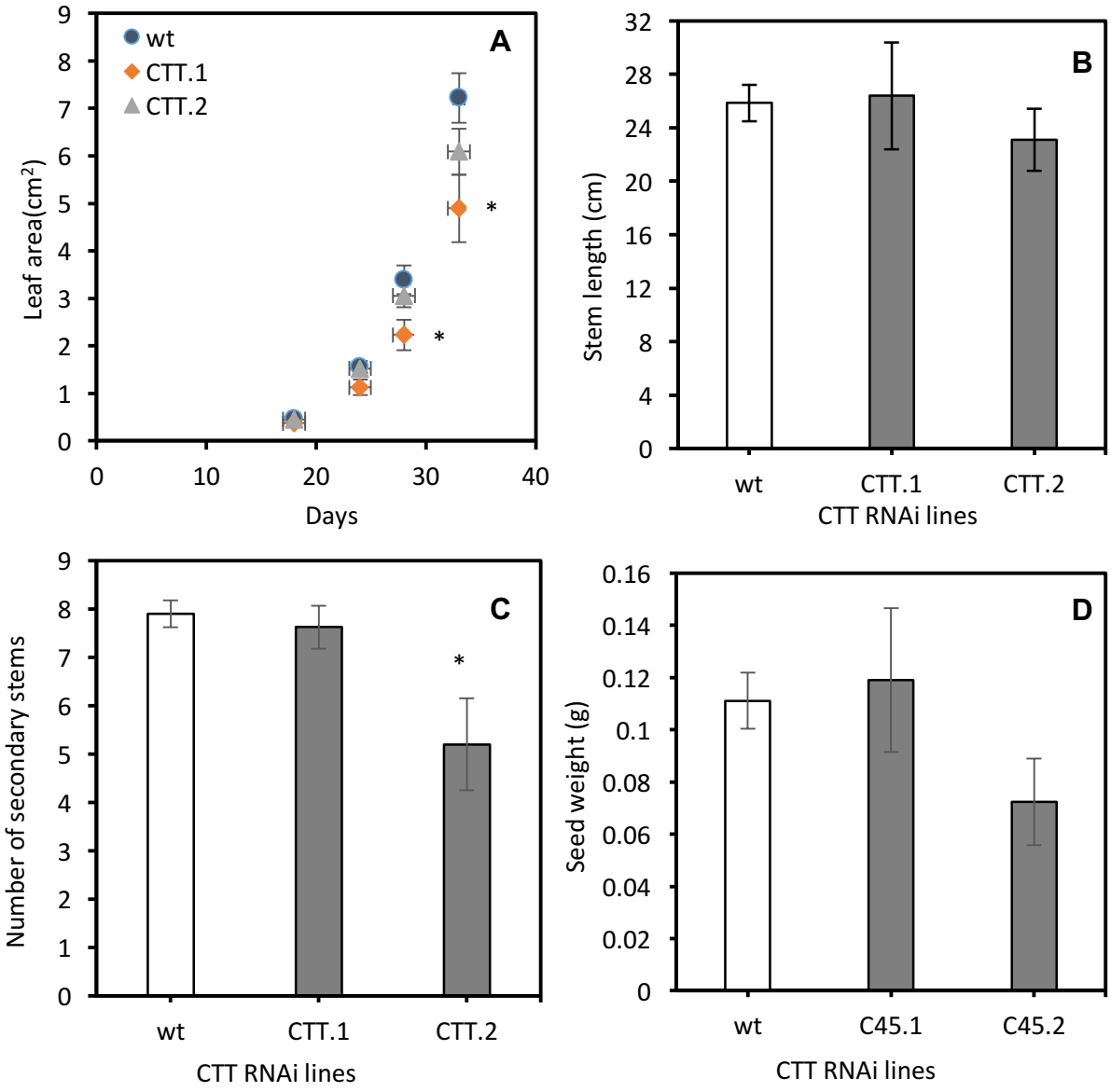

Figure 5.8: Flowering phenotype of CTT::RNAi and wild type plants. Plants were grown directly on soil under a controlled environment in a short-day growth room (8 h light, 16 h dark, 22 °C). **(A)** The leaf area of two independent CTT RNAi lines. Numbers indicate growth period (days). **(B)** The stem length of two independent lines. **(C)** Number of secondary stems of the two independent lines. **(D)** Seed weight. Error bars indicate the standard error (SE) from 10 replicates. Significant changes from the WT were determined by one-way analysis of variance (ANOVA) for $p < 0.05$ and indicated by an asterisk.

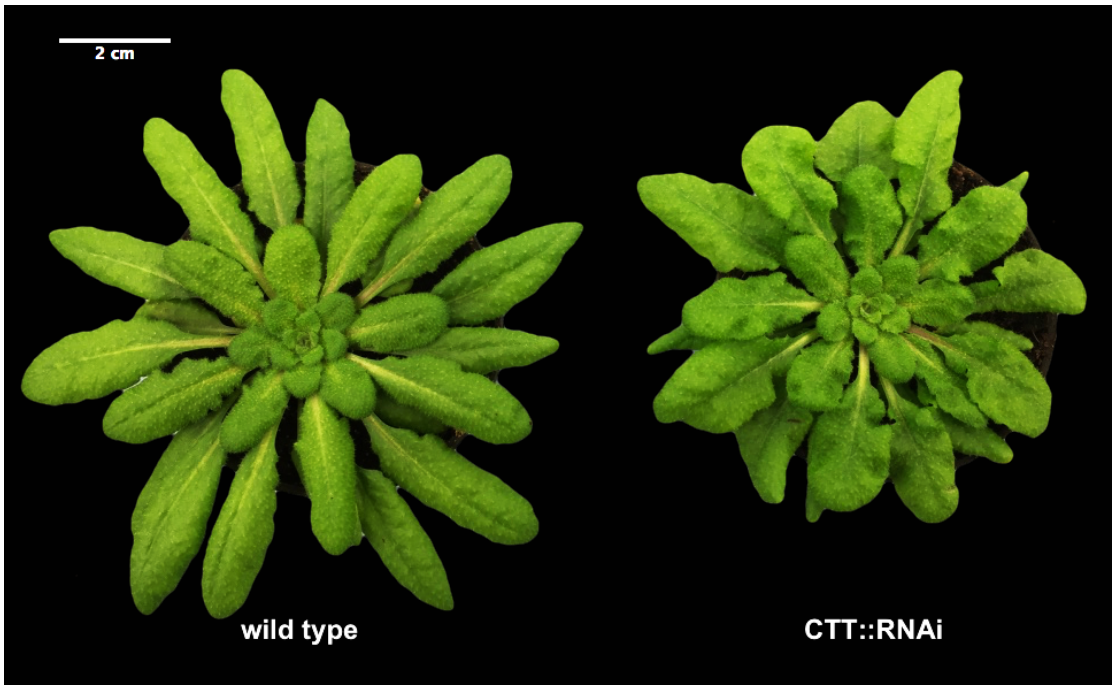

Figure 5.9: Phenotype of *Arabidopsis* CTTi::RNAi. Plants were grown directly in soil under a controlled environment in a short-day growth room (8 h light, 16 h dark, 22 °C). **(Left)** Wild-type *Arabidopsis* col.0 (WT), **(right)** CTT RNAi plant (CTT). Photos were taken when the plants were 50 days old.

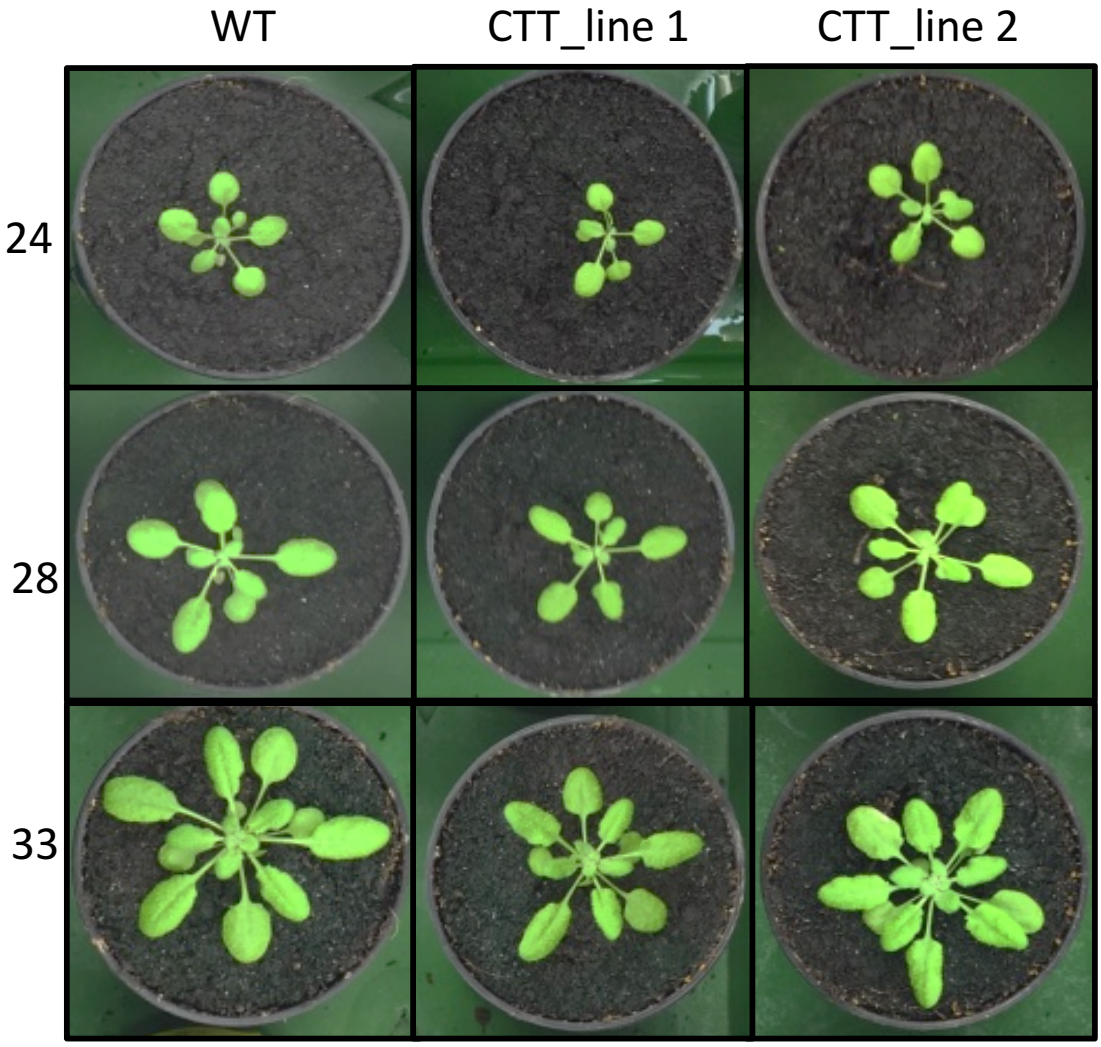

Figure 5.10: Phenotype of Arabidopsis CTT::RNAi. Plants were grown directly in soil under a controlled environment in a short-day growth room (8 h light, 16 h dark, 22 °C). Wild-type plants are shown in the left column (WT). Two CTT independent lines as shown, in the middle (CTT_line 1) and on the right (CTT_line 2). Numbers indicate the days of plant growth.

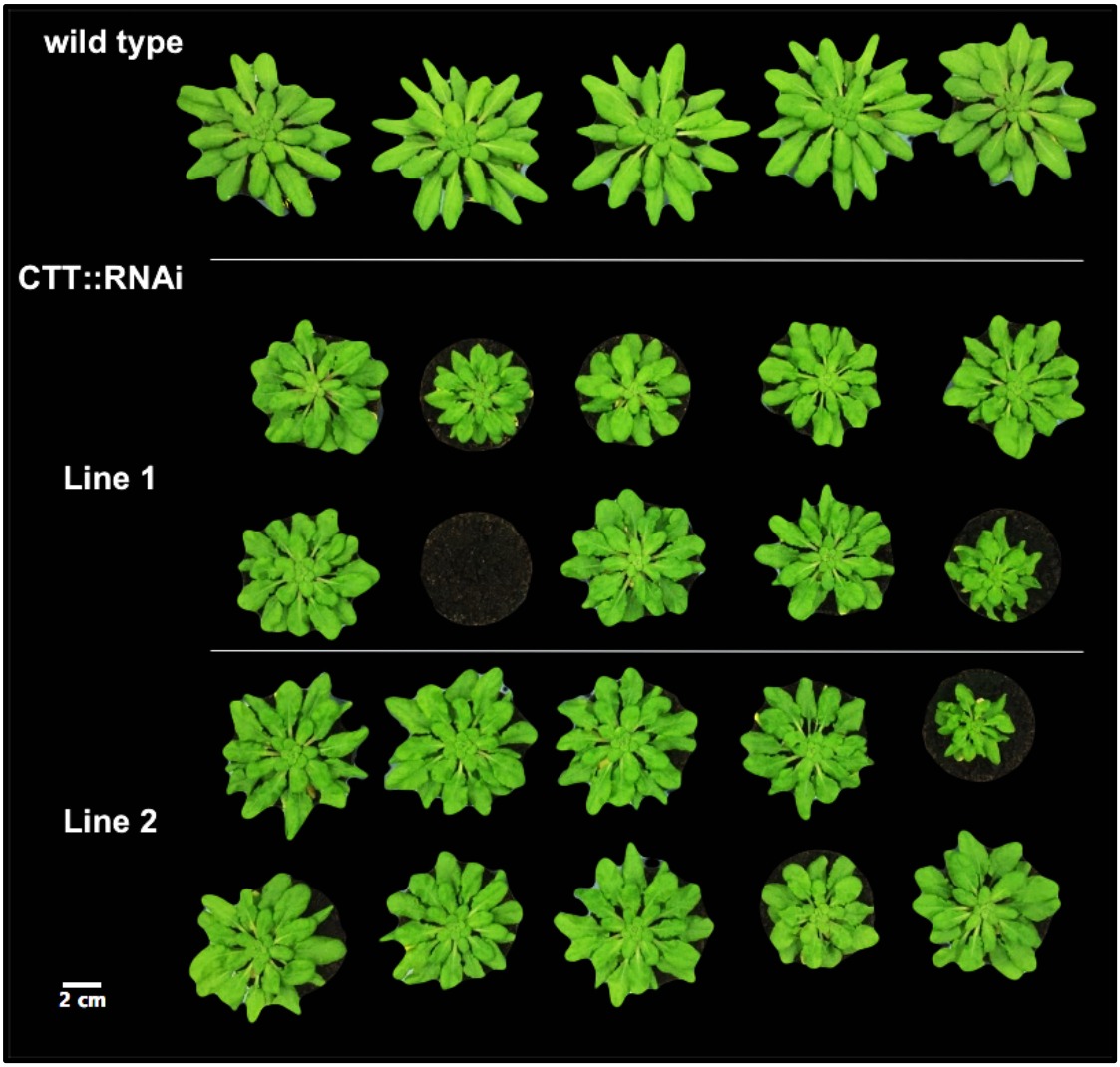

Figure 5.11: Phenotype of Arabidopsis CTTi::RNAi. Plants were grown directly in soil under a controlled environment in a short-day growth room (8 h light, 16 h dark, 22 °C). Wild-type plants (WT) are shown on the top. Two CTT independent lines are shown in the middle (CTT_line 1) and on the bottom (CTT_line 2). Photos were taken when the plants were 50 days old.

(A)

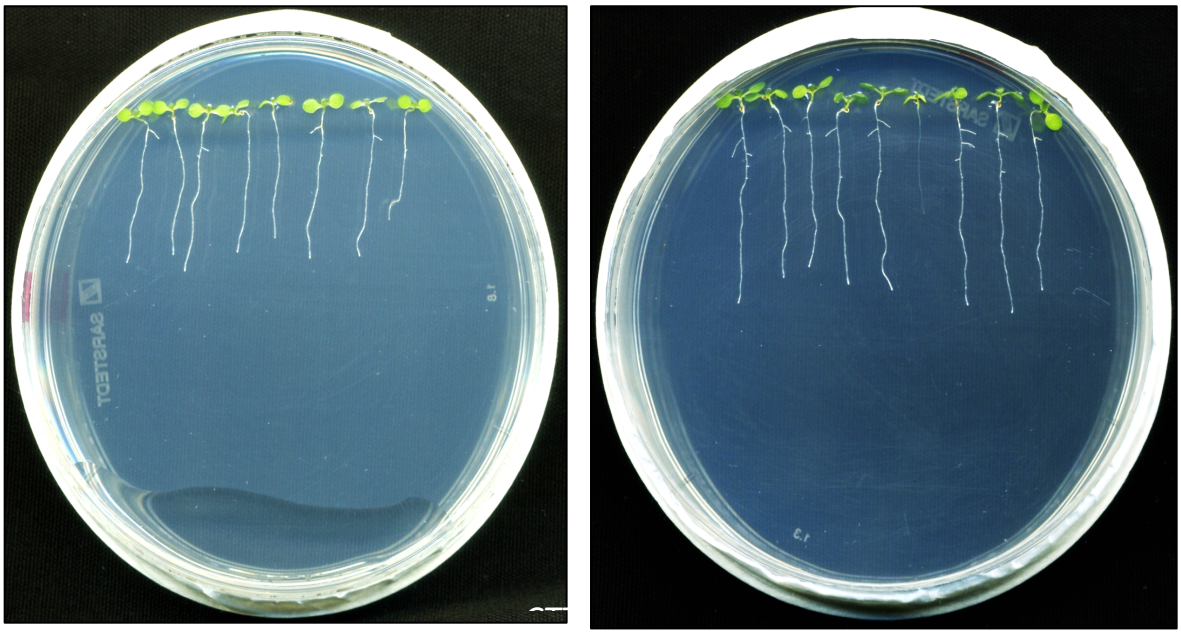

(B)

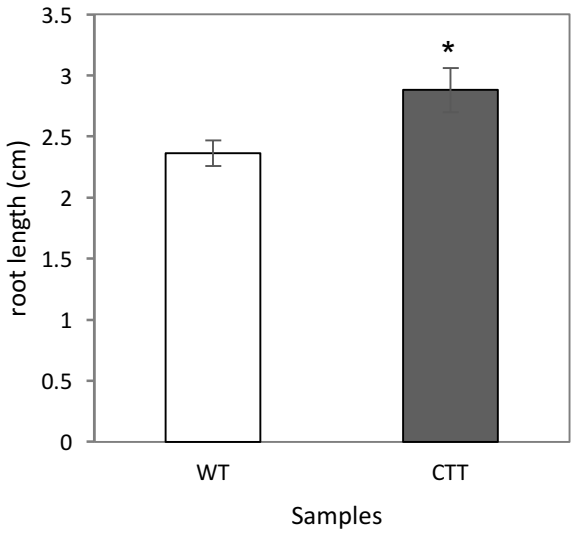

Figure 5.12: Length of CTT::RNAi root. (A) Seeds were grown on MS media and allowed to grow for 10 days. On the top, photos for the wild type **(wt**) are shown on the left and CTT RNAi root on the right. **(B)** bar chart represents the root length. Significant changes to the wild type were determined by one-way analysis of variance (ANOVA) for $p < 0.05$ and indicated by an asterisk**.**

5.2.3.2. Analysis of the influence of AtFolt1::RNAi absence on plant growth

To investigate the effect of AtFolt1 on plant growth, especially on leaf area and plant length, an experiment was performed on the Col_0 WT and the second generation of KO AtFolt1 plants (T2 plants). This experiment was set up for a short day (8 h light, 16 h dark, 22 °C). Two independent lines were grown directly in soil with triplicates of 10 plants, either WT or KO AtFolt1. After the first four leaves were completely grown, measurements of their surface area were taken. The results showed that the leaf area of AtFolt1 lines appeared slightly smaller than that of the WT, but the difference was not significant. In addition, the difference in stem length was not significant between AtFolt1 lines and the wild type, at about 21 cm and 25 cm, respectively. The secondary stems were not affected in the absence of the AtFolt1 gene, as no significant change occurred when compared to the WT (Figure 5.13). Therefore, it can be concluded that AtFolt1 does not affect plant growth, at least in the Arabidopsis phenotype.

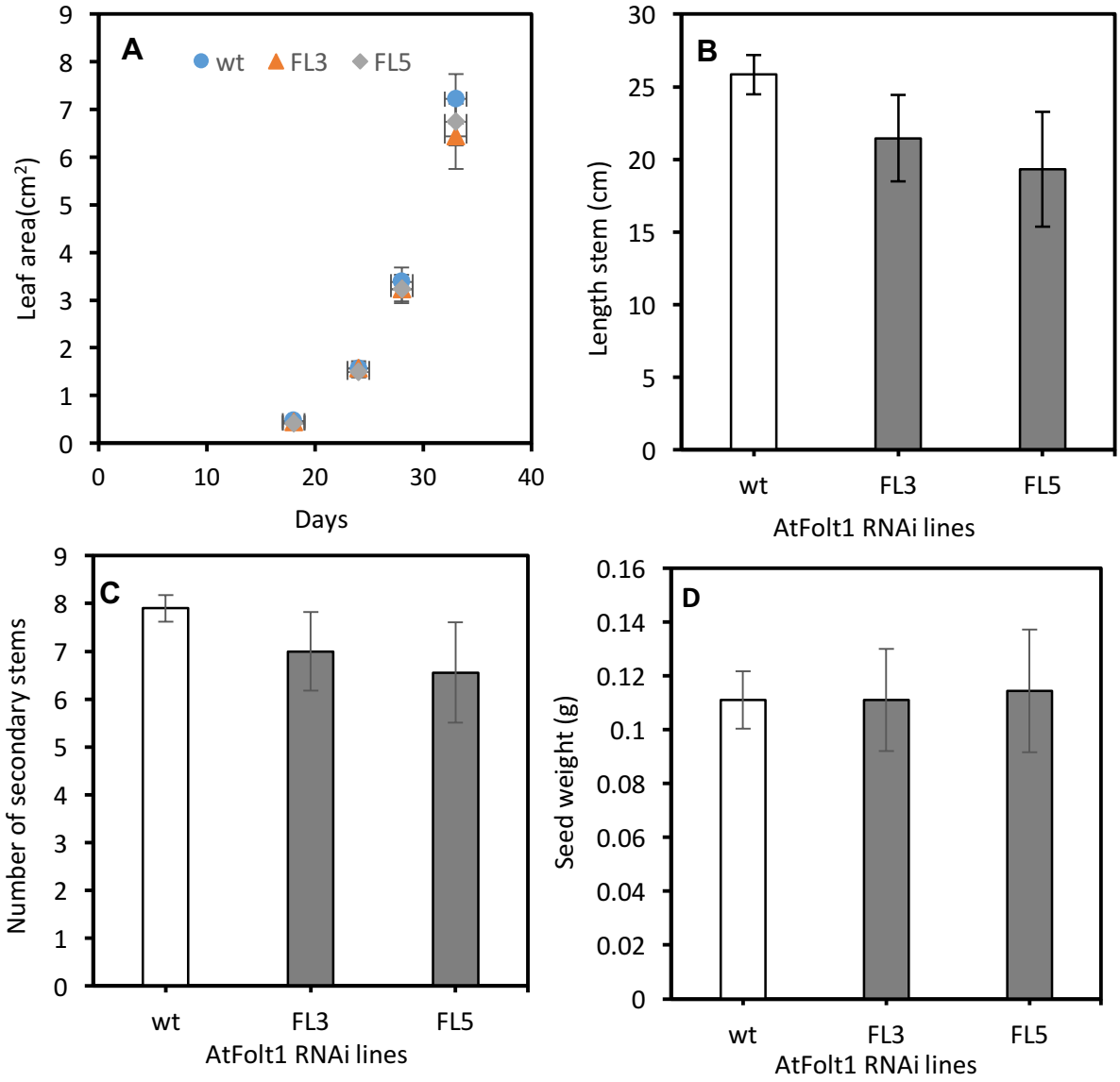

Figure 5.13: Flowering phenotype of AtFolt1::RNAi and wild type (WT) plants. Plants were grown directly in soil under a controlled environment in a short-day growth room (8 h light, 16 h dark, 22 °C). **(A)** Leaf area in two independent AtFolt1 lines (AtFolt1.1 and AtFolt1.2). **(B)** Length of the main stem of the individual lines. **(C)** The number of secondary stems of individual lines. Error bars indicate the standard deviation (SD) from 10 replicates. Significant changes from the WT were determined by one-way analysis of variance (ANOVA) for $p < 0.05$ and are indicated by an asterisk.

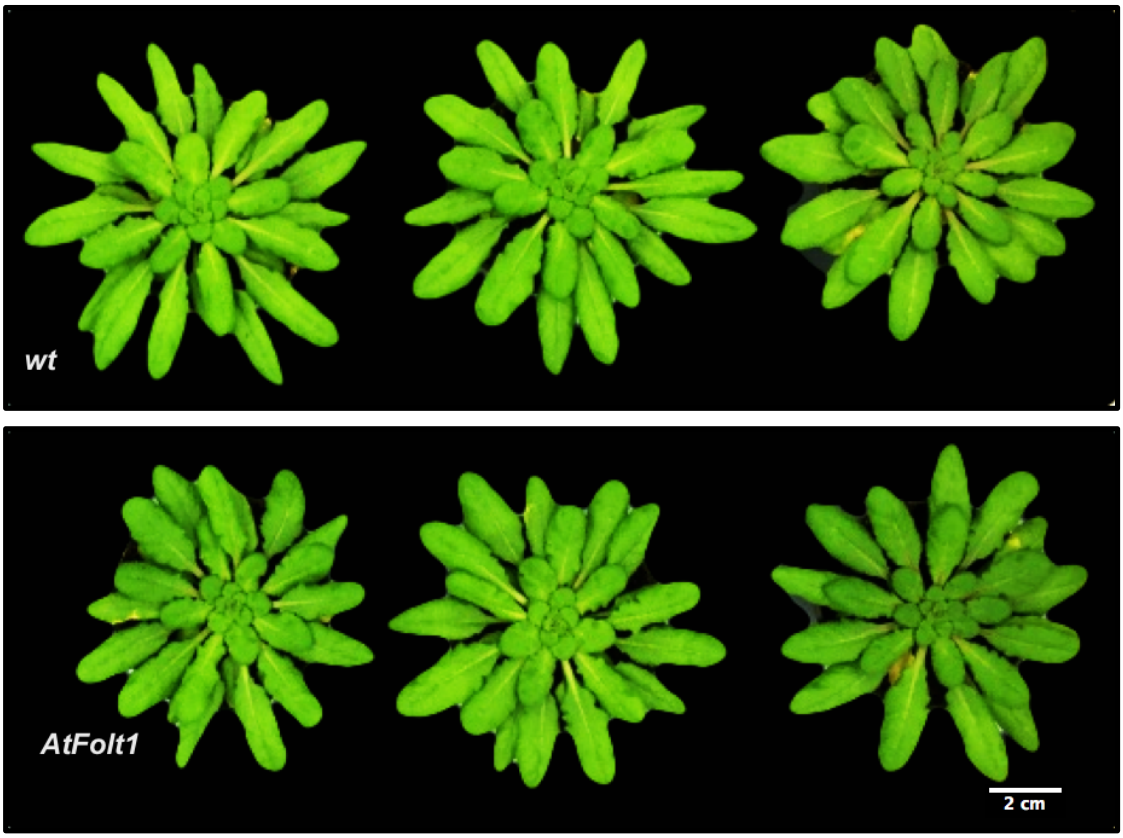

Figure 5.14: Phenotype of the Arabidopsis AtFolt1 RNAi plant. Plants were grown directly in soil under a controlled environment in a short-day growth room (8 h light, 16 h dark, 22 °C). Photos were taken when the plants were 50 days old.

(A)

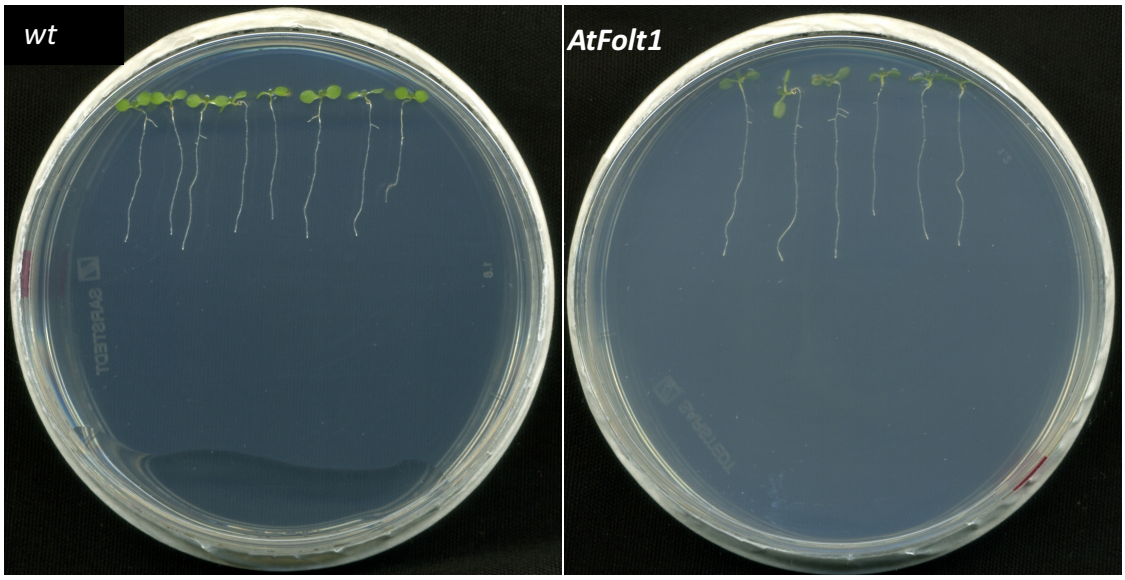

(B)

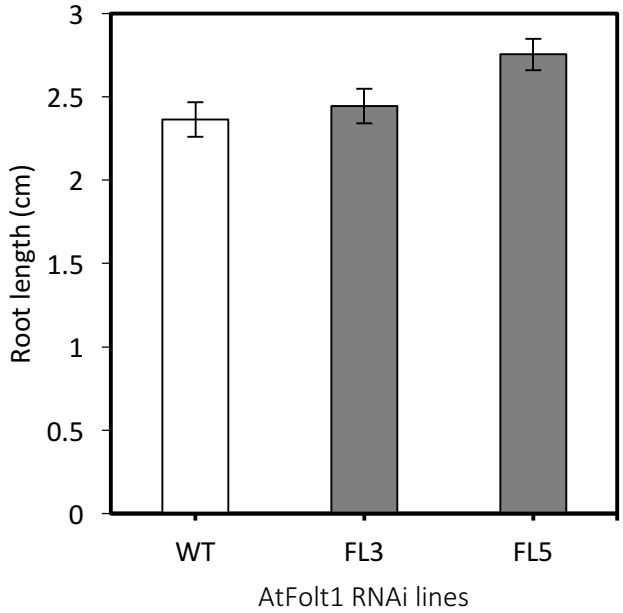

Figure 5.15: Length of AtFolt1 root. (A) Seeds were grown on MS media and allow to grow for 10 days. Photos for wild type (wt) root growth are on the left and AtFolt1 RNAi root growth on the right. **(B)** Bar chart represents the root length. Significant changes to the wild type were determined by one-way analysis of variance (ANOVA) for $p < 0.05$ and are indicated by an asterisk.

5.2.4. Is AtFolt1 or CTT a TPP carrier in *Arabidopsis thaliana*?

To answer the question of whether AtFolt1 or CTT is a TPP carrier in *Arabidopsis thaliana*, it was necessary to measure TPP in AtFolt1 and CTT transgenic plants. The experiment was set up to determine the TPP content by HPLC analysis. Plants were grown under controlled normal conditions in a short-day growth room (8 h light, 16 h dark, 22 °C). Then, thiamine was extracted from the leaves to carry out the HPLC analysis. The HPLC results showed that there was a reduction in the TPP levels, both in AtFolt1 and CTT, compared with the WT. The reduction of the TPP and thiamine in AtFolt1::RNAi lines were between 25 – 55 % and 56 – 62 %, respectively. Werease, the reduction of the TPP in CTT::RNAi lines was between 30 to 60 % and thiamine was not clearly detected and more investigations required (Figures 5.16 to 5.18).

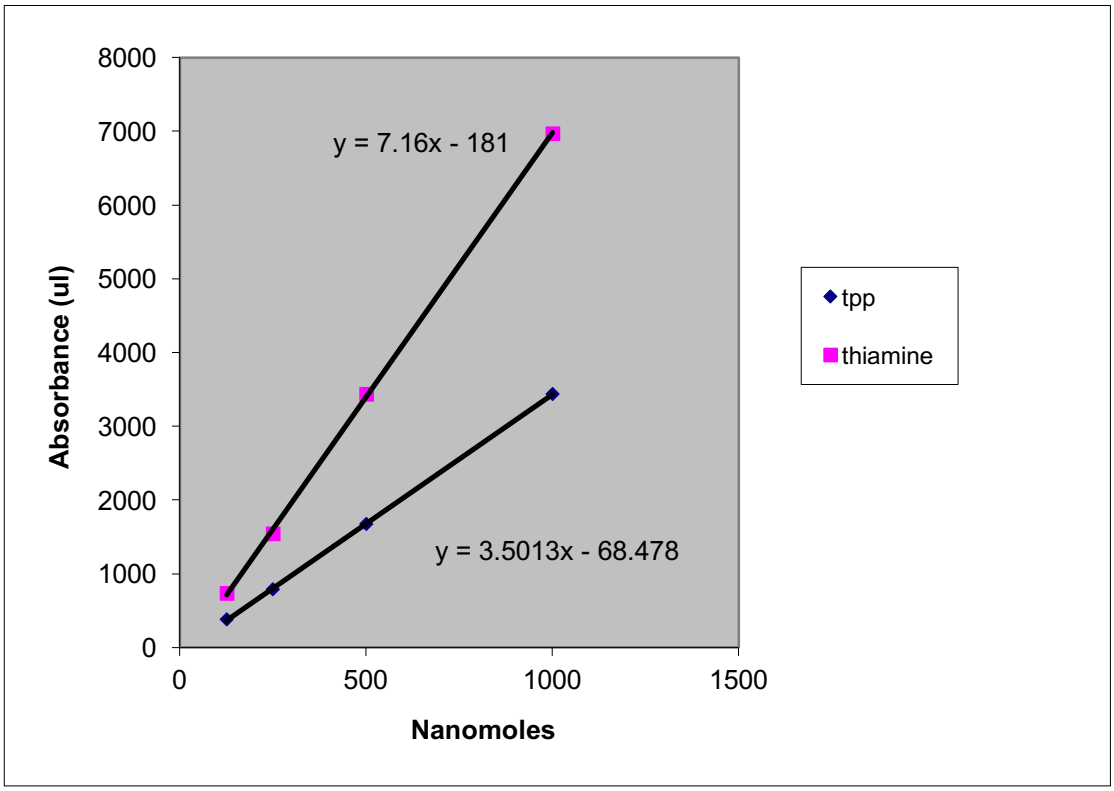

Figure 5.16: Standard thiamine and TPP curves plotted using reverse-phase chromatography. Thiamine and TPP were prepared with known quantities in 0.1% hydrochloric acid to the desired concentration to produce a standard curve.

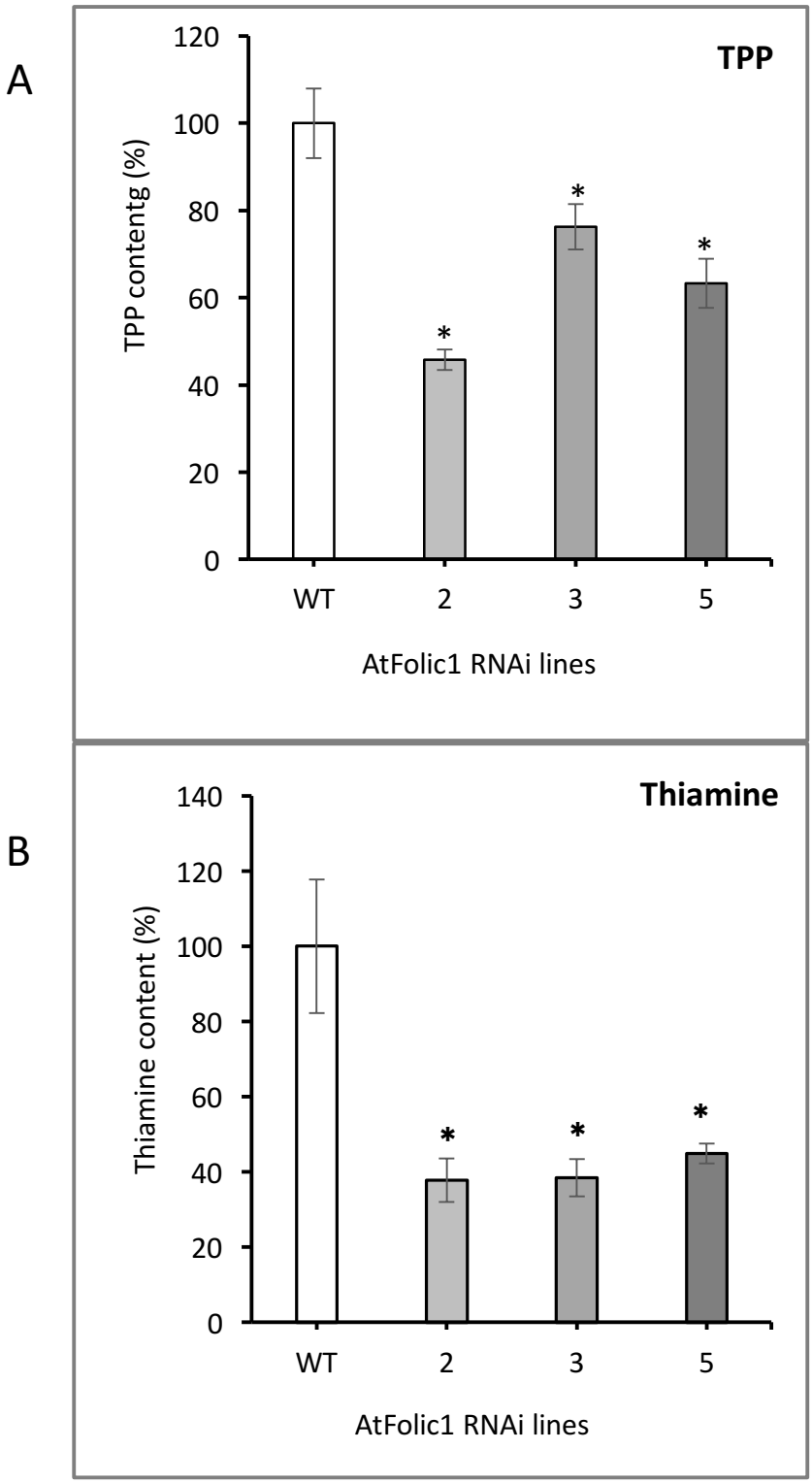

Figure 5.17: Quantification of the TPP levels determined in AtFolt1::RNAi and the wild type (WT). (A) Quantification of the TPP, **(B)** thiamine content in the leaves of three independent AtFolt1::RNAi lines and the WT. Plants were grown in soil in a short-day growth room (8 h light, 16 h dark, 22 °C). Thiamine was extracted from the AtFolt1 RNAi lines and WT leaves. Values are the average of six biological replicates, with the error bar representing the standard error (SE). Statistically significant changes for TPP content compared to the WT were determined by one-way analysis of variance (ANOVA). An asterisk indicates significance at $p < 0.05$.

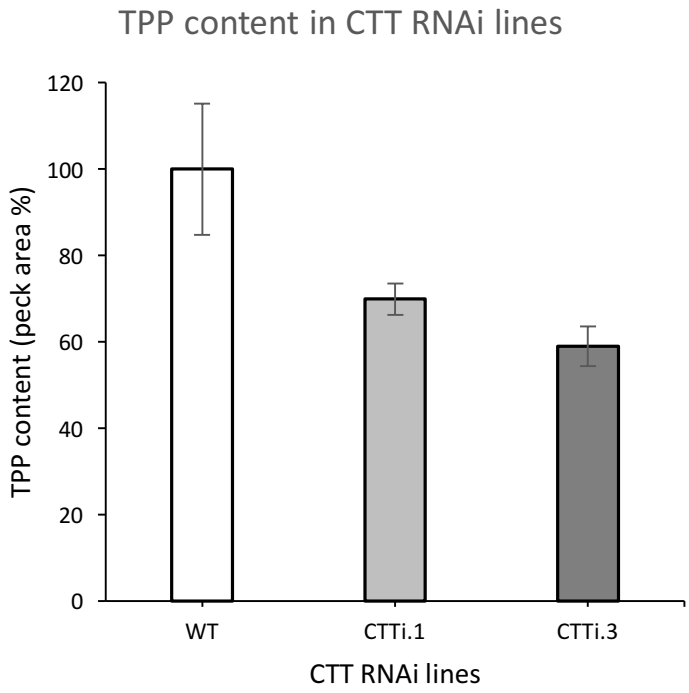

Figure 5.18: Quantification of TPP levels determined in CTT::RNAi and the wild type (WT). Quantification of the TPP content in the leaves of two independent CTT lines and the WT. Plants were grown in soil in a short-day growth room (8 h light, 16 h dark, 22 °C). Thiamine was extracted from CTT lines and WT leaves. Values are the average of three biological replicates, with the error bar representing the standard deviation (SD). Statistically significant changes for the TPP content compared to the WT were determined by one-way analysis of variance (ANOVA). An asterisk indicates significance at $p < 0.05$.

5.3. Discussion

TPP is an active form of thiamine; its synthesis only occurs in cytosol when thiamine is converted to TPP by thiamine diphosphokinase, which is a cytosolic enzyme (Ajjawi et al., 2007). TPP must be exported from cytosol to mitochondria and chloroplasts to be utilised as a cofactor for TPP-dependent enzymes in a number of metabolic pathways (Krampitz, 1969). In relation to the mitochondrial TPP, *Arabidopsis* AtTpc1 and AtTpc2 are reported to encode mitochondrial TPP carriers (Frelin et al., 2012). In terms of chloroplast, the current study identified two putative plastid TPP transporters, namely CTT and AtFolt1. The study focussed on the importance of CTT and AtFolt1 in *Arabidopsis thaliana* growth and the relation of these transporters to TPP levels.

CTT was identified as a member of the MCF (Millar and Heazlewood, 2003); however, the corresponding gene or protein has not yet been identified or characterised. Then, the CTT activity was inhibited using the RNAi technique. The findings showed that significant changes appeared in the secondary stems on the main stem of the plant. In addition, the leaf area and leaf shape were clearly affected. Previous research has shown that a reduction of thiamine in seeds will reduce the TPP availability in early seedlings, thereby, causing slow, chlorotic growth (Khozaei et al., 2015). According to this, the negative phenotype in our results may be due to a reduction in TPP levels, as our silico findings showed that CTT may be a TPP transporter. To study this hypothesis, the TPP level in the CTT transgenic *Arabidopsis* was determined using HPLC. The findings of the HPLC analysis showed a reduction in two independent lines of CTT by 30 – 60 % in relation to the WT level. This may explain the growth phenotypes on the CTT plants

due to the reduction of TPP, and CTT might has a relation to the TPP carrier in *Arabidopsis*. In contrast, regardless of whether CTT is a chloroplast TPP transporter, it may not be an individual chloroplast TPP transporter because TPP is required for enzymatic reaction in the chloroplast (Frank et al., 2007). To investigate this hypothesis, plastid TPP levels should be measured to determine the TPP level in the chloroplast.

Our second putative chloroplast TPP transporter, AtFolt1, was reported as a folate transporter in *Arabidopsis* (Bedhomme et al., 2005). However, this claim was recently investigated, and the researchers found that the absence of AtFolt1 did not affect the folate level in the chloroplast, and no phenotype appeared on the plants (Bedhomme et al., 2005). There are two possible reasons for this outcome: There may be an alternative folate pathway in plants, or it could be that AtFolt1 is not a folate carrier. I contrast, our in silico results indicated that AtFolt1 could have a similar function for mitochondrial TPP transporters in yeast, humans and plants, depending on the protein structure and the highly conserved region in the C-terminus. The AtFolt1 is located on the chloroplast membrane (Bedhomme et al., 2005). This suggests that AtFolt1 could be a TPP carrier that targets the chloroplast. To address this hypothesis, we inhibited AtFolt1 activity, and the findings agreed with those of a previous study carried out by (Bedhomme et al., 2005). No significant changes occurred in plant growth and in plants grown normally like the WT, at least under normal environmental conditions. However, the interesting results came when the TPP content was measured. HPLC analysis results presented a decrease in TPP levels between 25 to 55 % compared to the WT level.

In conclusion, CTT proved important for plants to grow normally, but AtFolt1 did not affect plant growth, at least under normal plant growth conditions. However, both CTT and AtFolt1 affected TPP levels in *Arabidopsis* leaves.

Chapter 6:

General discussion

Previous studies have shown that chloroplasts and mitochondria contain TPP-dependent enzymes. TPK catalyses the conversion of free thiamine to TPP; TPK is cytosolic, and this means that TPP is made in the cytosol. Two mitochondrial TPP carriers were identified in Arabidopsis, while no chloroplast TPP carriers have been identified (Frelin et al., 2012; Goyer, 2010; Rapala-Kozik et al., 2008; Ajjawi et al., 2007a). The main aims of this project were to identify the chloroplastic thiamine/TPP transporter(s) using plant mitochondrial transporter sequences and to determine the relative importance of different transporters for plant growth.

Comparative genomic analysis indicated that Arabidopsis has two putative chloroplast TPP transporters, AtFolt1 and CTT, based on similarity with previously identified TPP carriers, including Arabidopsis AtTpc1 and 2. This result is in agreement with previous studies that have shown that AtFolt1, CTT and TPP transporters belong to MCF (Picault et al., 2004; Millar and Heaziewood, 2003). The members of this family target mitochondria, chloroplasts or peroxisomal membranes (Palmieri et al., 2001; Haferkamp, 2007; Agrimi et al., 2011; Bernhardt et al., 2012). Our study indicated that both types of putative chloroplast TPP carriers (AtFolt1 and CTT) contain chloroplast transit peptides; therefore, they are likely to be located in the chloroplast envelope membrane. This was supported by a previous study that confirmed the localization of AtFolt1 in the chloroplast when the full-length coding sequence of AtFolt1 was produced containing tagged and transit expression was conducted in Arabidopsis (Bedhomme et al., 2005). The sequence analysis results presented here have shown that putative chloroplast TPP transporters share five functional motifs with TPP transporters. In addition, the predicted 3D models of the known TPP transporters generated in this study (Slc25a19, *yeast* Tpc1, *drosophila* Tpc, AtTpc1, AtTpc2, GRMZM2G118515 and GRMZM2G124911) and putative

chloroplast TPP transporters (AtFolt1 and CTT) were highly similar; this raises the possibility that AtFolt1 and CTT might share functions with these carriers. The limitation of this comparative study is that no crystal structure has been proposed for any TPP carriers. However, the function of Arabidopsis AtTpc1 and AtTpc2 was studied in yeast, and it was shown that both could restore TPP in *yeast* mitochondria when the yeast TPP transporter is inhibited (Tpc1) (Frelin et al., 2012). Other carriers were identified to be TPP transporters in other organisms: humans, yeast and drosophila (Iacopetta et al., 2010, Lindhurst et al., 2006, Marobbio et al., 2002). In humans, the knockout of Slc25a19 (the human TPP transporter) caused a reduction of TPP in mitochondria and an increase of TPP in the cytosol (Lindhurst et al., 2006). In yeast, Tpc1 mutant cells could not grow unless they were treated with auxotrophic thiamine, and their mitochondrial TPP level was decreased by inhibiting Tpc1 (Marobbio et al., 2002).

Evidence suggests that TMP is generated in the chloroplast and TPP in the cytosol. However, the location of the hydrolysis that converts TMP to thiamine remained unclear until recently, when TMP phosphatase was identified and a cytosolic localisation was demonstrated (Mimura et al., 2016, Goyer, 2010, Ajjawi et al., 2007). The implication of this finding is that it is TMP that is transported from the chloroplast to the cytosol, where it is then converted to thiamine. Thiamine is in turn converted to TPP, which is then redistributed to the mitochondria and chloroplast. It is proposed that either AtFolt1 or CTT may act as antiporters to transport TMP from the chloroplast to the cytosol and to transport TPP from the cytosol to the chloroplast. Recently, a thiamine transporter, PUT3 (AT5G05630), was identified in the phloem (Martinis et al., 2016). In this study, the PUT3 3D structural model was compared with the putative chloroplast and mitochondrial TPP carrier models. The

results showed that the predicted PUT3 structure differs from those of AtFolt1 and CTT, and the RMS values were 19.889 and 15.300, respectively. In addition, the PUT3 structure differs from those of AtTpc1 and AtTpc2 (Figures 6.1 and 6.2, respectively). This result provides further support for the proposal that AtFolt1 and CTT might be TMP/TPP transporters, which would mean that they could work as antiporters.

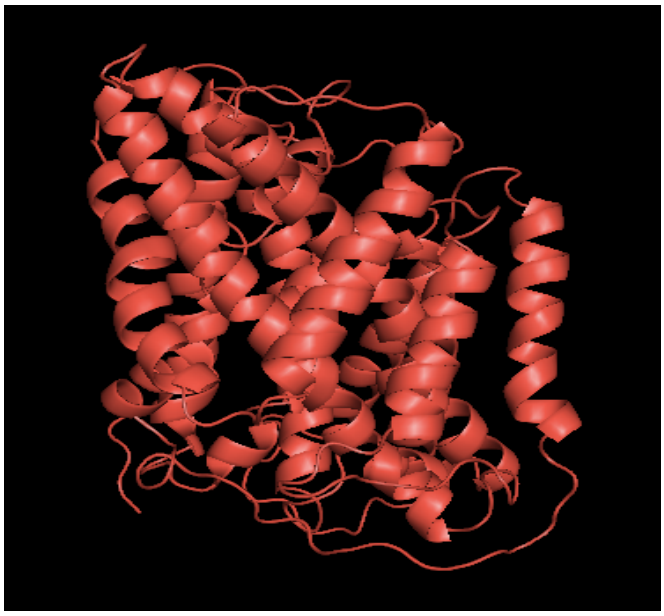

Figure 6.1: Predicted structure model of the Arabidopsis thiamine transporter protein (PUT3). The predicted structure model was produced using Phyre2 server, and alignment was performed using PyMol software.

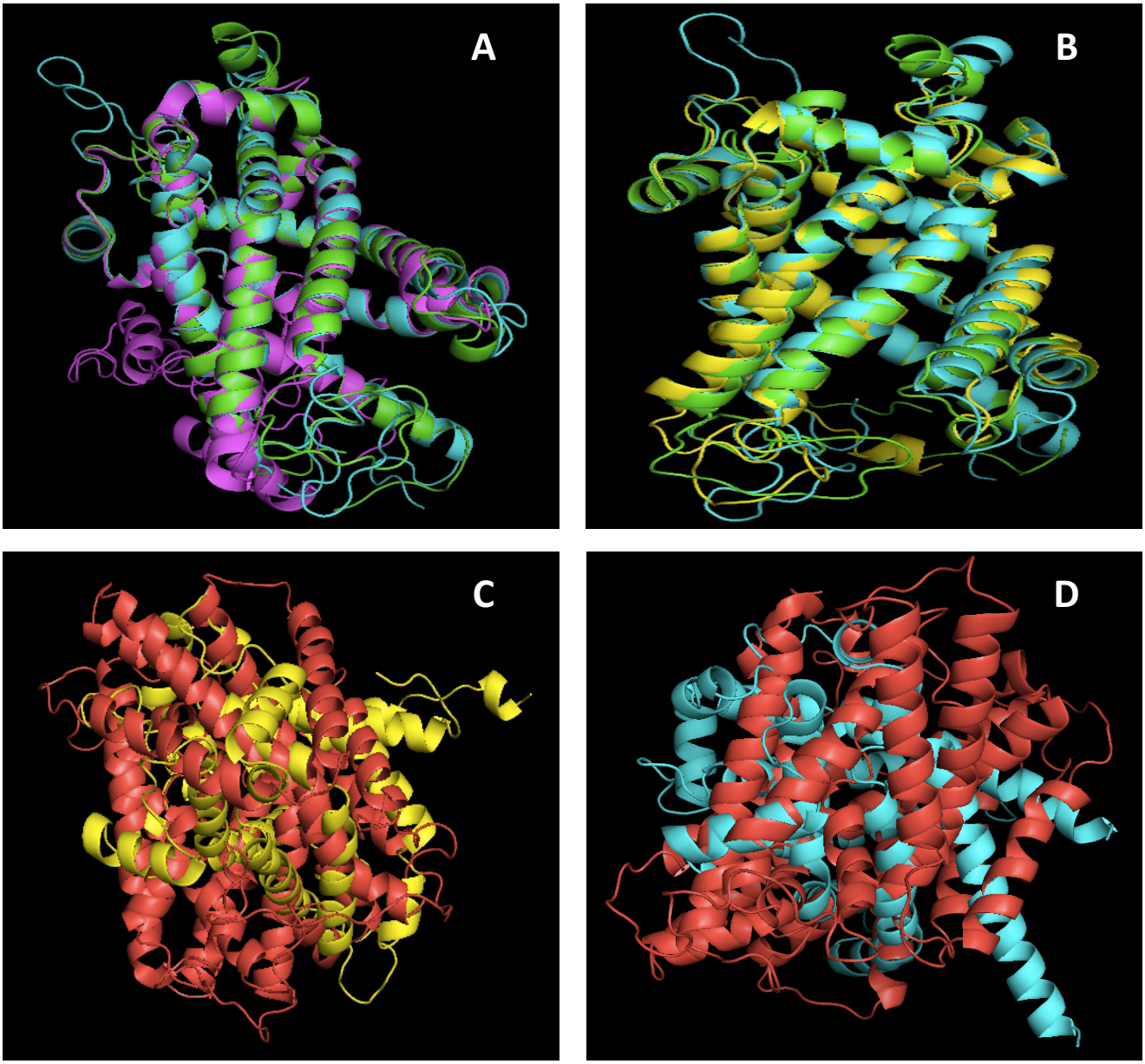

Figure 6.2: Comparative structure models of the Arabidopsis thiamine transporter protein (PUT3). 3D prediction models were obtained using the Phyre2 server. **(A)** CTT protein structure (magenta) was aligned with mitochondrial TPP carrier structures (AtTpc1 is green and AtTpc2 is cyan). **(B)** AtFolt1 protein structure (yellow) was aligned with AtTpc1 and AtTpc2. **(C)** Alignment of AtFolt1 (yellow) with PUT3 (red). **(D)** Alignment of AtTpc2 (blue) with PUT3 (red). The predicted structures were produced using Phyre2 server, and the alignment was performed using PyMol software.

The mitochondrial TPP transporters were interrupted to study the importance of these carriers in plant growth. The reductions in AtTpc1 and AtTpc2 transcription levels were ~80% and 60%–80%, respectively. They had similar effects on plant growth: shorter stems and a lower seed yield than the WT. With regard to roots, the AtTpc2 root was significantly affected, unlike that of the AtTpc1 plant, which resulted in a shorter AtTpc2 plant root length compared to that of WT. Interestingly, from the microarray data, the AtTpc2 expression was shown to be higher than the expression for AtTpc1 in the root, which suggests that the AtTpc2 protein may be the major functional isoform in these tissues.

These phenotypes could be explained by the fact that the knockdown of one of the mitochondrial TPP transporters (AtTpc1 and AtTpc2) could affect the mitochondrial TPP levels (not measured). Thus, a reduction in the TPP content in the mitochondria could affect TPP-dependent enzyme activity in the mitochondria and affect its production, thereby impacting plant growth. One of the TPP-dependent enzymes in the mitochondria is pyruvate dehydrogenase (PHD). Previous studies have shown that the reduction of the total mitochondrial PHD complex affected plant growth and produced plants that were much smaller than WT (Song and Liu, 2015). The mitochondrial PHD uses TPP as a cofactor to catalyse the oxidative decarboxylation of pyruvate to form acetyl-CoA, which is an important regulator in mitochondria (Tovar-Méndez et al., 2003). In addition, this reduction might also affect other TPP-dependent enzymes, such as α-ketoglutarate dehydrogenase and branched-chain α-keto acid dehydrogenase.

Chloroplasts contain TPP-dependent enzymes; therefore, they must import TPP from the cytosol, as TPK is cytosolic (Goyer, 2010, Ajjawi et al., 2007). Our results provide evidence that AtFolt1 and CTT are putative chloroplast TMP/TPP carriers based on the sequence similarity and 3D structural predictions (Chapter 4). The TPP level in AtFolt1 knockdown plants was found to be 25%–55% lower than that observed in WT plants. Thus, we hypothesised that as this TPP reduction did not influence plant growth in AtFolt1, the amount of thiamine available was adequate to produce the TPP required for the plant to grow normally under typical conditions. This data generally agrees with a previous study that showed that reducing TPP levels by ~50% relative to the wild-type level did not affect plant growth (Ajjawi et al., 2007). A noteworthy question is why was the TPP content reduced if the TPP synthesis occurred in the cytosol and AtFolt1 targeted the chloroplast? We hypothesised that the TPP reduction might be due to a reduction in the availability of thiamine content in the cytosol. If this hypothesis is true, the thiamine content should be found to be reduced. The thiamine content in AtFolt1 knockdown plants was determined, and it was found to be reduced relative to the content in WT plants. Interestingly, these data suggest that AtFolt1 could be responsible for the transportation and counter-transportation of TMP and TPP. To verify this hypothesis, the thiamine, TPP and TMP must be determined in the chloroplast of AtFolt1 transgenic plants, and the ability of AtFolt1 to transport these compounds must be demonstrated.

The TPP reduction in CTT::RNAi lines could be because the TPP content that was delivered to the chloroplast was inadequate in terms of functioning as an active co-factor for the TPP-dependent enzymes in the chloroplast. However, the TPP level was similar in AtFolt1 knockdown plants and did not affect leaf shape,

whereas in CTT knockdown it did. This could be because the phenotype observed in CTT::RNAi leaves could have led to CTT transporting more than one molecule to the chloroplast, or it could be an off-target effect. This may have been confirmed by a previous study which showed that CTT might be associated with the thylakoid adenosine triphosphate (ATP)/adenosine diphosphate (ADP) carrier (Haferkamp and Schmitz-Esser, 2012). Consequently, interrupting CTT activity might affect ATP/ADP and interrupt many different biological reactions within the chloroplast. To investigate this hypothesis, more investigations must be carried out to understand the reason for this phenotype observed on CTT::RNAi plant leaves.

In conclusion, the analysis of the mitochondrial TPP carriers (AtTpc1 and AtTpc2) showed that they had similar effects on plant growth when they were inhibited individually, except in relation to the influence of AtTpc2 on the root. This means that both mitochondrial TPP transporters are required for Arabidopsis to grow normally, at least under normal conditions. The knockdown of AtFolt1 did not affect plant growth, but it did affect the TPP level in the leaves, whereas CTT affected the TPP level and the leaves. Consequently, AtFolt1 could be a TMP/TPP antiporter.

Future work

To investigate the importance of mitochondrial TPP carriers in plants in greater detail, the inhibition of AtTpc1 and AtTpc2 activity should be explored in future studies. In addition, it is important to determine the TPP levels in the mitochondria of AtTpc1 or AtTpc2 transgenic plants to understand their role in TPP transportation.

Moreover, TPP, TMP, and thiamine in chloroplast must be determined to find out the effect of AtFolt1 and CTT on thiamine esters. Using yeast mutants of thiamine and TPP transporters, a complementation assay for AtFolt1 and CTT must be performed to confirm the functions of AtFolt1 and CTT.

References

AHN, I.-P., KIM, S., LEE, Y.-H. & SUH, S.-C. 2007. Vitamin B-1-induced priming is dependent on hydrogen peroxide and the NPR1 gene in Arabidopsis. *Plant Physiology,* 143**,** 838-848.

AIKAWA, H., WATANABE, I. S., FURUSE, T., IWASAKI, Y., SATOYOSHI, E., SUMI, T. & MOROJI, T. 1984. Low energy levels in thiamine-deficient encephalopathy. *Journal of Neuropathology & Experimental Neurology,* 43**,** 276-287.

AJJAWI, I., MILLA, M. A. R., CUSHMAN, J. & SHINTANI, D. K. 2007. Thiamin pyrophosphokinase is required for thiamin cofactor activation in Arabidopsis. *Plant molecular biology,* 65**,** 151-162.

AJJAWI, I., TSEGAYE, Y. & SHINTANI, D. 2007. Determination of the genetic, molecular, and biochemical basis of the Arabidopsis thaliana thiamin auxotroph th1. *Archives of Biochemistry and Biophysics,* 459**,** 107-114.

BAILEY, T. L. & ELKAN, C. 1994. Fitting a mixture model by expectation maximization to discover motifs in bipolymers.

BARILE, M., PASSARELLA, S. & QUAGLIARIELLO, E. 1990. Thiamine pyrophosphate uptake into isolated rat liver mitochondria. *Archives of biochemistry and biophysics,* 280**,** 352-357.

BEDHOMME, M., HOFFMANN, M., MCCARTHY, E. A., GAMBONNET, B., MORAN, R. G., RÉBEILLÉ, F. & RAVANEL, S. 2005. Folate metabolism in plants an arabidopsis homolog of the mammalian mitochondrial folate transporter mediates folate import into chloroplasts. *Journal of Biological Chemistry,* 280**,** 34823-34831.

BELANGER, F. C., LEUSTEK, T., CHU, B. Y. & KRIZ, A. L. 1995. Evidence for the thiamine biosynthetic pathway in higher-plant plastids and its developmental regulation. *Plant Molecular Biology,* 29**,** 809-821.

BELENKIY, R., HAEFELE, A., EISEN, M. B. & WOHLRAB, H. 2000. The yeast mitochondrial transport proteins: new sequences and consensus residues, lack of direct relation between consensus residues and transmembrane helices, expression patterns of the transport protein genes, and protein–protein interactions with other proteins. *Biochimica et Biophysica Acta (BBA)-Biomembranes,* 1467**,** 207-218.

BERNHARDT, K., WILKINSON, S., WEBER, A. P. & LINKA, N. 2012. A peroxisomal carrier delivers NAD+ and contributes to optimal fatty acid degradation during storage oil mobilization. *The Plant Journal,* 69**,** 1-13.

BINDER, S. 2010. Branched-chain amino acid metabolism in Arabidopsis thaliana. *The Arabidopsis Book***,** e0137.

BLASS, J. P. & GIBSON, G. E. 1977. Abnormality of a thiamine-requiring enzyme in patients with Wernicke-Korsakoff syndrome. *New England Journal of Medicine,* 297**,** 1367-1370.

BOCOBZA, S., ADATO, A., MANDEL, T., SHAPIRA, M., NUDLER, E. & AHARON, A. 2007. Riboswitch-dependent gene regulation and its evolution in the plant kingdom. *Genes & Development,* 21**,** 2874-2879.

BUBBER, P., KE, Z.-J. & GIBSON, G. E. 2004. Tricarboxylic acid cycle enzymes following thiamine deficiency. *Neurochemistry international,* 45**,** 1021-1028.

BUTTERWORTH, R. F., KRIL, J. J. & HARPER, C. G. 1993. Thiamine-Dependent Enzyme Changes in the Brains of Alcoholics: Relationship to the Wernicke-

Korsakoff Syndrome. *Alcoholism: Clinical and Experimental Research,* 17**,** 1084-1088.
CHABREGAS, S. M., LUCHE, D. D., FARIAS, L. P., RIBEIRO, A. F., VAN SLUYS, M. A., MENCK, C. F. M. & SILVA-FILHO, M. C. 2001. Dual targeting properties of the N-terminal signal sequence of Arabidopsis thaliana THI1 protein to mitochondria and chloroplasts. *Plant Molecular Biology,* 46**,** 639-650.
CHABREGAS, S. M., LUCHE, D. D., VAN SLUYS, M. A., MENCK, C. F. M. & SILVA-FILHO, M. C. 2003. Differential usage of two in-frame translational start codons regulates subcellular localization of Arabidopsis thaliana THI1. *Journal of Cell Science,* 116**,** 285-291.
CHATTERJEE, A., JURGENSON, C. T., SCHROEDER, F. C., EALICK, S. E. & BEGLEY, T. P. 2007. Biosynthesis of thiamin thiazole in eukaryotes: Conversion of NAD to an advanced intermediate. *Journal of the American Chemical Society,* 129**,** 2914-2922.
CHATTERJEE, A., SCHROEDER, F. C., JURGENSON, C. T., EALICK, S. E. & BEGLEY, T. P. 2008. Biosynthesis of the thiamin-thiazole in eukaryotes: Identification of a thiazole tautomer intermediate. *Journal of the American Chemical Society,* 130**,** 11394-11398.
CLOUGH, S. & BENT, A. 1997. Simplified Arabidopsis transformation protocol. *Brief version for those who are familiar with the method*.
CROFT, M. T., MOULIN, M., WEBB, M. E. & SMITH, A. G. 2007. Thiamine biosynthesis in algae is regulated by riboswitches. *Proceedings of the National Academy of Sciences,* 104**,** 20770-20775.
EMANUELSSON, O., NIELSEN, H., BRUNAK, S. & VON HEIJNE, G. 2000. Predicting subcellular localization of proteins based on their N-terminal amino acid sequence. *Journal of molecular biology,* 300**,** 1005-1016.
EMANUELSSON, O., NIELSEN, H. & VON HEIJNE, G. 1999. ChloroP, a neural network-based method for predicting chloroplast transit peptides and their cleavage sites. *Protein Science,* 8**,** 978-984.
ENGLER, C., KANDZIA, R. & MARILLONNET, S. 2008. A one pot, one step, precision cloning method with high throughput capability. *PloS one,* 3**,** e3647.
FATTAL-VALEVSKI, A. 2011. Thiamine (vitamin B1). *Journal of Evidence-Based Complementary & Alternative Medicine,* 16**,** 12-20.
FOURNIER, H. & BUTTERWORTH, R. F. 1990. Effects of thiamine deficiency on thiamine-dependent enzymes in regions of the brain of pregnant rats and their offspring. *Metabolic brain disease,* 5**,** 77-84.
FRANK, R., LEEPER, F. & LUISI, B. 2007. Structure, mechanism and catalytic duality of thiamine-dependent enzymes. *Cellular and molecular life sciences,* 64**,** 892-905.
FRELIN, O., AGRIMI, G., LAERA, V. L., CASTEGNA, A., RICHARDSON, L. G. L., MULLEN, R. T., LERMA-ORTIZ, C., PALMIERI, F. & HANSON, A. D. 2012. Identification of mitochondrial thiamin diphosphate carriers from Arabidopsis and maize. *Functional & Integrative Genomics,* 12**,** 317-326.
FROMMER, W. B. & NINNEMANN, O. 1995. Heterologous expression of genes in bacterial, fungal, animal, and plant cells. *Annual review of plant biology,* 46**,** 419-444.
GENNARO, A., ANNAMARIA, R., PASQUALE, S. & FERDINANDO, P. 2011. The human gene SLC25A17 encodes a peroxisomal transporter of coenzyme A, FAD and NAD+. *Biochemical Journal,* 443**,** 241-247.

GOYER, A. 2010. Thiamine in plants: Aspects of its metabolism and functions. *Phytochemistry,* 71**,** 1615-1624.
HAFERKAMP, I. 2007. The diverse members of the mitochondrial carrier family in plants. *FEBS letters,* 581**,** 2375-2379.
HAFERKAMP, I. & SCHMITZ-ESSER, S. 2012. The plant mitochondrial carrier family: functional and evolutionary aspects.
HEINRICH, C., STADLER, H. & WEISER, H. 1973. The effect of thiamine deficiency on the acetylcoenzymeA and acetylcholine levels in the rat brain. *Journal of neurochemistry,* 21**,** 1273-1281.
HIRAI, S. & KODAMA, H. 2008. RNAi vectors for manipulation of gene expression in higher plants. *The Open Plant Science Journal,* 2.
HOOPER, C. M., TANZ, S. K., CASTLEDEN, I. R., VACHER, M. A., SMALL, I. D. & MILLAR, A. H. 2014. SUBAcon: a consensus algorithm for unifying the subcellular localization data of the Arabidopsis proteome. *Bioinformatics,* 30**,** 3356-3364.
IACOPETTA, D., CARRISI, C., DE FILIPPIS, G., CALCAGNILE, V. M., CAPPELLO, A. R., CHIMENTO, A., CURCIO, R., SANTORO, A., VOZZA, A., DOLCE, V., PALMIERI, F. & CAPOBIANCO, L. 2010. The biochemical properties of the mitochondrial thiamine pyrophosphate carrier from Drosophila melanogaster. *Febs Journal,* 277**,** 1172-1181.
JENKINS, A. H., SCHYNS, G., POTOT, S., SUN, G. & BEGLEY, T. P. 2007. A new thiamin salvage pathway. *Nature chemical biology,* 3**,** 492-497.
JULLIARD, J. H. & DOUCE, R. 1991. BIOSYNTHESIS OF THE THIAZOLE MOIETY OF THIAMIN (VITAMIN-B1) IN HIGHER-PLANT CHLOROPLASTS. *Proceedings of the National Academy of Sciences of the United States of America,* 88**,** 2042-2045.
JURGENSON, C. T., BEGLEY, T. P. & EALICK, S. E. 2009. The structural and biochemical foundations of thiamin biosynthesis. *Annual review of biochemistry,* 78**,** 569-603.
KAPLAN, R. 2001. Structure and function of mitochondrial anion transport proteins. *Journal of Membrane Biology,* 179**,** 165-183.
KELLEY, L. A. & STERNBERG, M. J. 2009. Protein structure prediction on the Web: a case study using the Phyre server. *Nature protocols,* 4**,** 363-371.
KHOZAEI, M., FISK, S., LAWSON, T., GIBON, Y., SULPICE, R., STITT, M., LEFEBVRE, S. C. & RAINES, C. A. 2015. Overexpression of Plastid Transketolase in Tobacco Results in a Thiamine Auxotrophic Phenotype. *The Plant Cell Online,* 27**,** 432-447.
KONG, D., ZHU, Y., WU, H., CHENG, X., LIANG, H. & LING, H.-Q. 2008. AtTHIC, a gene involved in thiamine biosynthesis in Arabidopsis thaliana. *Cell Research,* 18**,** 566-576.
KRAMPITZ, L. O. 1969. Catalytic functions of thiamin diphosphate. *Annual review of biochemistry,* 38**,** 213-40.
KRUGER, N. J. & VON SCHAEWEN, A. 2003. The oxidative pentose phosphate pathway: structure and organisation. *Current Opinion in Plant Biology,* 6**,** 236-246.
LANGE, B. M., WILDUNG, M. R., MCCASKILL, D. & CROTEAU, R. 1998. A family of transketolases that directs isoprenoid biosynthesis via a mevalonate-independent pathway. *Proceedings of the National Academy of Sciences,* 95**,** 2100-2104.

LARKIN, M. A., BLACKSHIELDS, G., BROWN, N., CHENNA, R., MCGETTIGAN, P. A., MCWILLIAM, H., VALENTIN, F., WALLACE, I. M., WILM, A. & LOPEZ, R. 2007. Clustal W and Clustal X version 2.0. *bioinformatics,* 23**,** 2947-2948.

LECLERE, S., RAMPEY, R. A. & BARTEL, B. 2004. IAR4, a gene required for auxin conjugate sensitivity in Arabidopsis, encodes a pyruvate dehydrogenase E1 alpha homolog. *Plant Physiology,* 135**,** 989-999.

LEE, T. C. & LANGSTON-UNKEFER, P. J. 1985. Pyruvate decarboxylase from Zea mays LI Purification and partial characterization from mature kernels and anaerobically treated roots. *Plant physiology,* 79**,** 242-247.

LI, H.-M. & CHIU, C.-C. 2010. Protein transport into chloroplasts. *Plant Biology,* 61**,** 157.

LINDHURST, M. J., FIERMONTE, G., SONG, S., STRUYS, E., DE LEONARDIS, F., SCHWARTZBERG, P. L., CHEN, A., CASTEGNA, A., VERHOEVEN, N., MATHEWS, C. K., PALMIERI, F. & BIESECKER, L. G. 2006. Knockout of Slc25a19 causes mitochondrial thiamine pyrophosphate depletion, embryonic lethality, CNS malformations, and anemia. *Proceedings of the National Academy of Sciences of the United States of America,* 103**,** 15927-15932.

LINDQVIST, Y., SCHNEIDER, G., ERMLER, U. & SUNDSTROM, M. 1992. 3-DIMENSIONAL STRUCTURE OF TRANSKETOLASE, A THIAMINE DIPHOSPHATE DEPENDENT ENZYME, AT 2.5 ANGSTROM RESOLUTION. *Embo Journal,* 11**,** 2373-2379.

LINKA, N. & WEBER, A. P. 2010. Intracellular metabolite transporters in plants. *Molecular Plant,* 3**,** 21-53.

LOIS, L. M., CAMPOS, N., PUTRA, S. R., DANIELSEN, K., ROHMER, M. & BORONAT, A. 1998. Cloning and characterization of a gene from Escherichia coli encoding a transketolase-like enzyme that catalyzes the synthesis of D-1-deoxyxylulose 5-phosphate, a common precursor for isoprenoid, thiamin, and pyridoxol biosynthesis. *Proceedings of the National Academy of Sciences,* 95**,** 2105-2110.

LU, J. & FRANK, E. L. 2008. Rapid HPLC measurement of thiamine and its phosphate esters in whole blood. *Clinical chemistry,* 54**,** 901-906.

LUNN, J. E. 2007. Compartmentation in plant metabolism. *Journal of Experimental Botany,* 58**,** 35-47.

MACHADO, C. R., DEOLIVEIRA, R. L. C., BOITEUX, S., PRAEKELT, U. M., MEACOCK, P. A. & LENCK, C. F. M. 1996. Thi1, a thiamine biosynthetic gene in Arabidopsis thaliana, complements bacterial defects in DNA repair. *Plant Molecular Biology,* 31**,** 585-593.

MAROBBIO, C. M. T., VOZZA, A., HARDING, M., BISACCIA, F., PALMIERI, F. & WALKER, J. E. 2002. Identification and reconstitution of theyeast mitochondrial transporter for thiamine pyrophosphate. *Embo Journal,* 21**,** 5653-5661.

MARTIN, P. R., SINGLETON, C. K. & HILLER-STURMHOFEL, S. 2003. The role of thiamine deficiency in alcoholic brain disease. *Alcohol Research and Health,* 27**,** 134-142.

MARTINIS, J., GAS-PASCUAL, E., SZYDLOWSKI, N., CRÈVECOEUR, M., GISLER, A., BÜRKLE, L. & FITZPATRICK, T. B. 2016. Long distance transport of thiamine (vitamin B1) is concomitant with that of polyamines in Arabidopsis. *Plant physiology***,** pp. 00009.2016.

MENG, L. & FELDMAN, L. 2010. A rapid TRIzol-based two-step method for DNA-free RNA extraction from Arabidopsis siliques and dry seeds. *Biotechnology journal,* 5**,** 183-186.
MILLAR, A. H. & HEAZLEWOOD, J. L. 2003. Genomic and proteomic analysis of mitochondrial carrier proteins in Arabidopsis. *Plant physiology,* 131**,** 443-453.
MIMURA, M., ZALLOT, R., NIEHAUS, T. D., HASNAIN, G., GIDDA, S. K., NGUYEN, T. N., ANDERSON, E. M., MULLEN, R. T., BROWN, G. & YAKUNIN, A. F. 2016. Arabidopsis TH2 Encodes the Orphan Enzyme Thiamin Monophosphate Phosphatase. *The Plant Cell,* 28**,** 2683-2696.
MIRANDA-RIOS, J. 2007. The THI-box riboswitch, or how RNA binds thiamin pyrophosphate. *Structure,* 15**,** 259-265.
PALMIERI, F. 1994. Mitochondrial carrier proteins. *FEBS letters,* 346**,** 48-54.
PALMIERI, F. 2004. The mitochondrial transporter family (SLC25): physiological and pathological implications. *Pflügers Archiv,* 447**,** 689-709.
PALMIERI, L., ROTTENSTEINER, H., GIRZALSKY, W., SCARCIA, P., PALMIERI, F. & ERDMANN, R. 2001. Identification and functional reconstitution of the yeast peroxisomal adenine nucleotide transporter. *The EMBO journal,* 20**,** 5049-5059.
PALMIERI, L., RUNSWICK, M. J., FIERMONTE, G., WALKER, J. E. & PALMIERI, F. 2000. Yeast mitochondrial carriers: bacterial expression, biochemical identification and metabolic significance. *Journal of bioenergetics and biomembranes,* 32**,** 67-77.
PENG, C., UYGUN, S., SHIU, S.-H. & LAST, R. L. 2015. The impact of the branched-chain ketoacid dehydrogenase complex on amino acid homeostasis in Arabidopsis. *Plant physiology,* 169**,** 1807-1820.
PICAULT, N., HODGES, M., PALMIERI, L. & PALMIERI, F. 2004. The growing family of mitochondrial carriers in Arabidopsis. *Trends in plant science,* 9**,** 138-146.
POHL, M., SPRENGER, G. A. & MULLER, M. 2004. A new perspective on thiamine catalysis. *Current Opinion in Biotechnology,* 15**,** 335-342.
RAPALA-KOZIK, M., KOWALSKA, E. & OSTROWSKA, K. 2008. Modulation of thiamine metabolism in Zea mays seedlings under conditions of abiotic stress. *Journal of experimental botany,* 59**,** 4133-4143.
RAPALA-KOZIK, M., OLCZAK, M., OSTROWSKA, K., STAROSTA, A. & KOZIK, A. 2007. Molecular characterization of the thi3 gene involved in thiamine biosynthesis in Zea mays: cDNA sequence and enzymatic and structural properties of the recombinant bifunctional protein with 4-amino-5-hydroxymethyl-2-methylpyrimidine (phosphate) kinase and thiamine monophosphate synthase activities. *Biochemical Journal,* 408**,** 149-159.
RASCHKE, M., BUERKLE, L., MUELLER, N., NUNES-NESI, A., FERNIE, A. R., ARIGONI, D., AMRHEIN, N. & FITZPATRICK, T. B. 2007. Vitamin B1 biosynthesis in plants requires the essential iron-sulfur cluster protein, THIC. *Proceedings of the National Academy of Sciences of the United States of America,* 104**,** 19637-19642.
RIBEIRO, A., PRAEKELT, U., AKKERMANS, A. D. L., MEACOCK, P. A., VANKAMMEN, A., BISSELING, T. & PAWLOWSKI, K. 1996. Identification of agthi1, whose product is involved in biosynthesis of the thiamine precursor thiazole, in actinorhizal nodules of Alnus glutinosa. *Plant Journal,* 10**,** 361-368.

RIVOAL, J., RICARD, B. & PRADET, A. 1990. PURIFICATION AND PARTIAL CHARACTERIZATION OF PYRUVATE DECARBOXYLASE FROM ORYZA-SATIVA L. *European Journal of Biochemistry,* 194**,** 791-797.

ROHMER, M. 1999. The discovery of a mevalonate-independent pathway for isoprenoid biosynthesis in bacteria, algae and higher plants. *Natural Product Reports,* 16**,** 565-574.

SCHENK, G., DUGGLEBY, R. G. & NIXON, P. F. 1998. Properties and functions of the thiamin diphosphate dependent enzyme transketolase. *International Journal of Biochemistry & Cell Biology,* 30**,** 1297-1318.

SCHRÖDINGER, L. 2015. The PyMOL molecular graphics system, version 1.8. *There is no corresponding record for this reference*.

SCHWACKE, R., FLÜGGE, U.-I. & KUNZE, R. 2004. Plant membrane proteome databases. *Plant Physiology and Biochemistry,* 42**,** 1023-1034.

SENECOFF, J. F. & MEAGHER, R. B. 1993. ISOLATING THE ARABIDOPSIS-THALIANA GENES FOR DENOVO PURINE SYNTHESIS BY SUPPRESSION OF ESCHERICHIA-COLI MUTANTS. *Plant Physiology,* 102**,** 387-399.

SONG, L. & LIU, D. 2015. Mutations in the three Arabidopsis genes that encode the E2 subunit of the mitochondrial pyruvate dehydrogenase complex differentially affect enzymatic activity and plant growth. *Plant cell reports,* 34**,** 1919-1926.

SPARKES, I. A., RUNIONS, J., KEARNS, A. & HAWES, C. 2006. Rapid, transient expression of fluorescent fusion proteins in tobacco plants and generation of stably transformed plants. *Nature protocols,* 1**,** 2019-2025.

SPRENGER, G. A., SCHORKEN, U., WIEGERT, T., GROLLE, S., DEGRAAF, A. A., TAYLOR, S. V., BEGLEY, T. P., BRINGERMEYER, S. & SAHM, H. 1997. Identification of a thiamin-dependent synthase in Escherichia coli required for the formation of the 1-deoxy-D-xylulose 5-phosphate precursor to isoprenoids, thiamin, and pyridoxol. *Proceedings of the National Academy of Sciences of the United States of America,* 94**,** 12857-12862.

TAMURA, K., PETERSON, D., PETERSON, N., STECHER, G., NEI, M. & KUMAR, S. 2011. MEGA5: molecular evolutionary genetics analysis using maximum likelihood, evolutionary distance, and maximum parsimony methods. *Molecular biology and evolution,* 28**,** 2731-2739.

TEIGE, M., MELZER, M. & SUSS, K. H. 1998. Purification, properties and in situ localization of the amphibolic enzymes D-ribulose 5-phosphate 3-epimerase and transketolase from spinach chloroplasts. *European Journal of Biochemistry,* 252**,** 237-244.

TOVAR-MÉNDEZ, A., MIERNYK, J. A. & RANDALL, D. D. 2003. Regulation of pyruvate dehydrogenase complex activity in plant cells. *European Journal of Biochemistry,* 270**,** 1043-1049.

TROSTLER, N. & SKLAN, D. 1978. Lipogenesis in the brain of thiamine-deficient rat pups. *Journal of nutritional science and vitaminology,* 24**,** 105-111.

WACHTER, A., TUNC-OZDEMIR, M., GROVE, B. C., GREEN, P. J., SHINTANI, D. K. & BREAKER, R. R. 2007. Riboswitch control of gene expression in plants by splicing and alternative 3 ' end processing of mRNAs. *Plant Cell,* 19**,** 3437-3450.

WANG, G. N., DING, X. H., YUAN, M., QIU, D. Y., LI, X. H., XU, C. G. & WANG, S. P. 2006. Dual function of rice OsDR8 gene in disease resistance and thiamine accumulation. *Plant Molecular Biology,* 60**,** 437-449.

WEI, T. & WANG, A. 2008. Biogenesis of cytoplasmic membranous vesicles for plant potyvirus replication occurs at endoplasmic reticulum exit sites in a COPI-and COPII-dependent manner. *Journal of virology,* 82**,** 12252-12264.

Appendices

Appendix 1: Primers used in this study.

Oligo names		Sequence 5' to 3'	gene	Size of fragment (bp)
scr_CTTSALK_152353	F	ATACAAATCAATTCCGGAGGC	CTT	1186
	R	ATGATGATGACGACGAGGAAG		
scr_CTTSALK_012760	F	AACAAATTGTGGAAGCATTGC	CTT	1025
	R	TGATACGGTCAAGAGGAGCAG		
scr_M3salk_43C	F	AGGCCACAAATGTTACAGCAC	AtTpc1	1132
	R	GTATCCGTTTGACCTATTGCG		
Scr_5Sail_127_G03	F	GGGTCCGTCTCTTGAACATT	AtTpc2	829
	R	CAGCGTAAGGCACAATCTCA		
scr_5GK	F	TCCACCCAACTCTCAAATCC	AtTpc2	884
	R	AGCAAAGCTGGCACATTACC		
RT_CTT2	F	GAGTGCGAAGAAGGCGATAG	CTT	229
	R	AGATGTCATGCCAGCACAAG		
RT_CTT1	F	GAGCACGATTACAGCAACGA	AtFolt1	158
	R	TGTGATGGAAGACGCAGGTA		
RT_Tpc1	F	TAGCTTCGGGCACTGTTTCT	AtTpc1	150
	R	TCTGCCCTAAACCGTCAAAC		
RT_Tpc2	F	TCCACCCAACTCTCAAATCC	AtTpc2	187
	R	TTAATCTGTCCCGGCTCATC		
RT_M5sail_127	F	GGTAATGTGCCAGCTTTGCT	AtTpc2	159
	R	ACATCCTGCTAACGCTCCAC		
qPCR_CTT	F	GGACAACAGAGTGCGAAGAA	CTT	134
	R	TGGACCGCACTGTAAGGTAA		
qPCR_CTT1	F	GCTTTATGCAGGCTTCTTCC	AtFolt1	127
	R	AGCAGGGCTGAGTTTCTCAT		
qPCR_Tpc2i	F	ATCCCCTTGATGTGGTCAAA	AtTpc2	236
	R	CTCCAACCAATCGGAGGTAA		
qPCR_Folici	F	GAGCACGATTACAGCAACGA	AtFolt1	158
	R	TGTGATGGAAGACGCAGGTA		
qPCR_CTTi	F	GGGCTTATAGGCTTGTACCG	CTT	118
	R	GCTTCTCACTTGTGGCGATA		
qPCR_Tpc1i	F	TAGCTTCGGGCACTGTTTCT	AtTpc1	150
	R	TCTGCCCTAAACCGTCAAAC		
clo_Foic_CDS	F	CACCATGGCGGCGTCGTG	AtFolt1	927
	R	CTAATCTTTTGTTGTTGGATGCTG		
CLO_CTT_CDS91	F	CACCATGGAAGAAGACAGAGCGATTC	CTT	1143
	R	TTGAGCTTGGTCTCGATTCC		

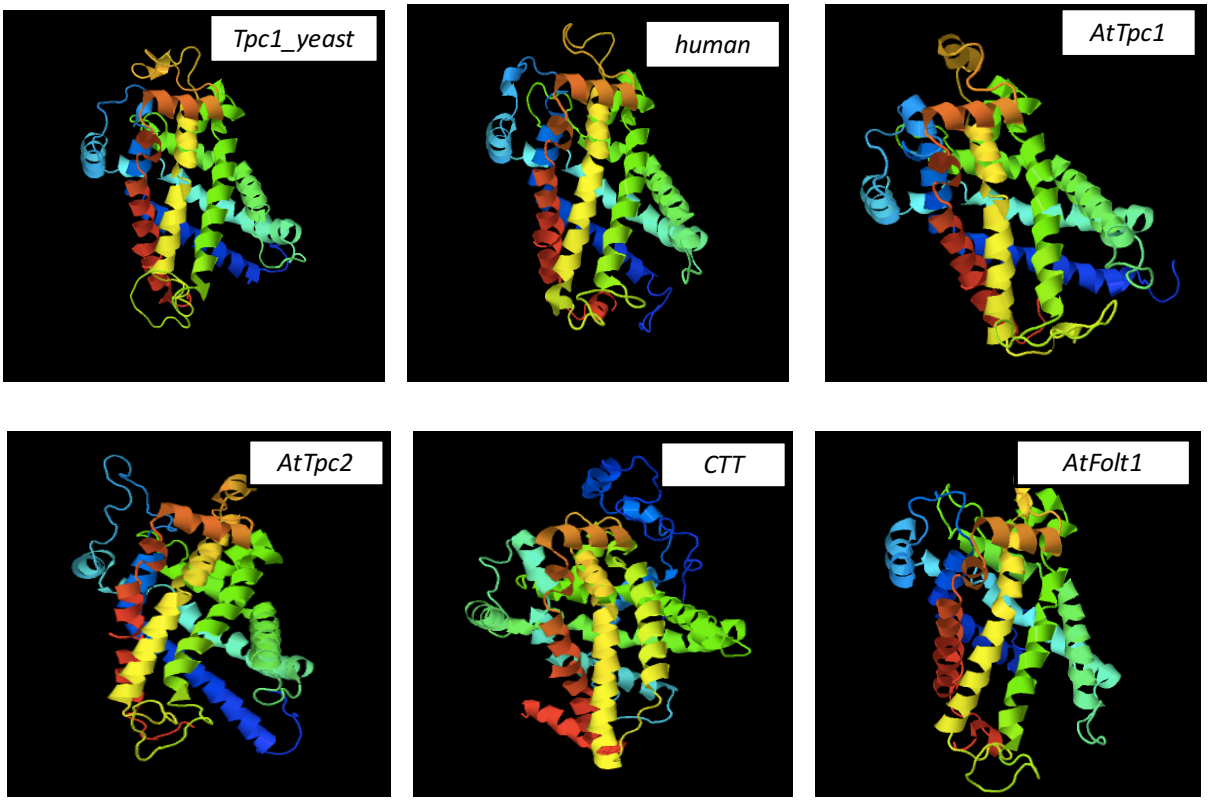

Figure A2: Prediction of TPP transporter protein structures in plants. 3D models were obtained using the Phyre2 server. From the left, **(Tpc1)** is TPP carrier in yeast, **(human)** is TPP carrier in human, **(AtTpc1)** is mitochondrial TPP transporter in Arabidopsis (AT3G21390), **(AtTpc2)** is a second mitochondrial TPP transporter in Arabidopsis (AT5G48970), **(CTT)** is a putative TPP transporter in Arabidopsis, **(AtFolt1)** is a second putative chloroplast TPP transporter in Arabidopsis.

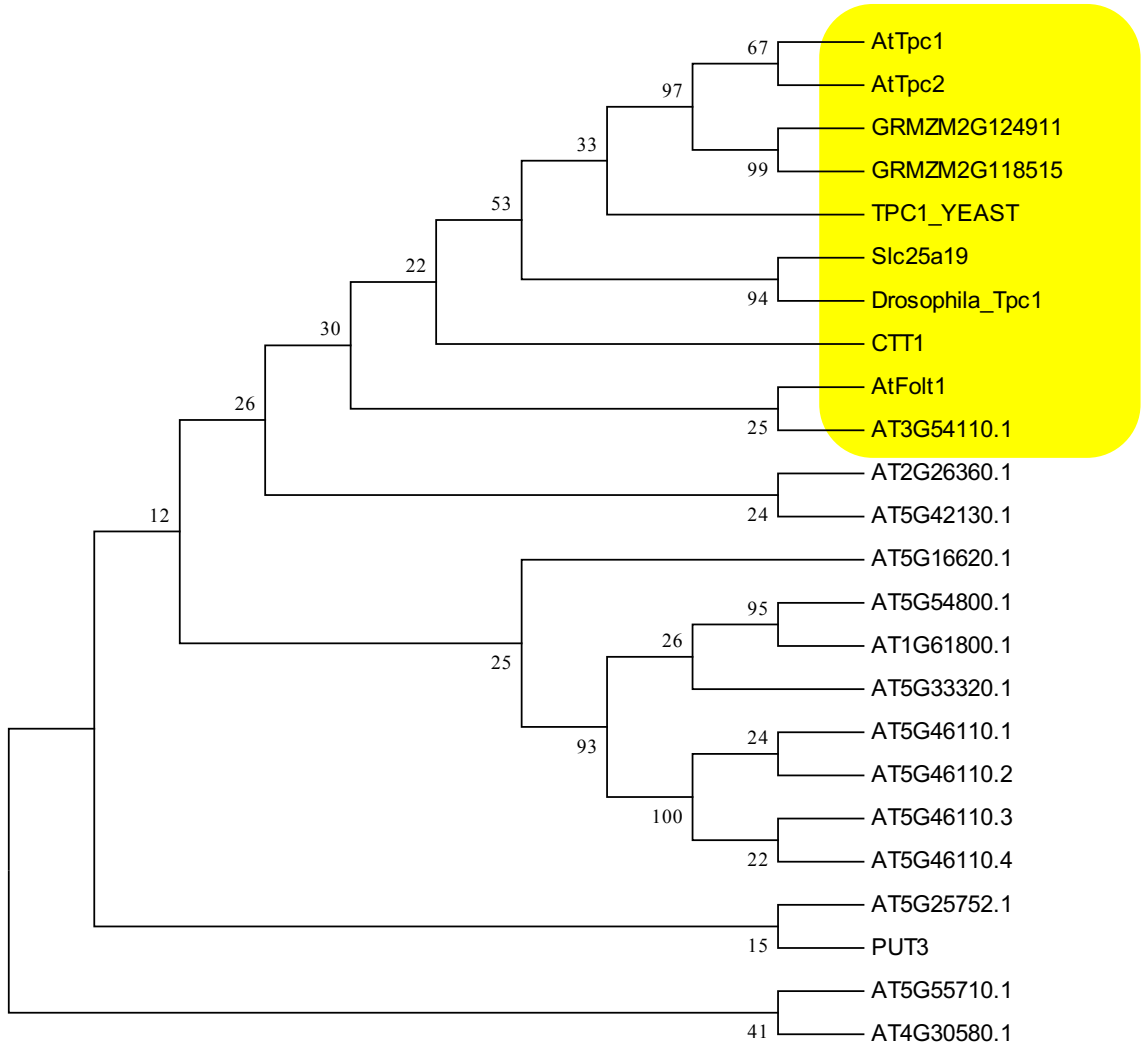

Figure A1: Phylogenetic analysis of the known TPP transporters from yeast, humans and all other chloroplast membranes. Sequences were aligned using ClustalW; the tree was constructed using the Maximum Likelihood method based on the JTT model. The bootstrap values (%) for 1000 replicates are shown next to the nodes. Only the tree's topology is shown; the branch lengths are not proportional to the estimated number of amino acid substitutions. The red squares indicate the known TPP carriers, and the blue squares indicate the putative chloroplast transporters. Mitochondrial TPP carrier in humans (SLC25A19), mitochondrial TPP carrier 1 in yeast (TPC1_yeast), mitochondrial TPP carrier in Drosophila (TPC1_Drosophila), Arabidopsis mitochondrial TPP transporters (AtTpc1 and AtTpc2), Zea mays mitochondrial TPP transporters (GRMZM2G118515 and GRMZM2G124911) and plant mitochondrial TPP transporter, AtTpc1 and AtTpc2. AT3G51870 is Arabidopsis unknown protein and AT5G66380 is Arabidopsis folate transporter.

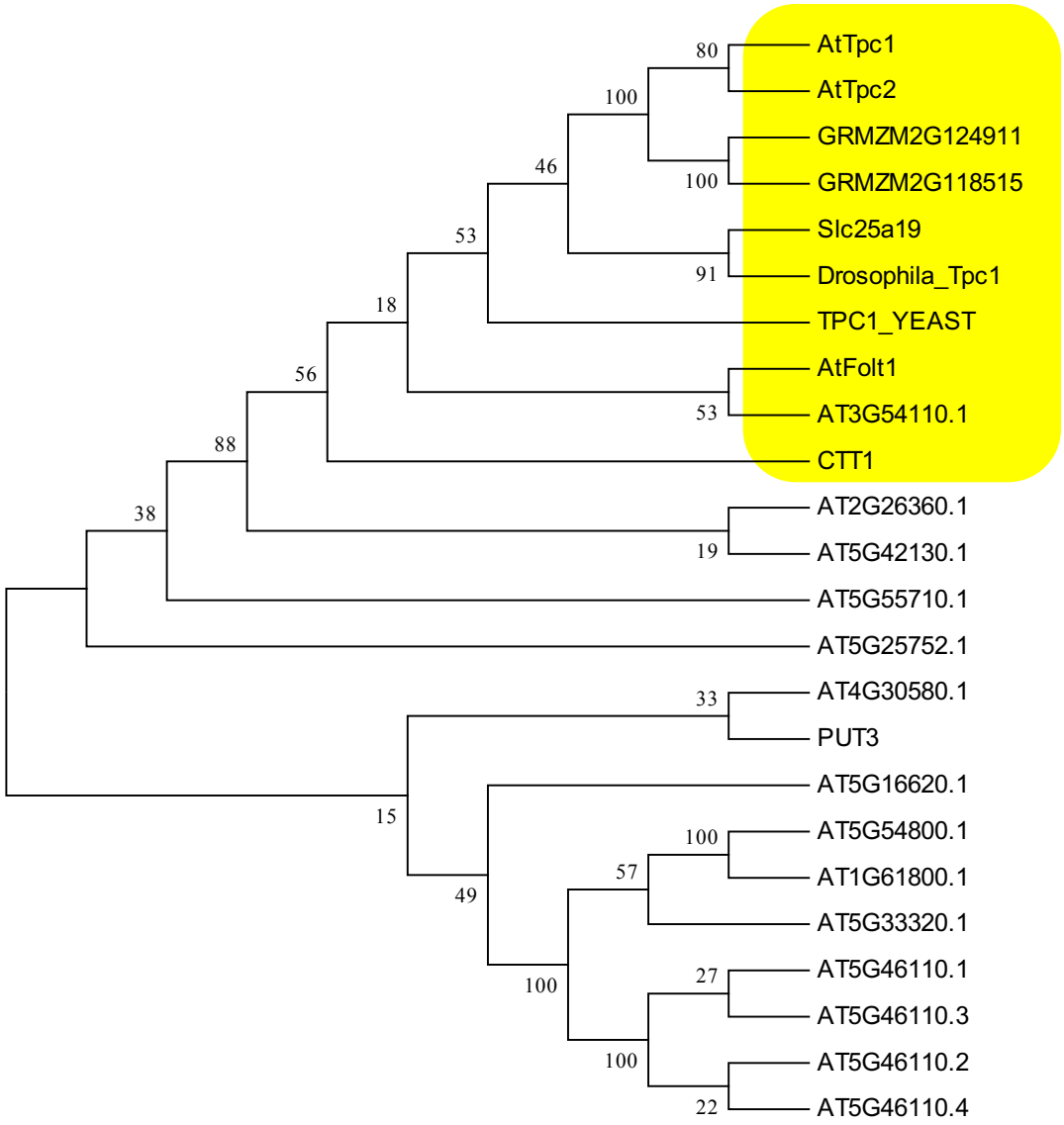

Figure A2: Phylogenetic analysis of the known TPP transporters from yeast, humans and all other chloroplast membranes. Sequences were aligned using ClustalW; the tree was constructed using minimum evolution tree method of MEGA5. The bootstrap values (%) for 1000 replicates are shown next to the nodes. Only the tree's topology is shown; the branch lengths are not proportional to the estimated number of amino acid substitutions. The red squares indicate the known TPP carriers, and the blue squares indicate the putative chloroplast transporters. Mitochondrial TPP carrier in humans (SLC25A19), mitochondrial TPP carrier 1 in yeast (TPC1_yeast), mitochondrial TPP carrier in Drosophila (TPC1_Drosophila), Arabidopsis mitochondrial TPP transporters (AtTpc1 and AtTpc2), Zea mays mitochondrial TPP transporters (GRMZM2G118515 and GRMZM2G124911) and plant mitochondrial TPP transporter, AtTpc1 and AtTpc2. AT3G51870 is Arabidopsis unknown protein and AT5G66380 is Arabidopsis folate transporter.

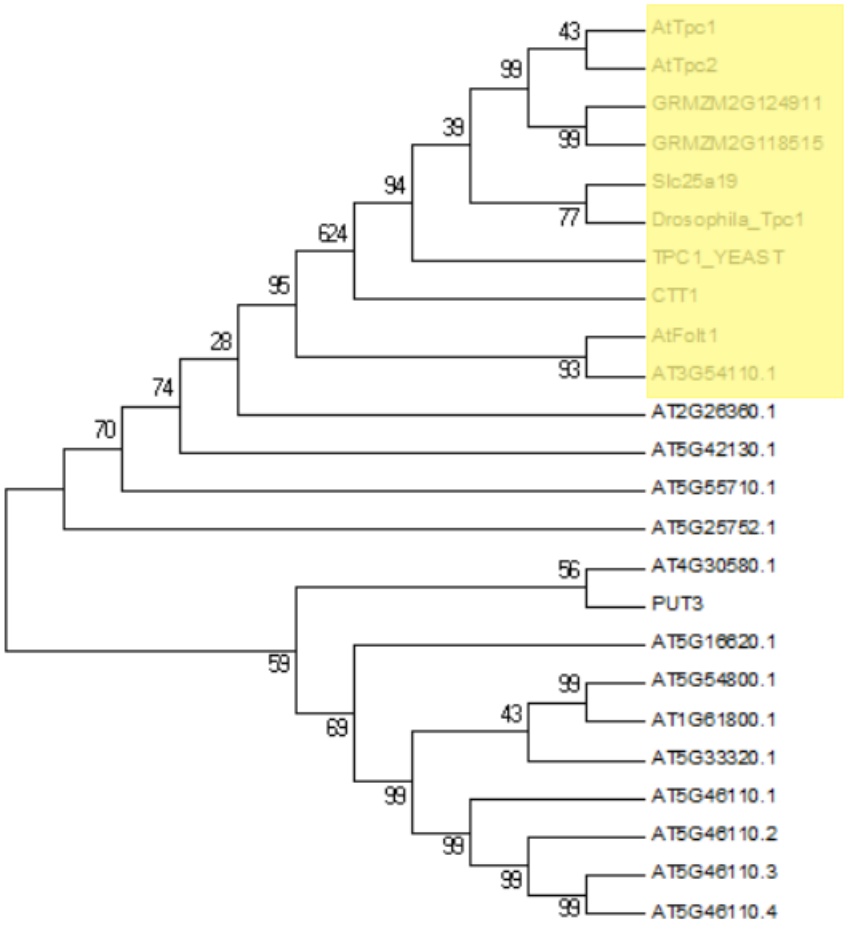

Figure A3: Phylogenetic analysis of the known TPP transporters from yeast, humans and all other chloroplast membranes. Sequences were aligned using ClustalW; the tree was constructed using minimum evolution tree method of MEGA5. The interior test was used and test values (%) for 1000 replicates are shown next to the nodes. Only the tree's topology is shown; the branch lengths are not proportional to the estimated number of amino acid substitutions. The red squares indicate the known TPP carriers, and the blue squares indicate the putative chloroplast transporters. Mitochondrial TPP carrier in humans (SLC25A19), mitochondrial TPP carrier 1 in yeast (TPC1_yeast), mitochondrial TPP carrier in Drosophila (TPC1_Drosophila), Arabidopsis mitochondrial TPP transporters (AtTpc1 and AtTpc2), Zea mays mitochondrial TPP transporters (GRMZM2G118515 and GRMZM2G124911) and plant mitochondrial TPP transporter, AtTpc1 and AtTpc2. AT3G51870 is Arabidopsis unknown protein and AT5G66380 is Arabidopsis folate transporter.

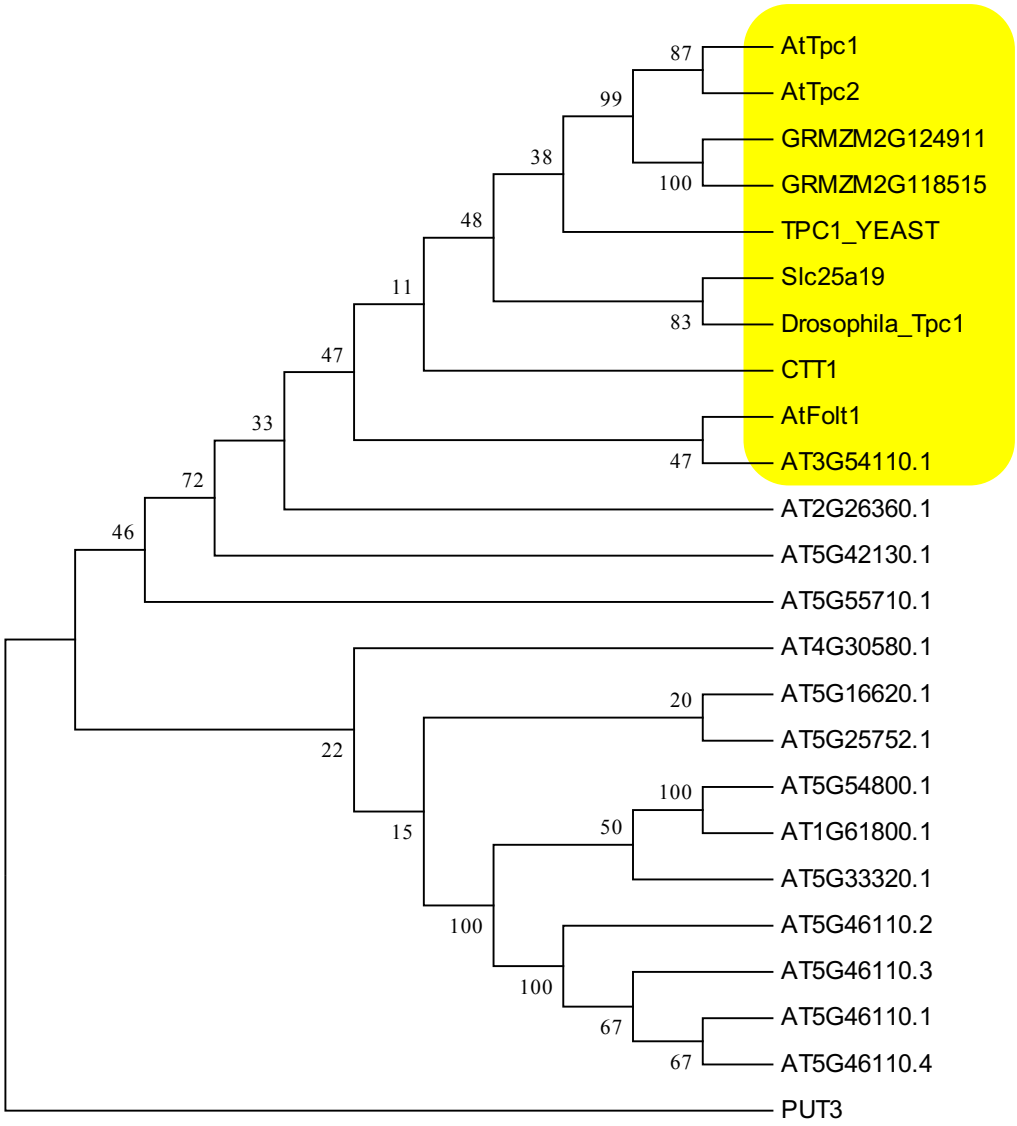

Figure A4: Phylogenetic analysis of the known TPP transporters from yeast, humans and all other chloroplast membranes. Sequences were aligned using ClustalW; the tree was constructed using maximum parsimony tree method of MEGA5. The bootstrap values (%) for 1000 replicates are shown next to the nodes. Only the tree's topology is shown; the branch lengths are not proportional to the estimated number of amino acid substitutions. The red squares indicate the known TPP carriers, and the blue squares indicate the putative chloroplast transporters. Mitochondrial TPP carrier in humans (SLC25A19), mitochondrial TPP carrier 1 in yeast (TPC1_yeast), mitochondrial TPP carrier in Drosophila (TPC1_Drosophila), Arabidopsis mitochondrial TPP transporters (AtTpc1 and AtTpc2), Zea mays mitochondrial TPP transporters (GRMZM2G118515 and GRMZM2G124911) and plant mitochondrial TPP transporter, AtTpc1 and AtTpc2. AT3G51870 is Arabidopsis unknown protein and AT5G66380 is Arabidopsis folate transporter.

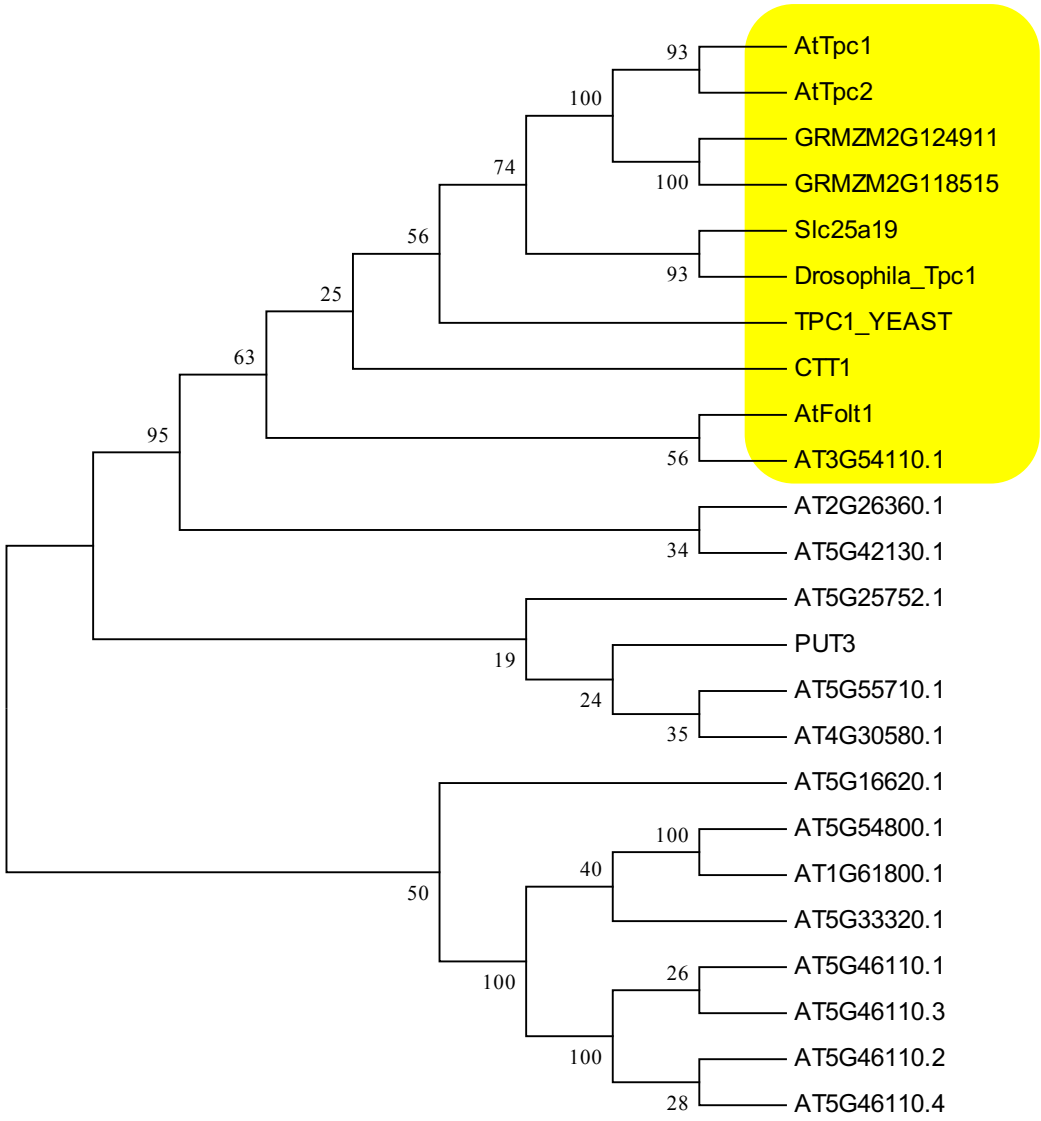

Figure A5: Phylogenetic analysis of the known TPP transporters from yeast, humans and all other chloroplast membranes. Sequences were aligned using ClustalW; the tree was constructed using neighbour- joining tree method of MEGA5. The bootstrap values (%) for 1000 replicates are shown next to the nodes. Only the tree's topology is shown; the branch lengths are not proportional to the estimated number of amino acid substitutions. The red squares indicate the known TPP carriers, and the blue squares indicate the putative chloroplast transporters. Mitochondrial TPP carrier in humans (SLC25A19), mitochondrial TPP carrier 1 in yeast (TPC1_yeast), mitochondrial TPP carrier in Drosophila (TPC1_Drosophila), Arabidopsis mitochondrial TPP transporters (AtTpc1 and AtTpc2), Zea mays mitochondrial TPP transporters (GRMZM2G118515 and GRMZM2G124911) and plant mitochondrial TPP transporter, AtTpc1 and AtTpc2. AT3G51870 is Arabidopsis unknown protein and AT5G66380 is Arabidopsis folate transporter.

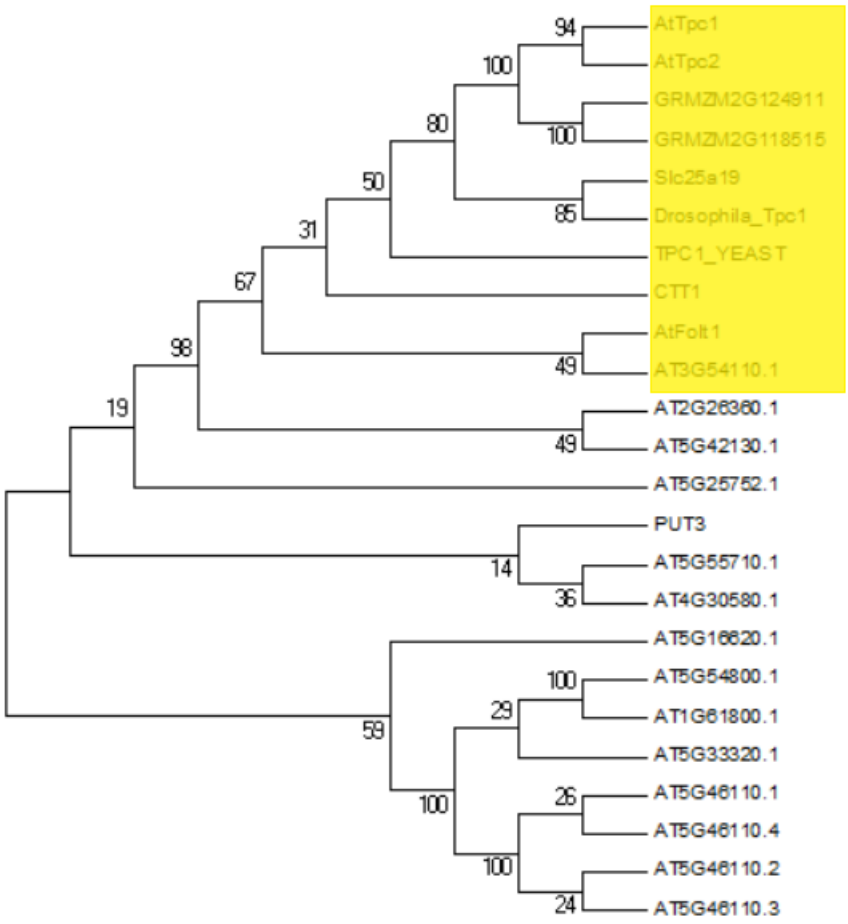

Figure A6: Phylogenetic analysis of the known TPP transporters from yeast, humans and all other chloroplast membranes. Sequences were aligned using ClustalW; the tree was constructed using UPGMA tree method of MEGA5. The bootstrap values (%) for 1000 replicates are shown next to the nodes. Only the tree's topology is shown; the branch lengths are not proportional to the estimated number of amino acid substitutions. The red squares indicate the known TPP carriers, and the blue squares indicate the putative chloroplast transporters. Mitochondrial TPP carrier in humans (SLC25A19), mitochondrial TPP carrier 1 in yeast (TPC1_yeast), mitochondrial TPP carrier in Drosophila (TPC1_Drosophila), Arabidopsis mitochondrial TPP transporters (AtTpc1 and AtTpc2), Zea mays mitochondrial TPP transporters (GRMZM2G118515 and GRMZM2G124911) and plant mitochondrial TPP transporter, AtTpc1 and AtTpc2. AT3G51870 is Arabidopsis unknown protein and AT5G66380 is Arabidopsis folate transporter.

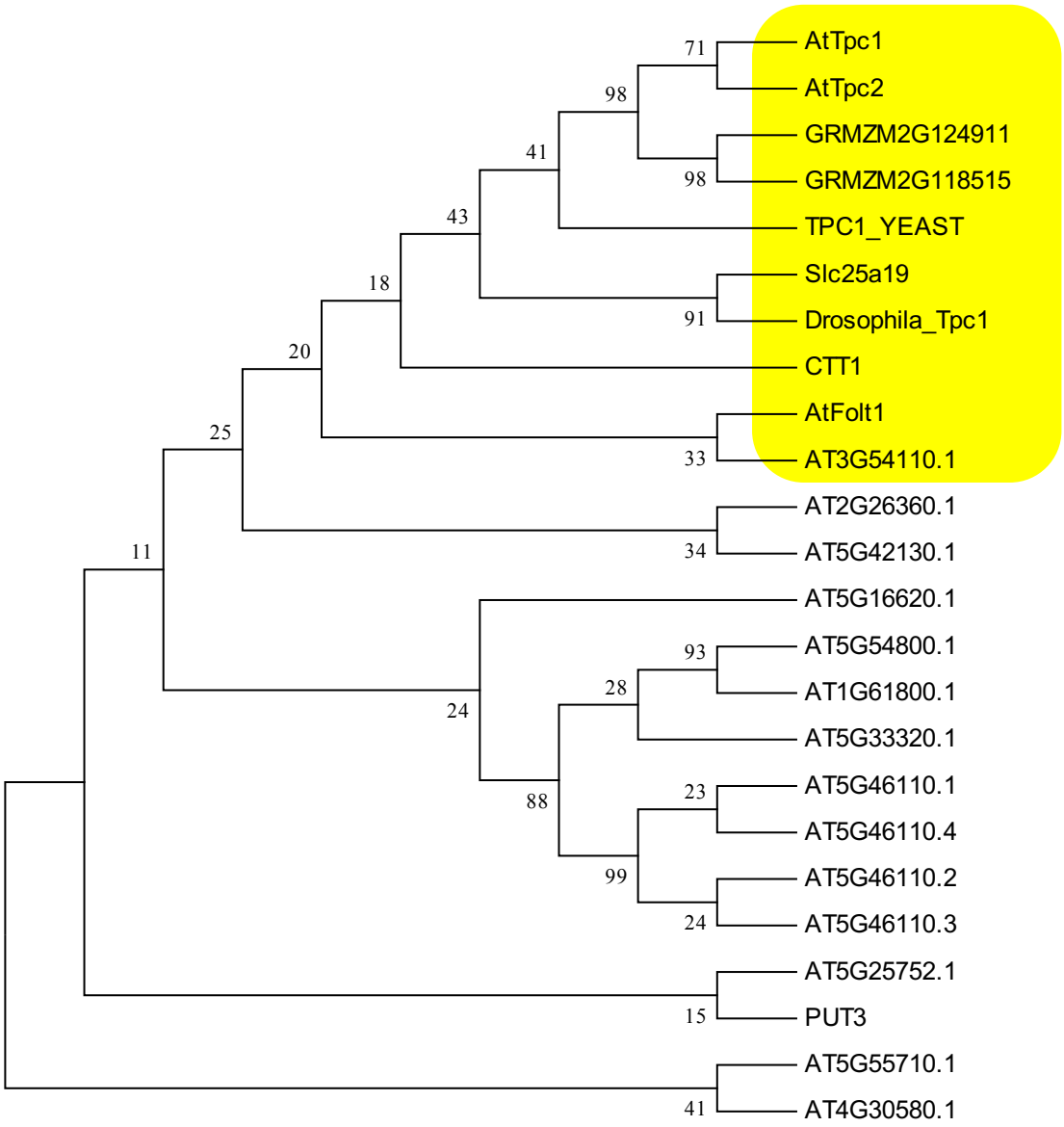

Figure A7: Phylogenetic analysis of the known TPP transporters from yeast, humans and all other chloroplast membranes. Sequences were aligned using ClustalW; the tree was constructed using the Maximum Likelihood method based on the Whelan And Goldman model. The bootstrap values (%) for 1000 replicates are shown next to the nodes. Only the tree's topology is shown; the branch lengths are not proportional to the estimated number of amino acid substitutions. The red squares indicate the known TPP carriers, and the blue squares indicate the putative chloroplast transporters. Mitochondrial TPP carrier in humans (SLC25A19), mitochondrial TPP carrier 1 in yeast (TPC1_yeast), mitochondrial TPP carrier in Drosophila (TPC1_Drosophila), Arabidopsis mitochondrial TPP transporters (AtTpc1 and AtTpc2), Zea mays mitochondrial TPP transporters (GRMZM2G118515 and GRMZM2G124911) and plant mitochondrial TPP transporter, AtTpc1 and AtTpc2. AT3G51870 is Arabidopsis unknown protein and AT5G66380 is Arabidopsis folate transporter.

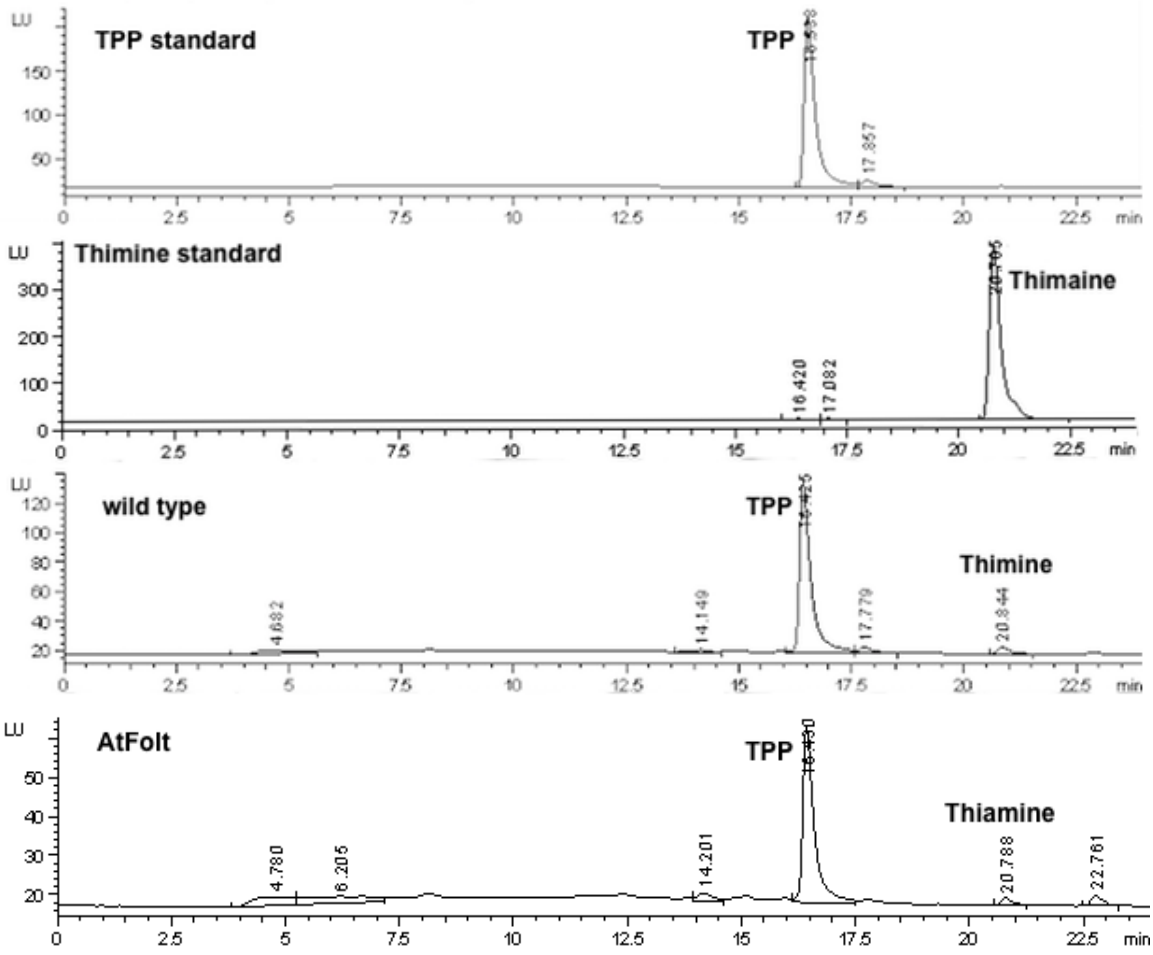

Figure A8: Quantification of the TPP levels determined in AtFolt1::RNAi and the wild type (WT). A representative HPLC profile of the TPP collected from the leaves of *Arabidopsis* AtFolt1 lines (AtFolt1) and the WT.

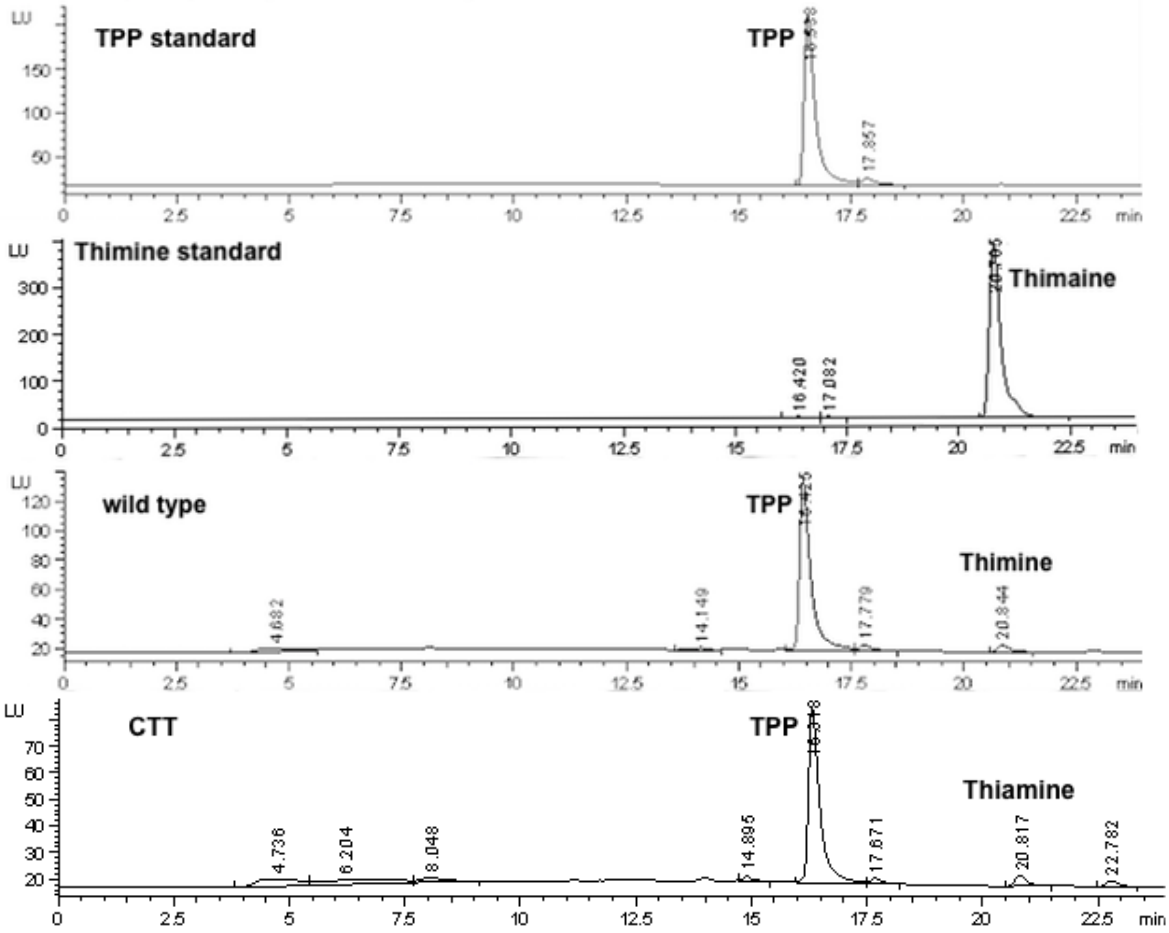

Figure A8: Quantification of TPP levels determined in CTT::RNAi and the wild type (WT). Representative HPLC profile of the TPP collected from the leaves of Arabidopsis CTT lines and the WT.